The Effect of a Perfectly Conducting Ground Plane
with a Symmetrically Located Semi-cylindrical
Hump on the Impedance and Field Distribution
of a Two-Wire Transmission Line

Lt Daniel F. Higgins
Air Force Weapons Laboratory

CLEARED
FOR PUBLIC RELEASE
PL/PA 5/19/95

Abstract

The effect of various ground contouring schemes on the im-
pedance and field distribution of horizontally polarized trans-
mission line EMP simulators is an important question. This note
considers the specific geometry of a semi-cylindrical hump or
mound symmetrically located below a two-wire transmission line.
A perfectly conducting ground and TEM mode propagation is as-
sumed. The field distribution and impedance of such a line are
calculated for a variety of hump sizes and transmission line
configurations. The results are compared to those of a similar
line above a ground without the hump (i.e., a planar ground)
and a similar line in free space. By means of these compari-
sons several "equivalent" ground contours are defined.

Acknowledgment

I wish to thank Mr. Terry Brown of the Dikewood Corporation for the considerable amount of computer programming involved in the preparation of this note. I would also like to thank Dr. Carl Baum for his interest and advice in the preparation of this work.

I. Introduction

     The use of TEM mode propagation of a transmission line to
simulate the free space EMP environment is a fairly well under-
stood EMP simulation technique. Present experience, however,
is almost totally limited to vertically polarized transmission
lines with one plate of the line being placed directly on the
ground. When one considers simulating the effects of EMP on
large aircraft however, one is forced to build horizontally
polarized transmission lines because of the difficulty of ro-
tating large test structures within the working volume. For a
horizontally polarized transmission line, one must consider the
effect of the neaby, imperfectly conducting earth on the quality
of simulation produced by transmission line.[1] In particular,
our purpose is to consider ways of contouring the ground below
the line so as to enhance the performance of the simulator sys-
tem.

     More specifically we shall consider here the effect of a
mound or hump in the ground located symmetrically below the
plates of the transmission line and running along the axis of
the line. The earth is considered perfectly conducting, TEM
mode propagation is assumed, and the transmission line is as-
sumed to be long; thus, we will consider only the two-dimen-
sional problem of fields in a cross-section of the line perpen-
dicular to the direction of propagation (see Figure 1).

     The simplest conceptual design for a horizontally polarized
simulator would consist of a parallel plate transmission line
above a planar ground. A dielectric test stand would be re-
quired to support the test object approximately in the center
of the transmission line. Now, in designing a large horizon-
tally polarized simulator of this type one is faced with sev-
eral conflicting problems. Because the ground tends to lower
the fields in the working volume and because of the problem of
flashover and arcing from the bottom of the plates to the
ground, one wants to place the transmission line as far as pos-
sible above the ground. On the other hand, due to cost and me-
chanical considerations, one wishes to minimize the height of
the dielectric test stand for supporting the test object in the
working volume. One method of solving this problem is to build
a mound of earth under the center of the transmission line.
The dielectric test support stand is built on top the mound,
thereby minimizing its height while at the same time the dis-
tance from the bottom of the plates to the ground is maximized.
(See Figure 1A.) In other words, the mound tends to put the
bottom of the test support stand nearer to the working volume
while still keeping a relatively large distance between the
transmission line plates and the ground.

     This mound at the center of transmission line serves sev-
eral purposes. First of all, the interaction between a test

3

aircraft and an earth with a mound below the aircraft is less than the interaction between the aircraft and a flat ground located at the top of the mound. Thus for a given height of test support stand, setting the support stand on a mound helps to decrease the undesirable interaction between the test object and the ground.

Another way in which this mound or hump can be used to enhance simulator performance is by reflecting certain undesirable high frequency sections of the pulser output away from the working volume. To understand this effect, consider a horizontally polarized transmission line above a flat earth. The high frequency portion of the pulse generator's output pulse (i.e., those frequencies corresponding to wavelengths less than the transmission line dimensions) will tend to expand along spherical wavefronts centered at the generator. These high frequencies would reflect off a flat ground right back into the working volume, thus distorting the environment there. (The reflected pulse would tend to cancel the electric field.) Using the limits of geometrical optics, however, one can easily see that a properly contoured ground would reflect these high frequencies away from the working volume, or at least disperse the reflected energy of the fields over a larger volume.

Thus we have seen several reasons for contouring the ground below a horizontally polarized transmission line. In this note a rather over-simplified geometry will be considered in order to make the problem tractable. We shall consider the effect of a semi-cylindrical hump attached to an otherwise flat ground plane on the fields produced by a two-wire transmission line (see Figure 1C). A two-wire line obviously varies from finite width parallel plates but should approximate a parallel plate line where the plate separation is greater than the plate width. Furthermore, a semi-cylindrical hump is probably not the optimal shape of the ground contour, but should still point out the main features of interest with regard to the electromagnetic effects of such a mound.

In this note we shall consider both the case of a line above a flat ground and the case of a line above a contoured ground. Variations in field strength and uniformity will be considered as a function of transmission line wire separation, distance to ground, and mound size. In addition, equivalent flat ground planes will be defined for various mound sizes in terms of equal transmission line impedances and equal field strengths at the center of the transmission line.

II.   The Two-Wire Line Above a Planar Ground

The complex potential function for a two-wire line above a flat ground (Case A) can be written as

4

$$\phi^{(A)} = u + iv = \ln\left[\frac{z + z_1}{z - z_1}\right] + \ln\left[\frac{z - z_2}{z + z_3}\right] \tag{1}$$

where

$$z_1 = a$$

$$z_2 = a - 2ib$$

$$z_3 = a + 2ib = z_2^*$$

and $2a$ is the wire separation and b is the distance of the wires above the ground plane (see Figure 1B). This equation for the potential is only strictly correct for line charges; i.e., in the limit as the wire radius $r_0 \to 0$. As long as r_0 is much smaller than other characteristic lengths, the above expression should be a good approximation of the potential, however.

Now, rather than writing out the real and imaginary parts of $\phi^{(A)}$ and taking derivatives to get the fields, let us continue to use complex notation. Consider the fact that since $\phi^{(A)}$ is an analytic function

$$\frac{\partial \phi^{(A)}}{\partial z} = \frac{\partial u}{\partial x} + i\frac{\partial v}{\partial x} \tag{2}$$

But a normalized electric field

$$\vec{e} = e_x \hat{x} + e_y \hat{y} \tag{3}$$

is defined by

$$e_x = -\frac{\partial u}{\partial x} \tag{4}$$

$$e_y = -\frac{\partial u}{\partial y} = \frac{\partial v}{\partial x} \tag{5}$$

Thus

$$\frac{\partial \phi}{\partial z} = -e_x + i e_y \tag{6}$$

Therefore, if one thinks of the vector $\vec{e}$ in terms of a complex number in the z-plane,

$$\vec{e} = \left[-\frac{\partial \phi}{\partial z} \right]^* \tag{7}$$

where * indicates the complex conjugate. Thus

$$\vec{e}^{(A)} = \left[-\frac{1}{z + z_1} + \frac{1}{z - z_1} - \frac{1}{z - z_2} + \frac{1}{z + z_3} \right]^* \tag{8}$$

Remember that $\vec{e}^{(A)}$ is really just a complex function whose real part equals $e_x(x,y)$ and imaginary part equals $e_y(x,y)$ when evaluated at $z = x + iy$.

The unnormalized field can be written as

$$\vec{E}^{(A)} = \frac{|\Delta V|}{2|u_o^{(A)}|} \vec{e}^{(A)} \tag{9}$$

where $|\Delta V|$ is the potential difference across the line in volts per meter and $u_o^{(A)}$ is the real part of $\phi^{(A)}$ evaluated on the surface of one of the wires. To find $u_o^{(A)}$, let $z = \xi - z_1$. Then

$$\phi^{(A)} = \ell n \left[\frac{\xi}{\xi - 2z_1} \right] + \ell n \left[\frac{\xi - z_2 - z_1}{\xi + z_3 - z_1} \right] \tag{10}$$

Now, assume ξ is very small, i.e.,

$$|\xi| = r_o \ll a,b \tag{11}$$

Then

$$|u_o^{(A)}| \simeq \ell n \left(\frac{2a}{r_o} \right) - \frac{1}{2} \ell n \left(1 + \frac{a^2}{b^2} \right) \tag{12}$$

Note that the inequality $r_o \ll a,b$ ensures that the second term in equation 12 is much smaller than the first term. In comparing field strengths, we will usually ignore this second term. However, in other cases (e.g., calculating the geometrical factors) it will be necessary to retain this term.

6

Now consider defining an efficiency factor, f_E, such that[2]

$$|\vec{E}|_{z=iy} = \frac{|\Delta V|}{2a} f_E \tag{13}$$

Then, from equation 9

$$f_E = \frac{a}{|u_o^{(A)}|} |\vec{e}^{(A)}|_{z=iy}$$

$$= \frac{2}{\ln\left(\frac{2a}{r_o}\right) - \frac{1}{2}\ln\left(1 + \frac{a^2}{b^2}\right)} \left[\frac{1}{\left(\frac{y}{a}\right)^2 + 1} - \frac{1}{\left(\frac{y}{a} + 2\frac{b}{a}\right)^2 + 1}\right] \tag{14}$$

One can also define a geometrical factor f_g (ref. 2)

$$f_g^{(A)} = \frac{\Delta u}{\Delta v} = \frac{|u_o^{(A)}|}{\pi} = \frac{1}{\pi}\ln\left(\frac{2a}{r_o}\right) - \frac{1}{2\pi}\ln\left(1 + \frac{a^2}{b^2}\right) \tag{15}$$

where the pulse impedance of the line is just

$$Z = \sqrt{\frac{\mu_o}{\varepsilon_o}} f_g \tag{16}$$

the inductance per unit length is

$$L' = \mu_o f_g \tag{17}$$

and the capacitance per unit length is

$$C' = \frac{\varepsilon_o}{f_g} \tag{18}$$

Now consider the previous expressions in the limit as b becomes very large. This special case is just a two-wire line in free space which is treated elsewhere.[2] It is easily seen that the expressions here just reduce to those in reference 2 as $b \to \infty$.

III. The Two-Wire Line Above a Ground with a Semi-cylindrical Hump

Now consider the case of a two-wire transmission line above a non-planar ground which is flat except for a semi-circular hump symmetrically located beneath the two-wire line (Case B). The hump has radius γ, the wires are separated by 2α and are a distance β above the planar part of the ground (see Figure 1B). Consider this geometry in the complex z-plane and the wires as line charges located at

$$z_1 = \alpha \tag{19}$$

$$z_2 = -\alpha \tag{20}$$

Now map the z-plane into the complex w-plane by the conformal transform

$$w = \frac{z + i\beta}{\gamma} + \frac{\gamma}{z + i\beta} \tag{21}$$

This transformation maps the entire non-planar ground in the z-plane onto the real axis of the w-plane. The wires are mapped onto the points

$$w_1 = \frac{\alpha + i\beta}{\gamma} + \frac{\gamma}{\alpha + i\beta}$$

$$= \alpha\mu + i\beta\nu \tag{22}$$

$$w_2 = \frac{-\alpha + i\beta}{\gamma} + \frac{\gamma}{-\alpha + i\beta}$$

$$= -\alpha\mu + i\beta\nu \tag{23}$$

where

$$\mu = \frac{1}{\gamma} + \frac{\gamma}{\alpha^2 + \beta^2} \tag{24}$$

$$\nu = \frac{1}{\gamma} - \frac{\gamma}{\alpha^2 + \beta^2} \tag{25}$$

Then the complex potential can be written as

$$\phi^{(B)} = \ln\left[\frac{w + w_1}{w - w_2}\right] + \ln\left[\frac{w - w_1}{w + w_2}\right] \tag{26}$$

Now, as before, define a normalized electric field

$$\vec{e}^{(B)} = \left[-\frac{\partial \phi^{(B)}}{\partial z}\right]^*$$

$$= \left[-\frac{\partial \phi^{(B)}}{\partial w}\frac{\partial w}{\partial z}\right]^*$$

$$= \left[\left(-\frac{1}{w + w_1} - \frac{1}{w - w_1} + \frac{1}{w + w_2} + \frac{1}{w - w_2}\right)\left(\frac{1}{\gamma} - \frac{\gamma}{(z + i\beta)^2}\right)\right]^* \tag{27}$$

The unnormalized field is just

$$\vec{E}^{(B)} = \frac{|\Delta V|}{2|u_0^{(B)}|}\,\vec{e}^{(B)} \tag{28}$$

where $|u_0^{(B)}|$ is obtained by letting $w = \xi - w_1$. Then

$$\phi^{(B)} = \ln\left(\frac{\xi}{\xi - w_2 - w_1}\right) + \ln\left(\frac{\xi - 2w_1}{\xi + w_2 - w_1}\right)$$

$$= \ln\left(\frac{\xi}{\xi - 2\alpha\mu}\right) + \ln\left(\frac{\xi - 2\alpha\mu - 2i\beta\nu}{\xi - 2\alpha\mu}\right) \tag{29}$$

Now, let $|\xi| = \mu r_0 << \alpha\mu, \beta\nu$. Then

$$|u_0^{(B)}| \simeq \ln\left(\frac{2\alpha}{r_0}\right) - \frac{1}{2}\ln\left(1 + \frac{\alpha^2\mu^2}{\beta^2\nu^2}\right) \tag{30}$$

where again in the limit as $r_0 \to 0$ only the first term is significant.

9

As for the flat ground plane, define an efficiency factor f_E

$$f_E^{(B)} = \frac{\alpha}{|u_o^{(B)}|} \, |\vec{e}^{(B)}|_{z=iy} \tag{31}$$

Now, note that

$$w_1 = -w_2^* \tag{32}$$

Thus

$$\frac{\partial \phi^{(B)}}{\partial w} = \frac{-w_2 + w_1}{w^2 + w(w_1 + w_2) + w_1 w_2} + \frac{+w_2 - w_1}{w^2 - w(w_1 + w_2) + w_1 w_2}$$

$$= \frac{2\alpha\mu}{w^2 + w(2i\beta\nu) - |w_1|^2} - \frac{2\alpha\mu}{w^2 - w(2i\beta\nu) - |w_1|^2} \tag{33}$$

giving

$$|\vec{e}^{(B)}|_{z=iy} = 2\alpha\mu \left| \left[\frac{1}{-\left(\frac{y+\beta}{\gamma} - \frac{\gamma}{y+\beta}\right)^2 - 2\beta\nu\left(\frac{y+\beta}{\gamma} - \frac{\gamma}{y+\beta}\right) - \alpha^2\mu^2 - \beta^2\nu^2} \right. \right.$$

$$\left. \left. - \frac{1}{-\left(\frac{y+\beta}{\gamma} - \frac{\gamma}{y+\beta}\right)^2 + 2\beta\nu\left(\frac{y+\beta}{\gamma} - \frac{\gamma}{y+\beta}\right) - \alpha^2\mu^2 - \beta^2\nu^2} \right] \left[\frac{1}{\gamma} + \frac{\gamma}{(y+\beta)^2} \right] \right| \tag{34}$$

As before we can also define f_g as

$$f_g^{(B)} \simeq \frac{|u_o^{(B)}|}{\pi} = \frac{1}{\pi} \ln\left(\frac{2\alpha}{r_o}\right) - \frac{1}{2\pi} \ln\left(1 + \frac{\alpha^2\mu^2}{\beta^2\nu^2}\right) \tag{35}$$

IV. Comparison of Ground Plane Effects

In the previous two sections of this note expressions have been derived for the geometrical factor and field distribution of a two-wire line above a planar ground (Case A) and above a

10

ground with a semi-cylindrical mound symmetrically located below the line (Case B). It was noted in section II that Case A has the limiting form of a two-wire line in free space as the ground plane is moved infinitely far away from the line (as $b \to \infty$). Similarly, it can be shown that Case A is the limiting form of Case B as the mound becomes very small (as $\gamma \to 0$).

However, in situations other than these limiting cases, one would like some means of comparing the effects of the ground plane. In particular, changes in the field distribution within the region between the two wires making up the transmission line must be considered, since the object being tested would be located in this area. Thus, in this section we will define several factors giving some quantitative measure of the various ground plane effects.

First consider the geometrical factor. Let

$$\Delta f_g \equiv f_g^{(A)} - f_g^{(B)}$$

$$= \frac{1}{2} \ell n \left(1 + \frac{\alpha^2 \mu^2}{\beta^2 \nu^2} \right) - \frac{1}{2} \ell n \left(1 + \frac{a^2}{b^2} \right)$$

$$= \ell n \left[\left(\frac{1 + \frac{\alpha^2 \mu^2}{\beta^2 \nu^2}}{1 + \frac{a^2}{b^2}} \right)^{1/2} \right] \tag{36}$$

To compare the effects of the various ground planes being considered, first have the wires of the line coincide by making

$$a \equiv \alpha \tag{37}$$

Then Δf_g just becomes a function of b, β, and γ. There are several interesting choices for b that can be made to compare Case A and Case B. One obvious choice is $b = \beta$. Another is $b = \beta - \gamma$. These choices put a planar ground at the bottom and top of the semi-circular hump, respectively. Another choice for b is to define some $b_{eff}^{(1)}$ such that $\Delta f_g = 0$; i.e.,

$$\frac{b_{eff}^{(1)}}{a} = \frac{\beta \nu}{\alpha \mu} = \left(\frac{\beta}{\alpha} \right) \left(\frac{\alpha^2 + \beta^2 - \gamma^2}{\alpha^2 + \beta^2 + \gamma^2} \right) \tag{38}$$

11

A second comparison one might make indicates the effect of the ground contouring on the efficiency factor, f_E. Define a relative change

$$\Delta f_E \equiv \frac{f_E^{(A)} - f_E^{(B)}}{f_E^{(A)}}$$

$$= \frac{\frac{a}{|u_o^{(A)}|} |\vec{e}^{(A)}|_{z=iy} - \frac{\alpha}{|u_o^{(B)}|} |\vec{e}^{(B)}|_{z=iy}}{\frac{a}{|u_o^{(A)}|} |\vec{e}^{(A)}|_{z=iy}} \tag{39}$$

As in equation 37, we assume $a \equiv \alpha$ for comparison purposes. Now consider equations 12 and 30 for $|u_o^{(A)}|$ and $|u_o^{(B)}|$, respectively. Note that in deriving both equations we have assumed that r_o is small, giving

$$\ln\left(\frac{2a}{r_o}\right) \gg \frac{1}{2} \ln\left(1 + \frac{a^2}{b^2}\right) \tag{40}$$

and

$$\ln\left(\frac{2\alpha}{r_o}\right) \gg \frac{1}{2} \ln\left(1 + \frac{\alpha^2 \mu^2}{\beta^2 \nu^2}\right) \tag{41}$$

Thus, one obtains the approximation

$$|u_o^{(A)}| \simeq |u_o^{(B)}| \tag{42}$$

which gives the result

$$\Delta f_E \simeq \frac{|\vec{e}^{(A)}|_{z=iy} - |\vec{e}^{(B)}|_{z=iy}}{|\vec{e}^{(A)}|_{z=iy}} \tag{43}$$

Due to symmetry, $\vec{e}$ evaluated along $z = iy$ has a zero y-component, indicating that Δf_E as approximated in equation 43 is just the relative difference in the normalized electric fields. As mentioned before, one can make several choices for b to compare Case A and Case B.

Now consider a more generalized parameter which compares the normalized electric fields everywhere in space. Let us first compare the transmission line above a planar ground with the same line in free space. Define

$$\Delta e^{(A)} \equiv \frac{\left| \vec{e}^{(A)}(b) - \vec{e}^{(A)}(b = \infty) \right|}{\left| \vec{e}^{(A)}(b = \infty) \right|} \tag{44}$$

where $\vec{e}^{(A)}(b = \infty)$ corresponds to a line in free space. The vector difference indicated above is just a simple subtraction of the complex numbers representing the electric field vectors. Thus, maintaining the field expressions in terms of complex numbers simplifies looking at field changes.

Similarly, the humped ground can be compared to the flat ground. Here let

$$\Delta e^{(B)} \equiv \frac{\left| \vec{e}^{(B)}(\beta) - \vec{e}^{(A)}(b) \right|}{\left| \vec{e}^{(A)}(b) \right|} \tag{45}$$

where several logical choices for b were discussed in considering Δf_g. One can also define another effective distance to the ground plane, $b_{eff}^{(2)}$, such that

$$\Delta e^{(B)} \Big|_{\substack{x=0 \\ y=0}} = 0 \tag{46}$$

This implies that

$$\vec{e}^{(B)}(\beta) \Big|_{z=0} = e^{(A)} \left(b_{eff}^{(2)} \right) \Big|_{z=0} \tag{47}$$

giving the result

$$\frac{b_{eff}^{(2)}}{a} = \frac{1}{2} \left\{ \left[\frac{a}{2} \vec{e}^{(B)} \Big|_{z=0} + 1 \right]^{-1} - 1 \right\}^{1/2} \tag{48}$$

Note that the definition of $\Delta e^{(B)}$ in equation 45 simply reduces to the expression for Δf_E in equation 43 when evaluated along the y-axis.

Now let us consider defining some quantitative measure of the uniformity of the fields produced. Let $\vec{e}(z)$ be the normalized field at any point in the z-plane. Consider the field at $z + \Delta z$, where z and Δz can be thought of as vectors or complex numbers; it is assumed that $|\Delta z| << |z|$. The field at the point $z + \Delta z$ is $\vec{e}(z + \Delta z)$. Then one measure of the change in the field is just $|\vec{e}(z + \Delta z) - \vec{e}(z)|$ where we take the magnitude of the vector difference in order to include changes in field direction as well as field magnitude. In general, $|\vec{e}(z + \Delta z) - \vec{e}(z)|$ will depend on the direction chosen for Δz. However, if $\vec{e}$ is derived from a complex potential function as done in this note, then $\vec{e}$ (when written as a complex function of z) is also an analytic function. Taking the limit as $|\Delta z|$ goes to zero, one can define a uniformity factor, U, such that

$$U = \frac{\displaystyle \lim_{|\Delta z| \to 0} \frac{|\vec{e}(z + \Delta z) - \vec{e}(z)|}{|\Delta z|}}{|\vec{e}(z)|/a} \tag{49}$$

Since $\vec{e}$ is analytic, the direction of Δz is immaterial and from the above definition

$$U = \frac{a\left|\frac{\partial \vec{e}}{\partial z}\right|}{|\vec{e}|} = \frac{a\left|\frac{\partial^2 \phi}{\partial z^2}\right|}{\left|\frac{\partial \phi}{\partial z}\right|} = a\left|\frac{\partial}{\partial z}\left[\ell n\left(\frac{\partial \phi}{\partial z}\right)\right]\right| \tag{50}$$

One can consider U(z) as a measure of the local uniformity at the point z since U depends only on the location z and how fast the field varies as one proceeds away from z.

Now let us apply this definition to the case being considered here. From equation 8

$$U^{(A)} = \frac{a\left|-\frac{1}{(z + z_1)^2} + \frac{1}{(z - z_1)^2} - \frac{1}{(z - z_2)^2} + \frac{1}{(z + z_3)^2}\right|}{|\vec{e}^{(A)}|} \tag{51}$$

Similarly, from equation 27

14

$$U^{(B)} = \frac{a\left|\frac{\partial}{\partial z}\vec{e}^{(B)}\right|}{\left|\vec{e}^{(B)}\right|} = \frac{a\left|\frac{\partial}{\partial z}\left[\frac{\partial \phi^{(B)}}{\partial w}\frac{\partial w}{\partial z}\right]\right|}{\left|\vec{e}^{(B)}\right|}$$

$$= \frac{a\left|\frac{\partial^2 \phi^{(B)}}{\partial w^2}\left(\frac{\partial w}{\partial z}\right)^2 + \frac{\partial \phi^{(B)}}{\partial w}\left(\frac{\partial^2 w}{\partial z^2}\right)\right|}{\left|\vec{e}^{(B)}\right|}$$

$$= \left(\frac{a}{\left|\vec{e}^{(B)}\right|}\right)\left|\left(\frac{1}{(w+w_1)^2} + \frac{1}{(w-w_1)^2} - \frac{1}{(w+w_2)^2} - \frac{1}{(w-w_2)^2}\right)\right.$$

$$\cdot \left(\frac{1}{\gamma} - \frac{\gamma}{(z+i\beta)^2}\right)^2$$

$$\left. + \left(\frac{1}{w+w_1} + \frac{1}{w-w_1} - \frac{1}{w+w_2} - \frac{1}{w-w_2}\right)\left(\frac{2\gamma}{(z+i\beta)^3}\right)\right| \qquad (52)$$

V. Discussion of Results

In the previous sections a number of expressions describing the impedance variation and field distribution were derived. In addition, certain figures of merit for comparing different ground geometries were defined. A number of these expressions were evaluated numerically and the results are shown in the attached figures. The number of graphs and figures is fairly large due to the number of independent parameters one can vary.

First, let us consider Figures 2 to 10. These figures show curvilinear square plots of the equipotential and stream lines of the complex potential function defined in equation 26. ($\gamma/\beta = 0$ corresponds to equation 1.) The equipotential lines correspond to u = constant while the streamlines correspond to v = constant where $\phi = u + iv$. The plots show the effect of varying the hump size for various β/α ratios. As would be expected, when the hump radius becomes comparable to the line spacing or the height above the ground, considerable changes in the field distribution can be seen, especially near the surface of the hump. (Similar plots for the two-wire line in free space can be found in reference 2. As in reference 1, u and v in the vicinity of the wire are plotted in increments of .05π up to u = π. For u > π, u and v are in increments of .1π. The u = π contour is easily seen on the graphs as the contour where every other v contour ends.)

15

While such equipotential plots are useful in seeing the overall field distribution, it is very difficult to directly read field strengths from such plots. Because of this, we have numerically evaluated equations 8 and 27 to find the normalized electric fields. The x- and y-components (the real and imaginary parts of $\vec{e}$) are plotted as a function of y along lines of constant x in Figures 11 to 29. Figures 11 to 14 show $e_x^{(A)}$ and $e_y^{(A)}$ with a planar ground at varying distances below the line. In Figures 15 to 29 $e_x^{(B)}$ and $e_y^{(B)}$ is plotted for variations both in the distance to the ground, β, and the radius of the mound, γ. The field is plotted only in the region between the wires ($x/\alpha < 1.0$) because we are primarily interested in the fields in this working volume between the "plates" of the transmission line. [Note also the step rise in some of the plots— these correspond to intersection with the surface of the semi- cylindrical hump.] From these plots it is easily seen that the effect of the ground on the field is most severe near the sur- face of the ground and becomes less as one goes out along the positive y-axis.

Now let us consider the results of numerical evaluation of several of the parameters defined in section IV. Figure 30 plots the change in geometrical factor, Δf_g, as a function of β for several values of b and γ. Figure 31 shows both $b_{eff}^{(1)}$ and $b_{eff}^{(2)}$ as a function of β with γ as a parameter. Thus Figure 31 can be used to find some flat ground geometry which is "equiva- lent" in some sense to the contoured ground under consideration.

Figures 32 and 33 are contour plots of the field deviation $\Delta e^{(A)}$. These figures plot lines of constant $\Delta e^{(A)}$ in the re- gion between the two wires making up the transmission line, thus giving an indication of the spatial distribution of field deviation in the working volume due to the ground plane. As one would expect, the deviations are largest as one approaches the ground plane.

Similarly, Figures 34-48 plot contours of the field devia- tion $\Delta e^{(B)}$, comparing the planar ground with the contoured ground. The plots show various β/α ratios with γ/β varied for each value of β/α. Furthermore, each contoured ground is com- pared with both a planar ground located at the bottom of the semi-circular hump and a planar ground tangent to the top of the hump (i.e., b = β and b = β - γ).

In Figures 49-57 contour plots of the uniformity factor $U^{(B)}$ (defined in equation 52) are presented for various β/α and γ/α ratios. (Note that γ/α = 0 corresponds to a planar ground, i.e., Case A.) Several interesting things can be seen from these local uniformity plots. First, note the minimum in $U^{(B)}$ on the y-axis slightly above the center of the transmission line. This minimum, indicating good field uniformity, would occur at the exact center of the line if the ground plane were absent and results from an "averaging" of the fields produced

16

by each of the two wires making up the transmission line. Note that as the ground plane is moved up and the hump becomes larger, this minimum is pushed further up the y-axis away from the center of the line. This effect would indicate that one should center the working volume of a horizontally polarized simulator above the geometric center of the transmission line for best field uniformity.

A second minimum can be seen near the surface of the hump approximately on a line from the center of the hump to the transmission line conductor at (α,o). This minimum results from the combination of fields from the wire at (α,o) and its image inside the semi-cylindrical hump of the ground plane. In fact, it can readily be seen that such a minimum would occur on a line connecting two parallel line charges of opposite sign. At some point depending on the charge magnitudes the field components along the connecting line will add while components perpendicular to the connecting line will tend to cancel, thus making the resultant field more uniform. This same effect can be seen in the equipotential plots (Figures 2-10). The areas where the curvilinear "squares" are most like a geometrical square are the areas of best uniformity.

VI. Summary

In this note, expressions for the geometrical factor and field distribution of a two-wire TEM mode transmission line above a perfectly conducting ground plane with a symmetrically located semi-cylindrical hump have been developed. These results have been compared to those of a similar line above a planar ground and various figures of merit for quantifying these comparisons have been defined. Several techniques for defining a planar ground "equivalent" to the contoured ground were discussed and the effect of the hump on field strength and uniformity are shown in the attached figures. The results indicate that certain ground contouring schemes similar to the idealized geometry considered here might well be used to enhance performance and reduce cost of a horizontally polarized simulator.

References

1. C. E. Baum, Sensor and Simulation Note 143, General Principles for the Design of ATLAS I and II, Part I: ATLAS: Electromagnetic Design Considerations for Horizontal Version, January 1972.

2. C. E. Baum, Sensor and Simulation Note 27, Impedances and Field Distributions for Symmetrical Two Wire and Four Wire Transmission Line Simulators, October 1966.
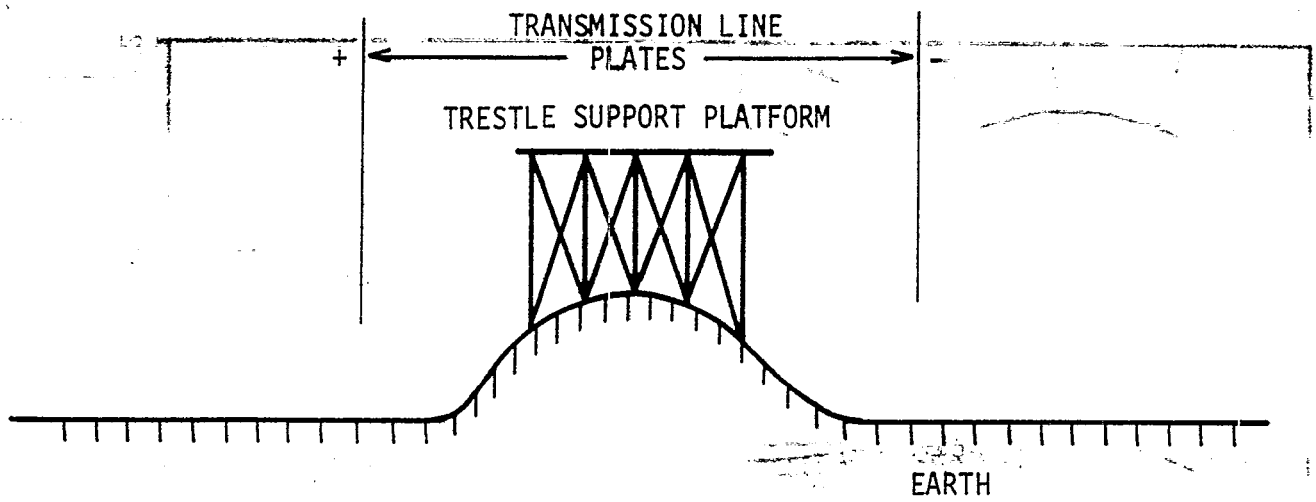
A. HORIZONTALLY POLARIZED TRANSMISSION LINE WITH CONTOURED EARTH BELOW
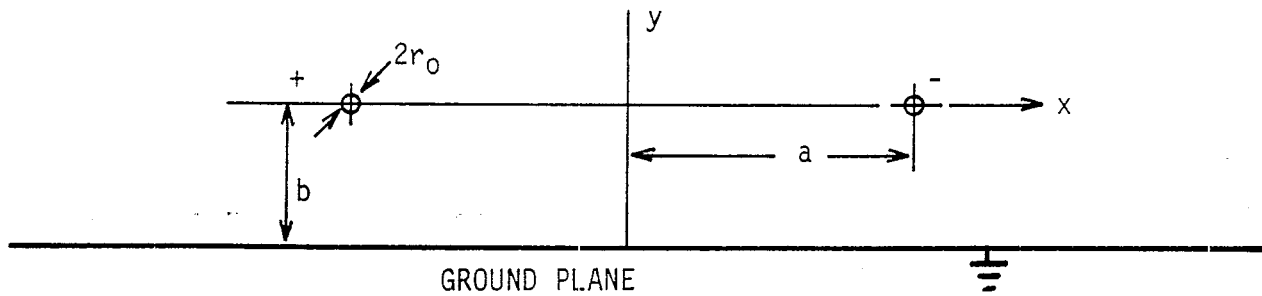
B. TWO WIRE LINE ABOVE A PLANAR GROUND (CASE A)
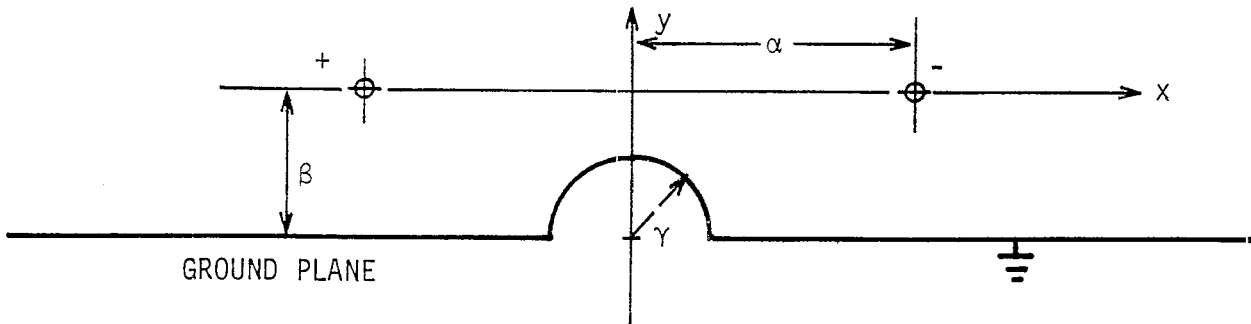
C. TWO WIRE LINE ABOVE A GROUND WITH A SYMMETRICALLY LOCATED SEMI-CYLINDRICAL HUMP (CASE B)

FIGURE 1. TRANSMISSION LINE CROSS-SECTIONAL GEOMETRIES
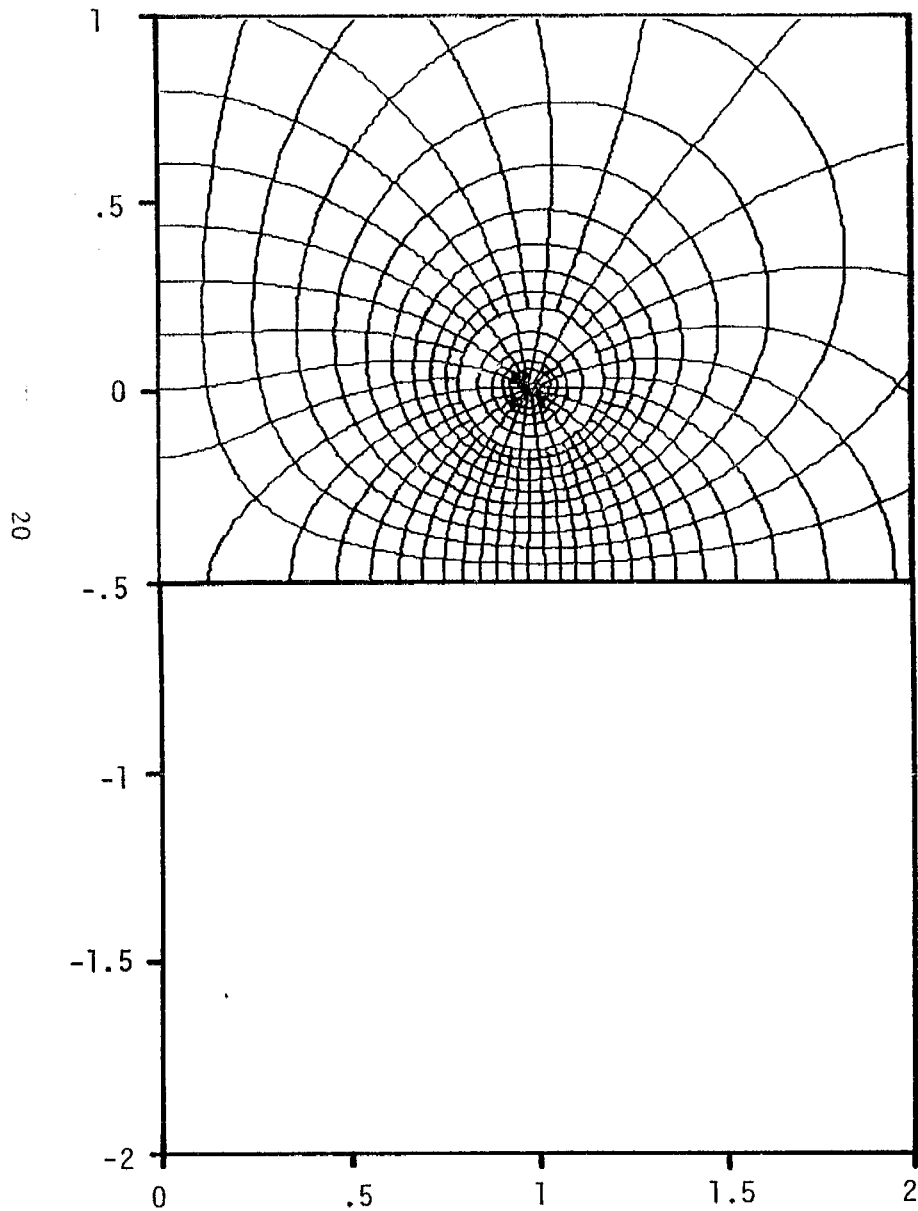
A. $\frac{\beta}{\alpha} = .5$, $\frac{\gamma}{\beta} = 0$
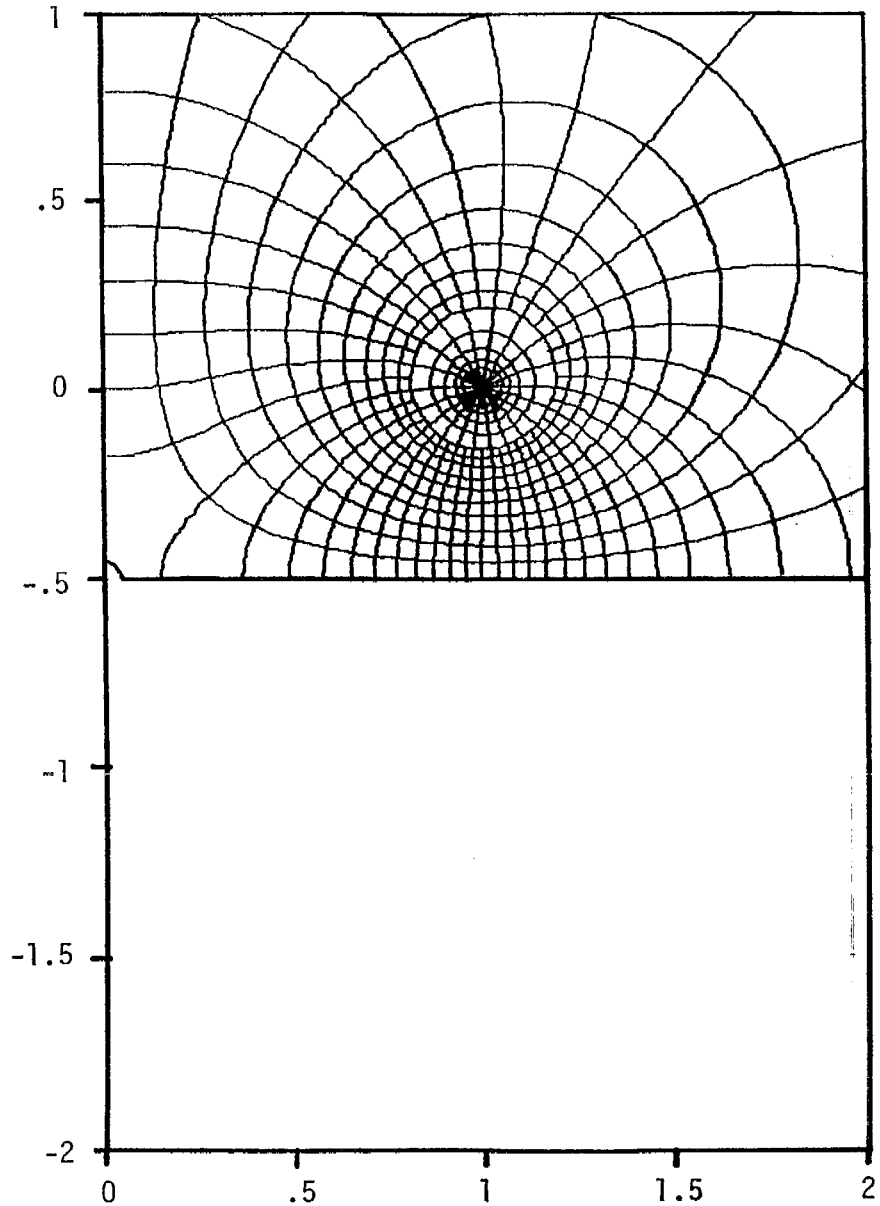
B. $\frac{\beta}{\alpha} = .5$, $\frac{\gamma}{\beta} = .1$

FIGURE 2. FIELD AND POTENTIAL DISTRIBUTION FOR SYMMETRICAL TWO WIRE TRANSMISSION LINE OVER A CONTOURED GROUND PLANE
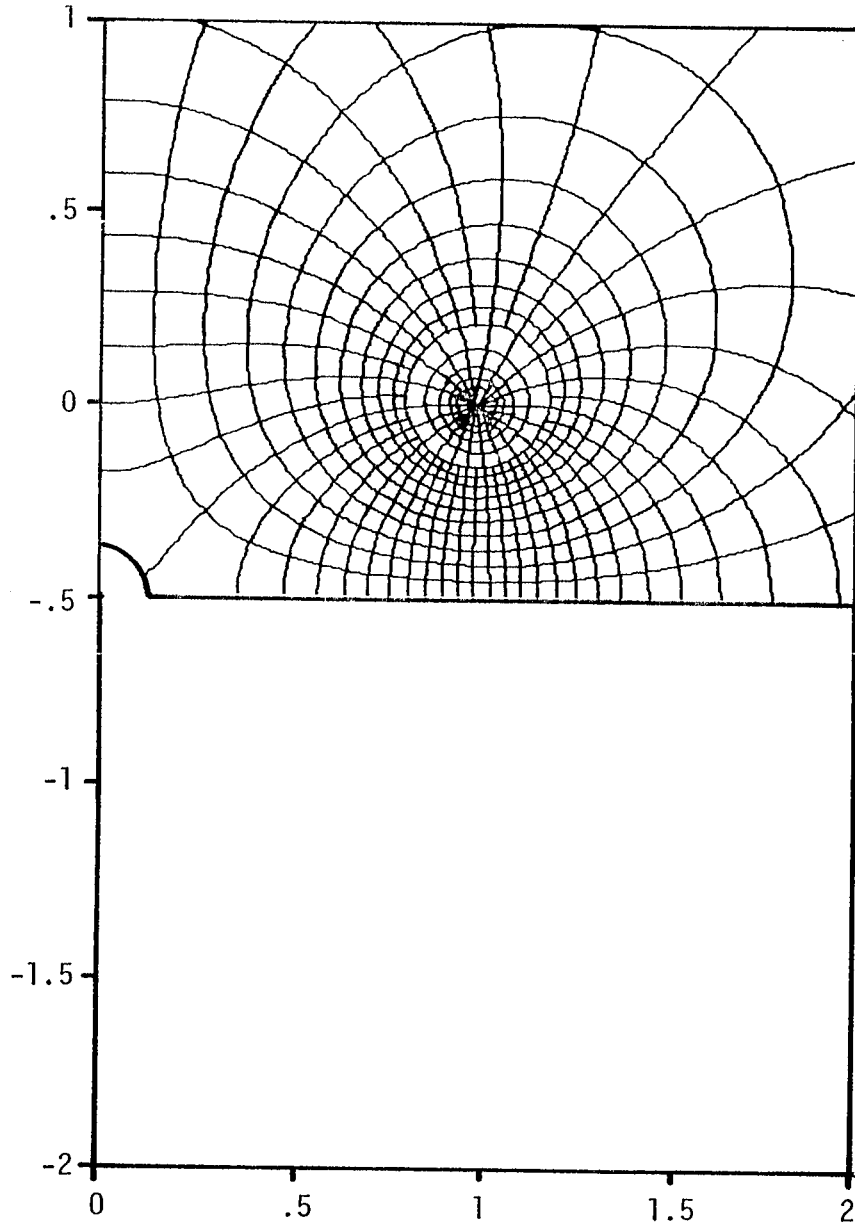
A. $\frac{\beta}{\alpha} = .5$, $\frac{\gamma}{\beta} = .25$
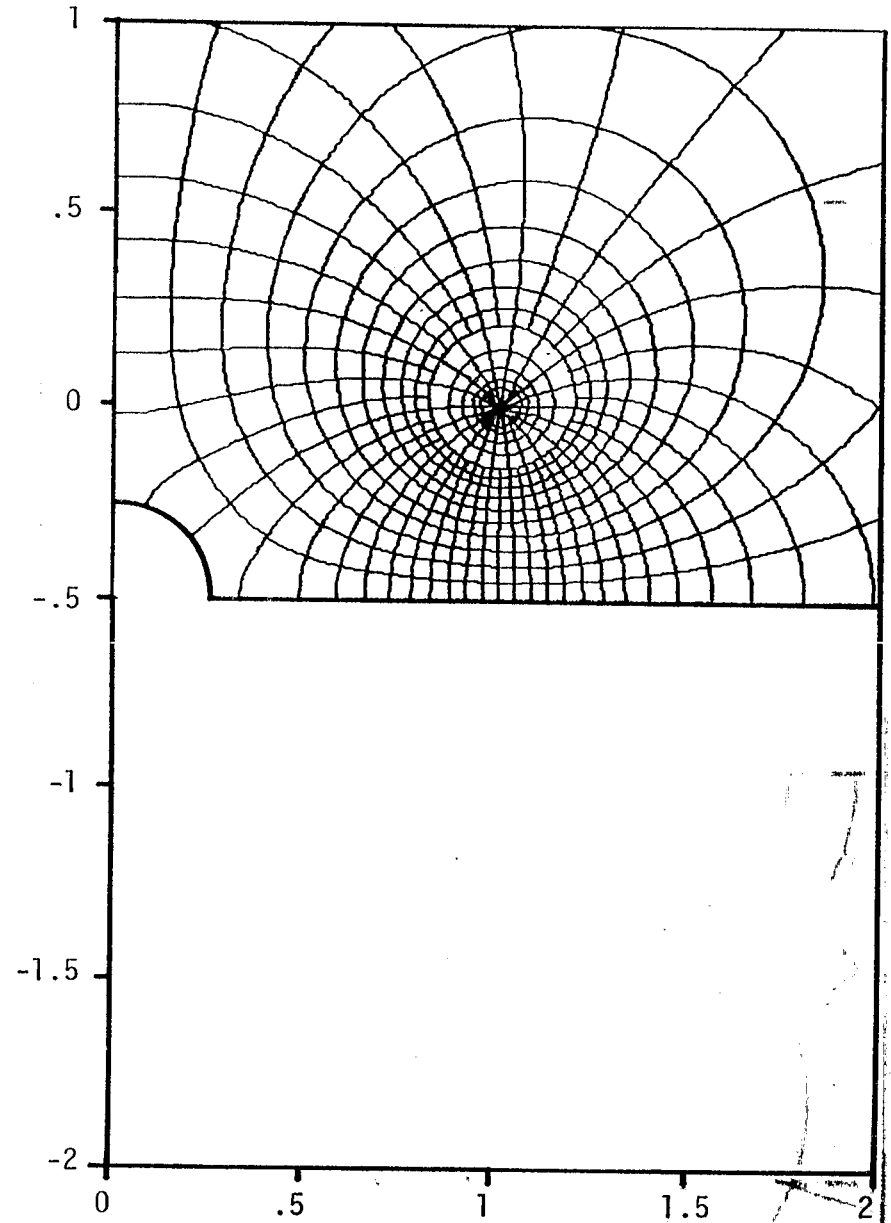
B. $\frac{\beta}{\alpha} = .5$, $\frac{\gamma}{\beta} = .5$

FIGURE 3. FIELD AND POTENTIAL DISTRIBUTION FOR SYMMETRICAL TWO WIRE TRANSMISSION LINE OVER A CONTOURED GROUND PLANE
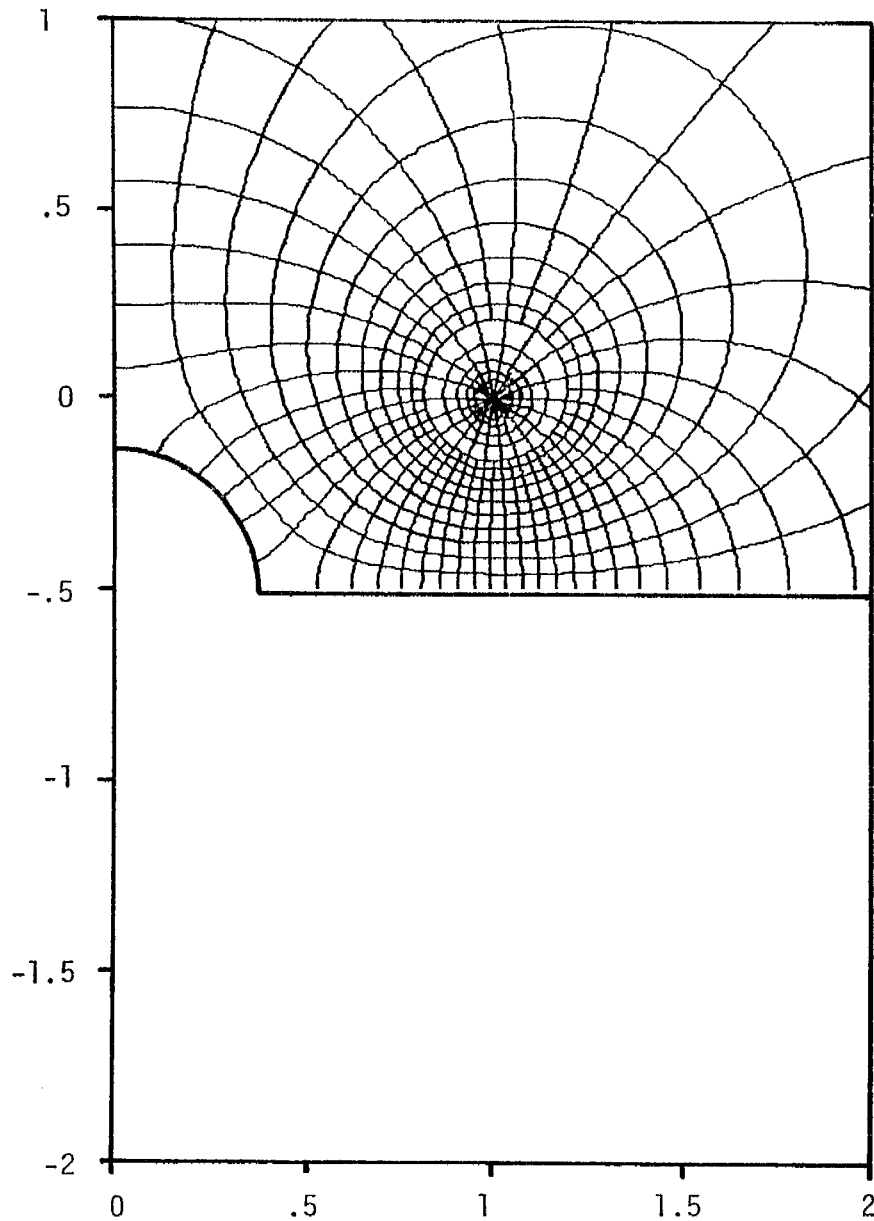
A. $\frac{\beta}{\alpha} = .5$, $\frac{\gamma}{\beta} = .75$
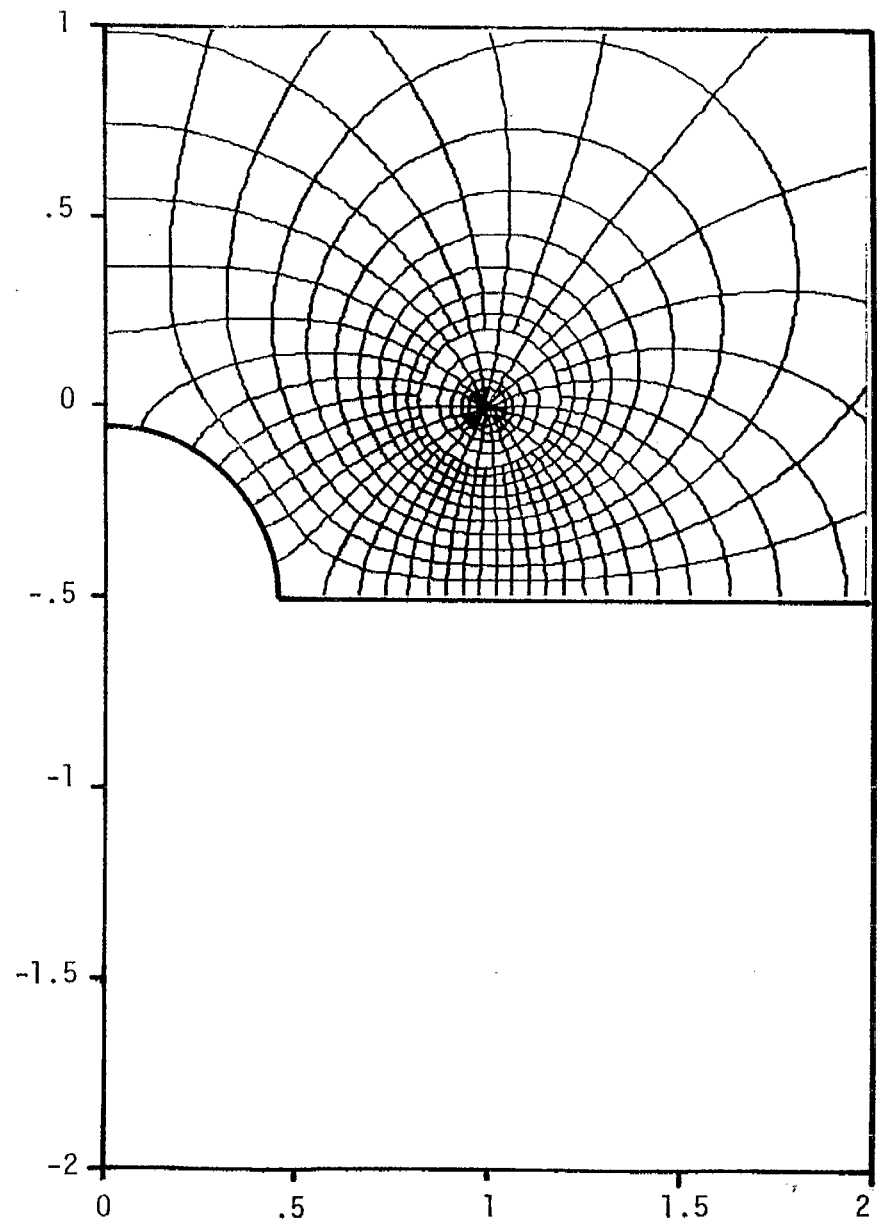
B. $\frac{\beta}{\alpha} = .5$, $\frac{\gamma}{\beta} = .9$

FIGURE 4.   FIELD AND POTENTIAL DISTRIBUTION FOR SYMMETRICAL TWO WIRE TRANSMISSION LINE OVER A CONTOURED GROUND PLANE
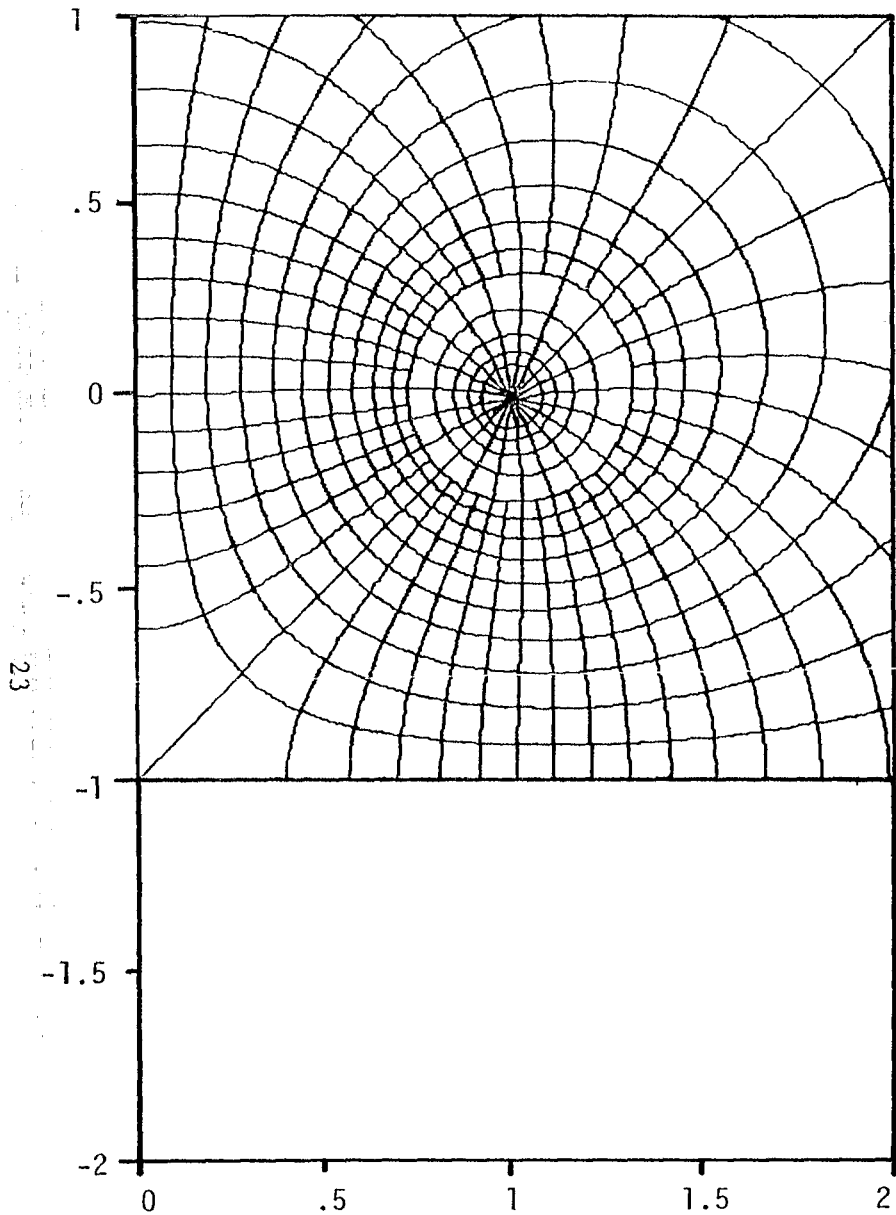
A. $\frac{\beta}{\alpha} = 1$, $\frac{\gamma}{\beta} = 0$
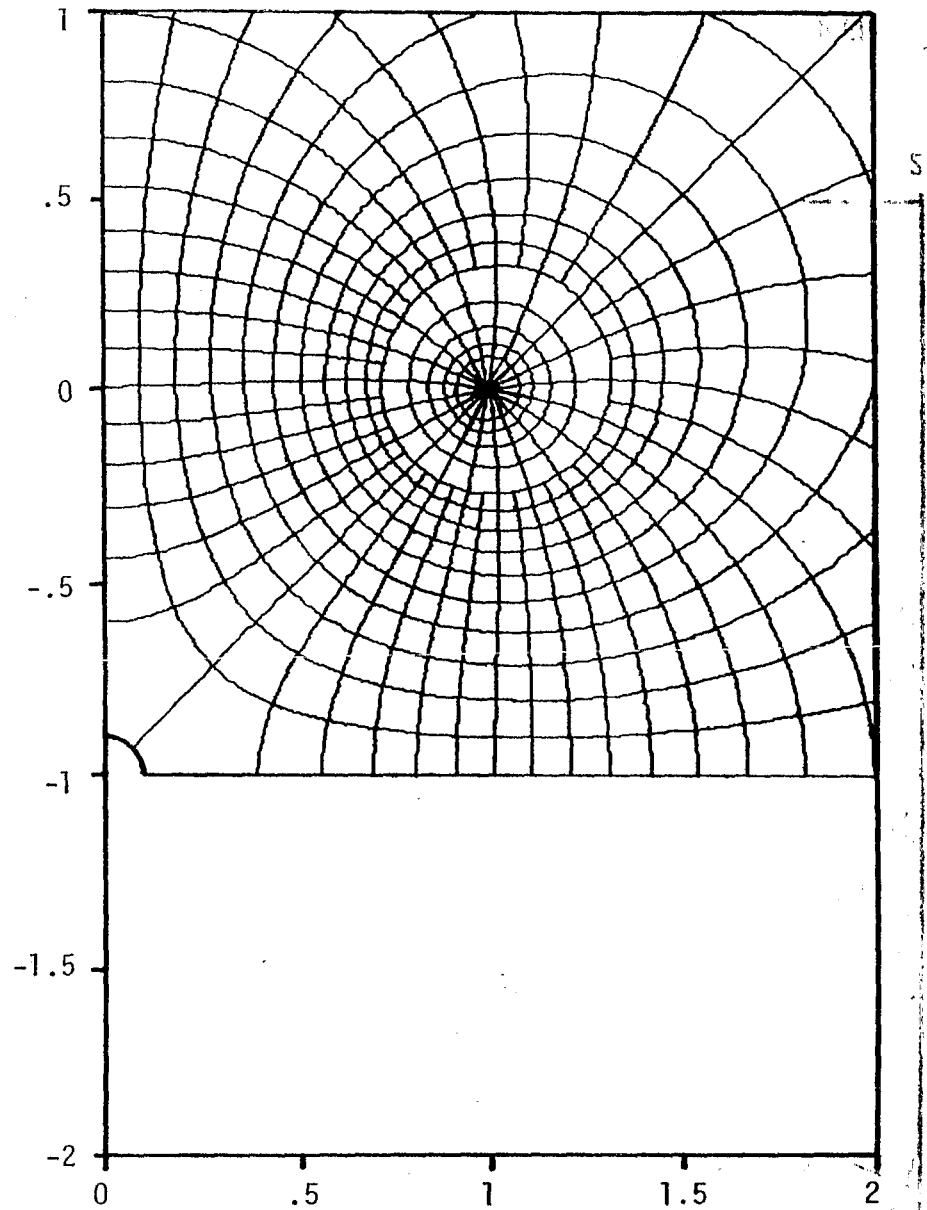
B. $\frac{\beta}{\alpha} = 1$, $\frac{\gamma}{\beta} = .1$

FIGURE 5.   FIELD AND POTENTIAL DISTRIBUTION FOR SYMMETRICAL TWO WIRE TRANSMISSION LINE OVER A CONTOURED GROUND PLANE
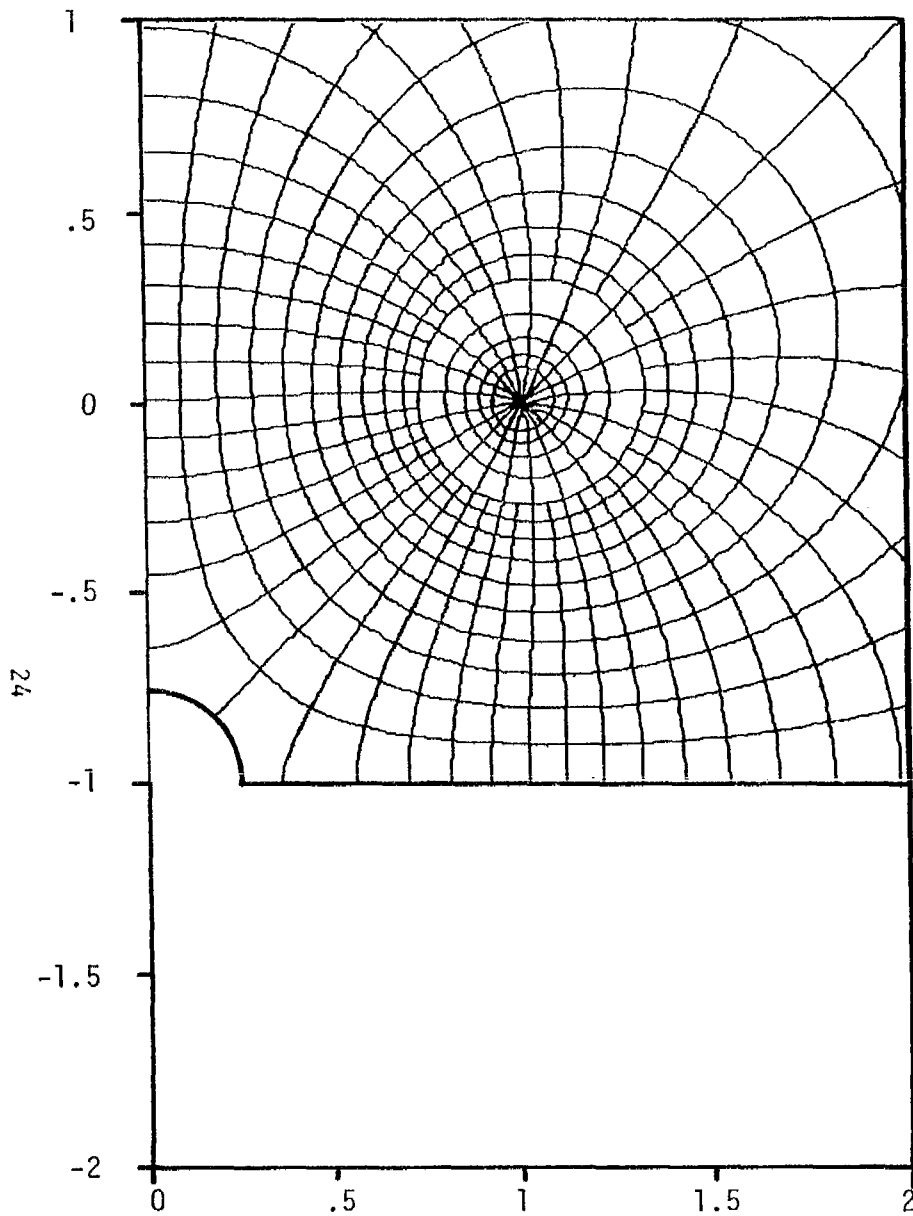
A. $\frac{\beta}{\alpha} = 1$, $\frac{\gamma}{\beta} = .25$
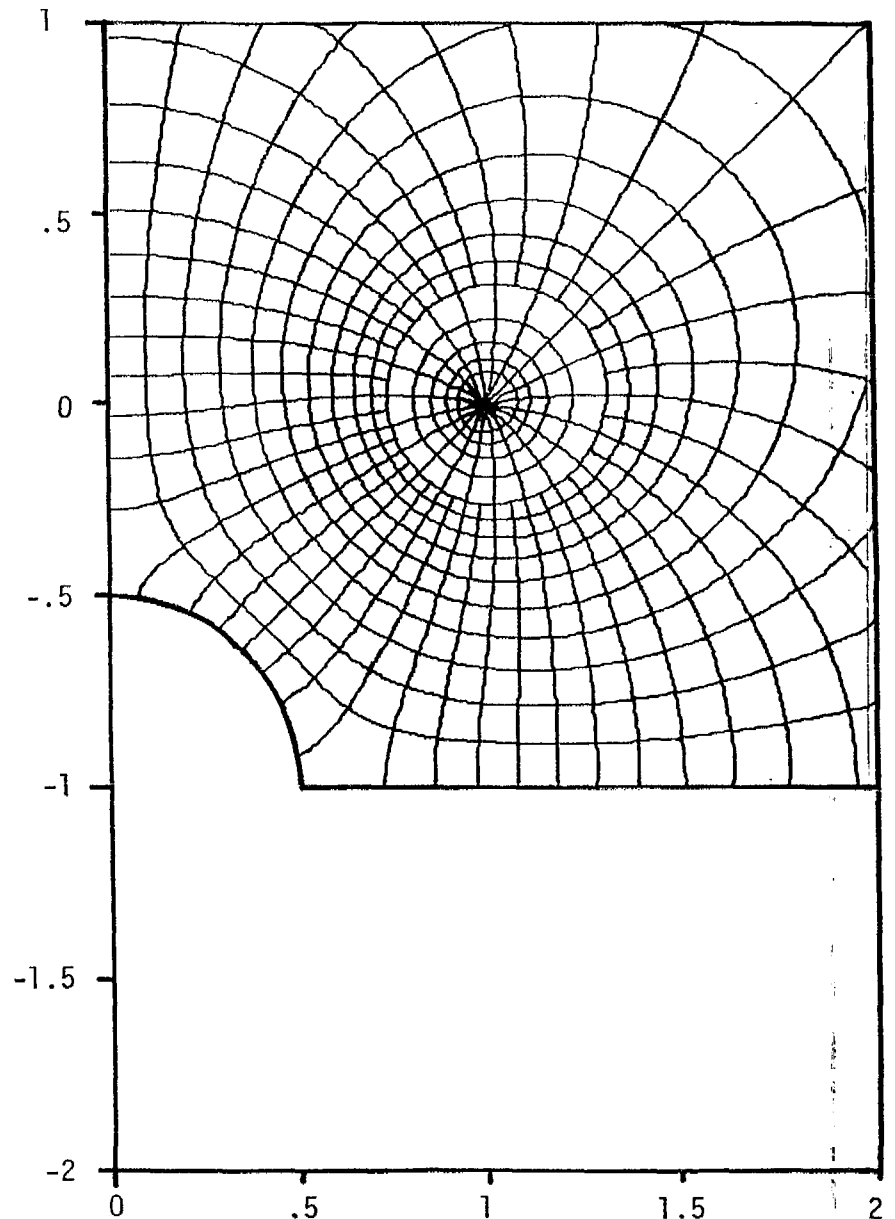
B. $\frac{\beta}{\alpha} = 1$, $\frac{\gamma}{\beta} = .5$

FIGURE 6. FIELD AND POTENTIAL DISTRIBUTION FOR SYMMETRICAL TWO WIRE TRANSMISSION LINE OVER A CONTOURED GROUND PLANE

24
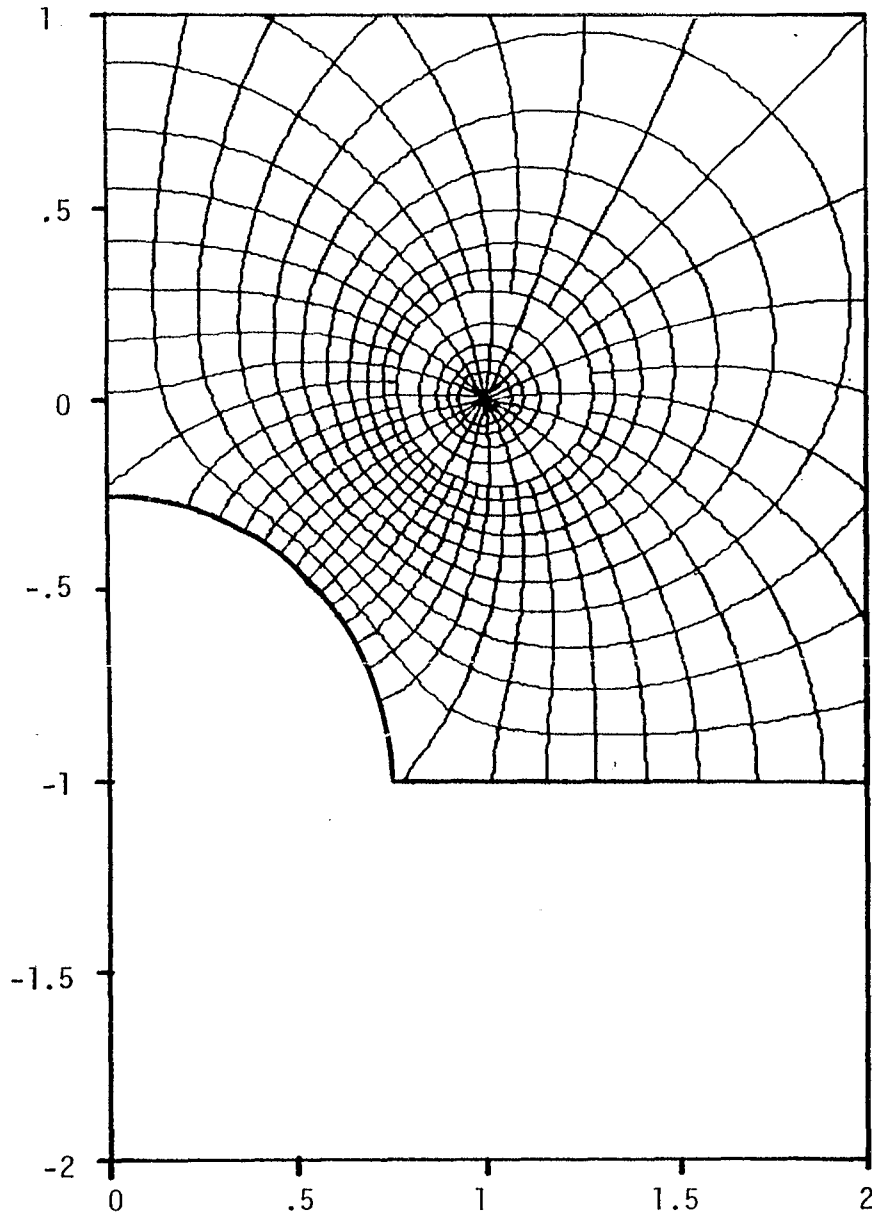
A. $\frac{\beta}{\alpha} = 1$, $\frac{\gamma}{\beta} = .75$
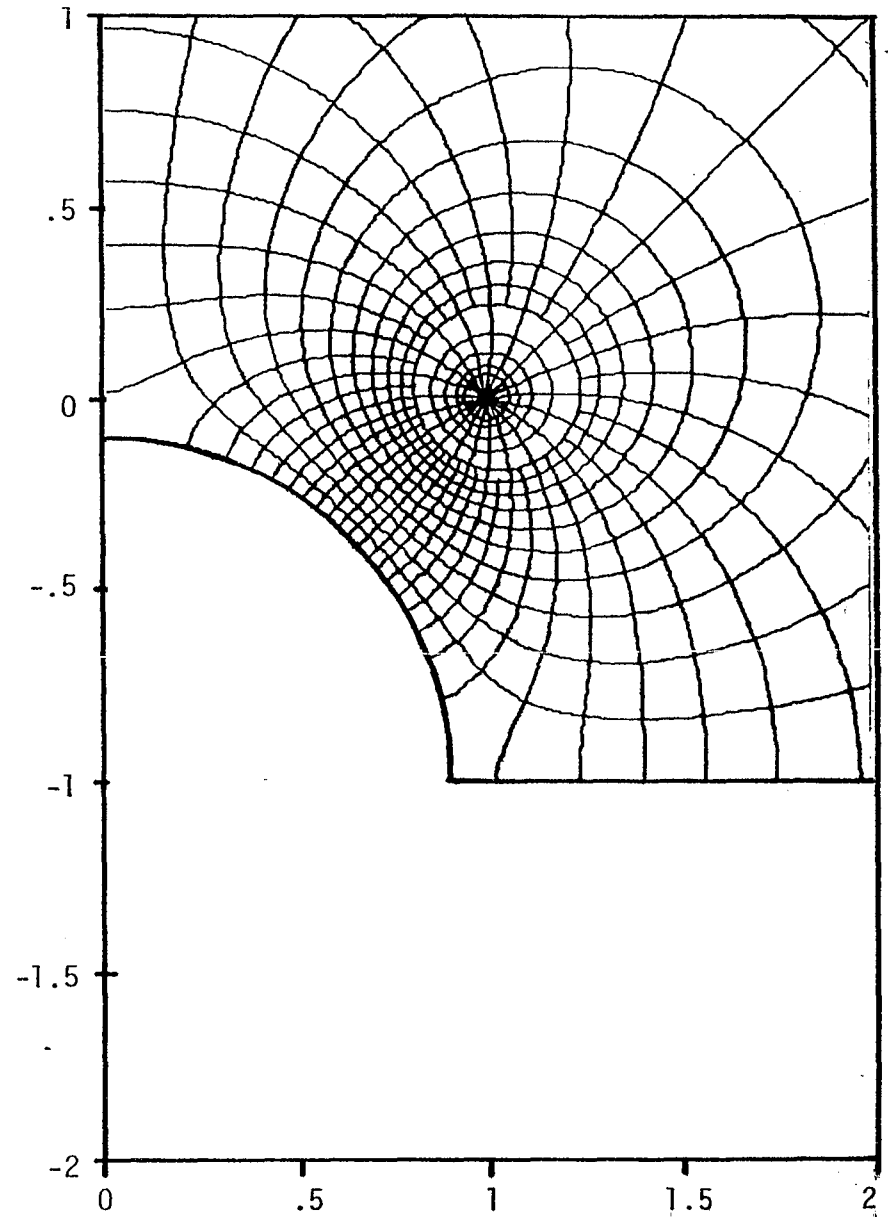
B. $\frac{\beta}{\alpha} = 1$, $\frac{\gamma}{\beta} = .9$

FIGURE 7. FIELD AND POTENTIAL DISTRIBUTION FOR SYMMETRICAL TWO WIRE TRANSMISSION LINE OVER A CONTOURED GROUND PLANE

A. $\frac{\beta}{\alpha} = 2$, $\frac{\gamma}{\beta} = 0$

B. $\frac{\beta}{\alpha} = 2$, $\frac{\gamma}{\beta} = .1$
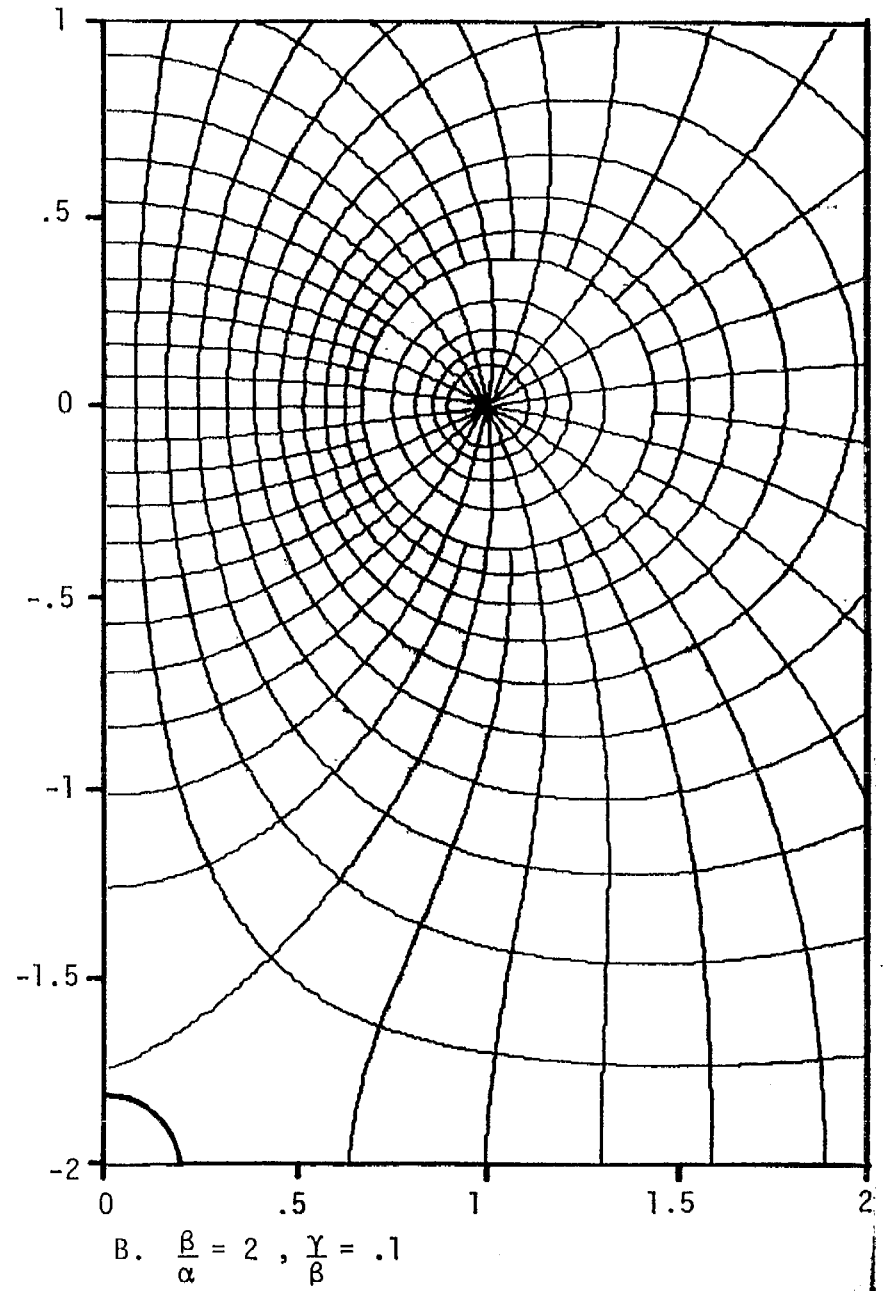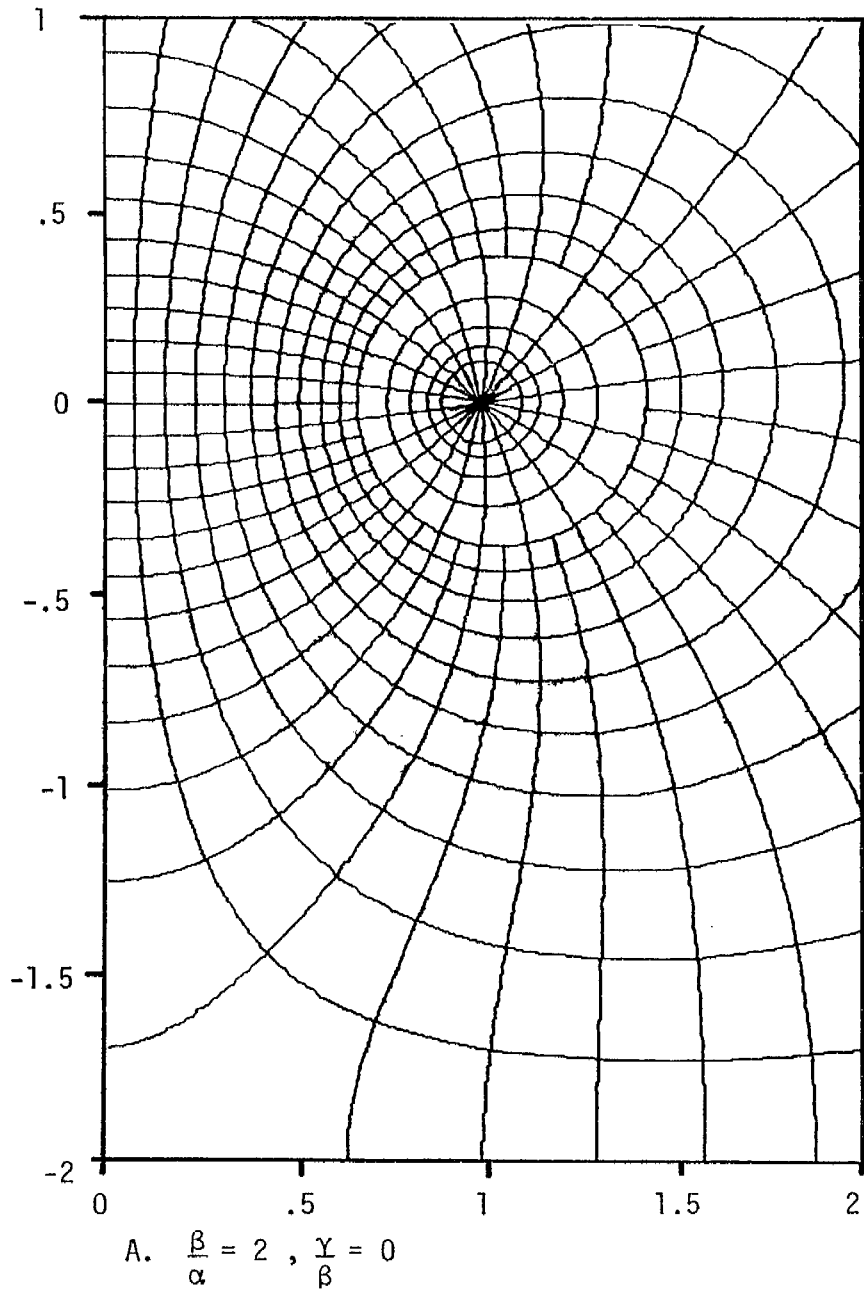
FIGURE 8.   FIELD AND POTENTIAL DISTRIBUTION FOR SYMMETRICAL TWO WIRE TRANSMISSION LINE OVER A CONTOURED GROUND PLANE

A. $\frac{\beta}{\alpha} = 2$, $\frac{\gamma}{\beta} = .25$

B. $\frac{\beta}{\alpha} = 2$, $\frac{\gamma}{\beta} = .5$
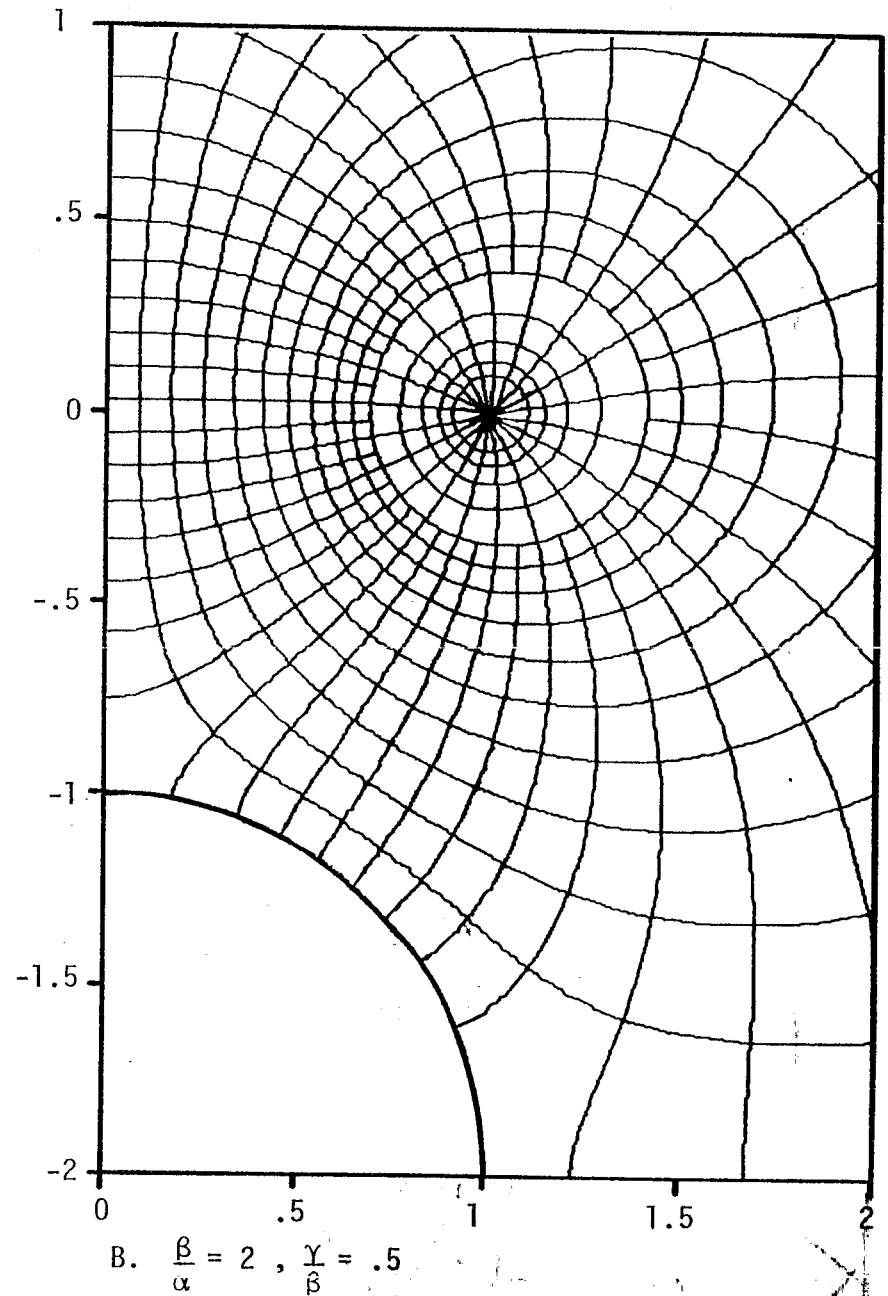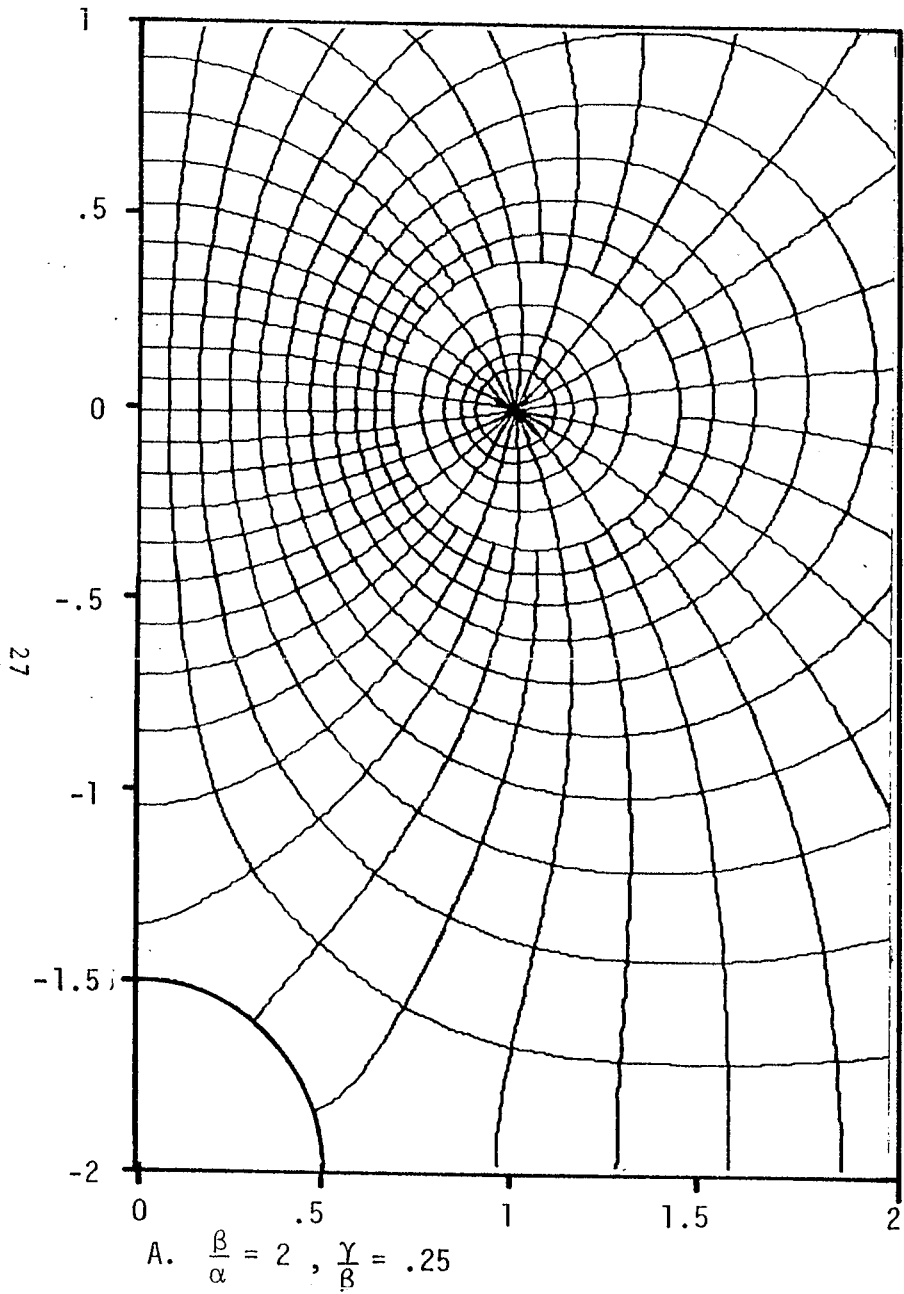
FIGURE 9. FIELD AND POTENTIAL DISTRIBUTION FOR SYMMETRICAL TWO WIRE TRANSMISSION LINE OVER A CONTOURED GROUND PLANE

27
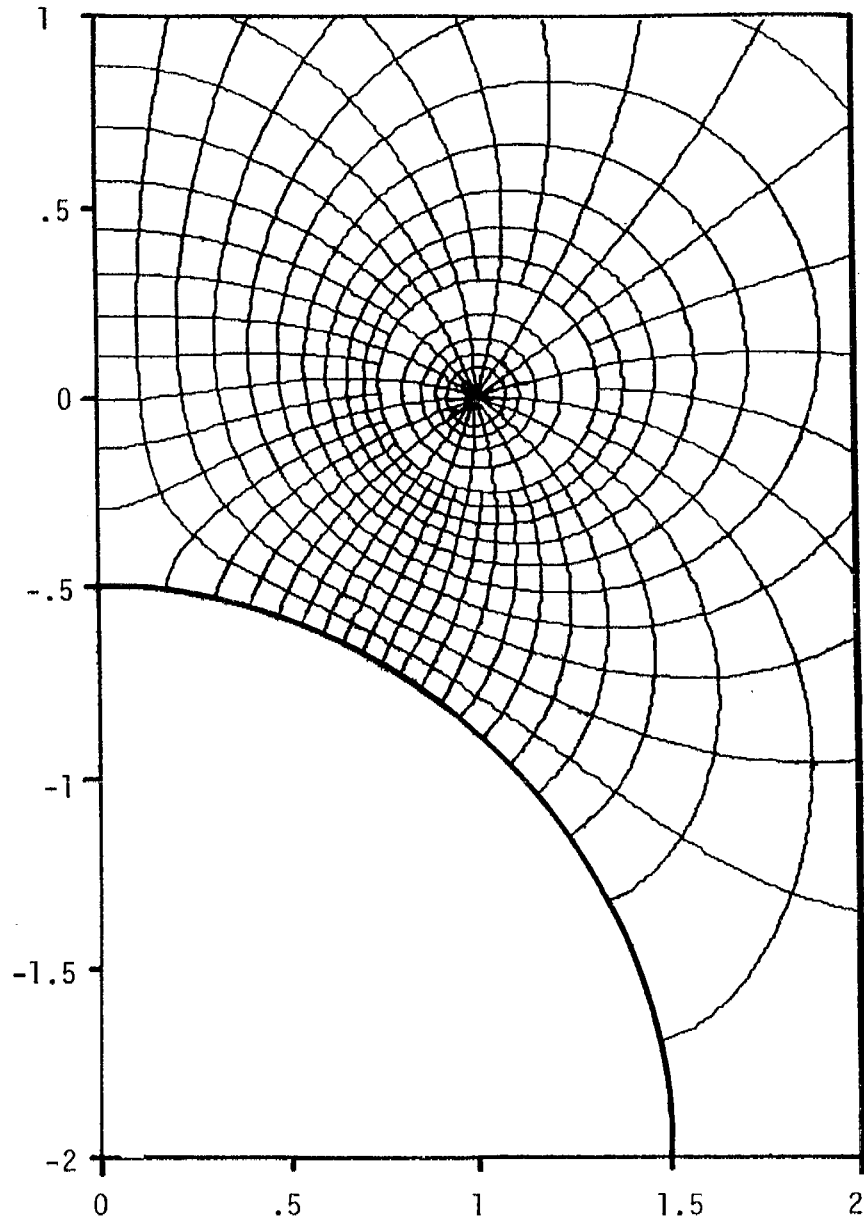
A. $\frac{\beta}{\alpha} = 2$, $\frac{\gamma}{\beta} = .75$
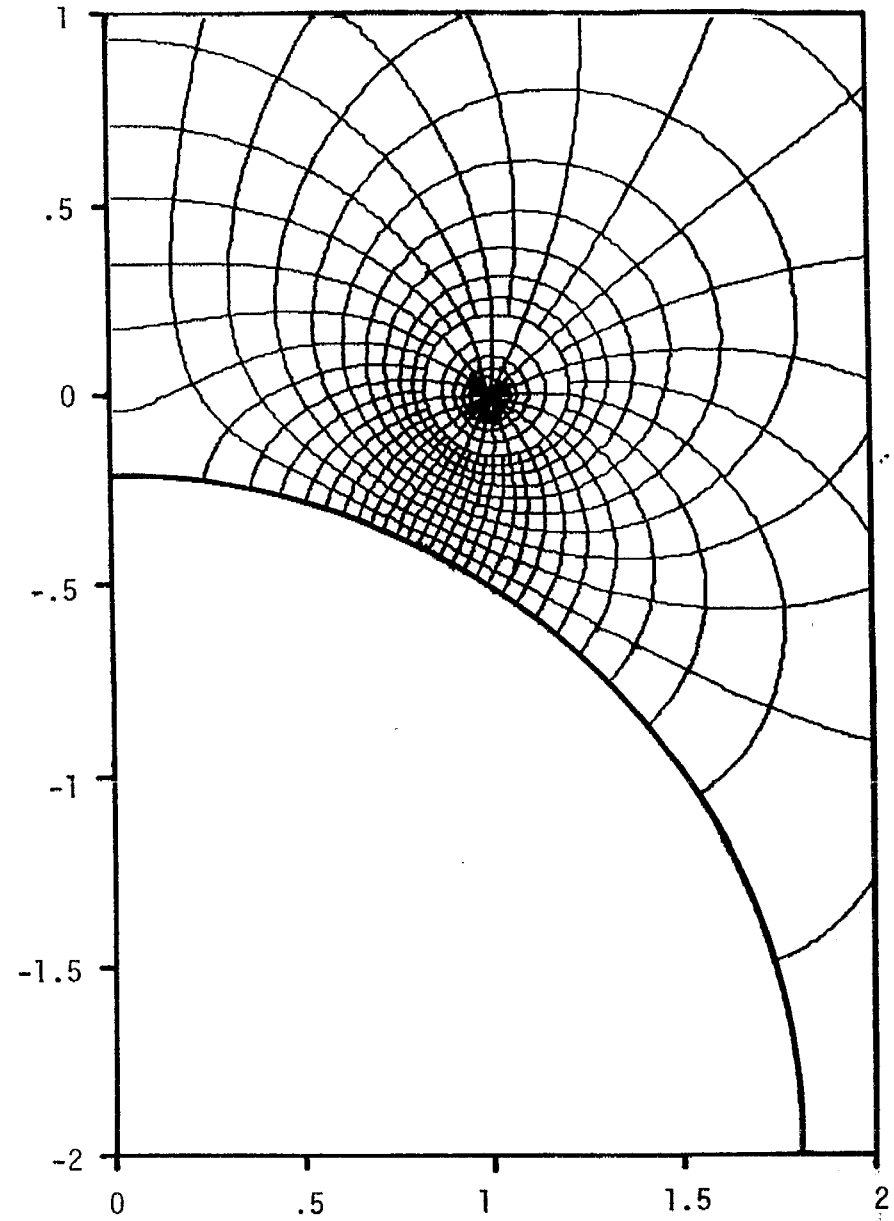
B. $\frac{\beta}{\alpha} = 2$, $\frac{\gamma}{\beta} = .9$

FIGURE 10. FIELD AND POTENTIAL DISTRIBUTION FOR SYMMETRICAL TWO WIRE TRANSMISSION LINE OVER A CONTOURED GROUND PLANE
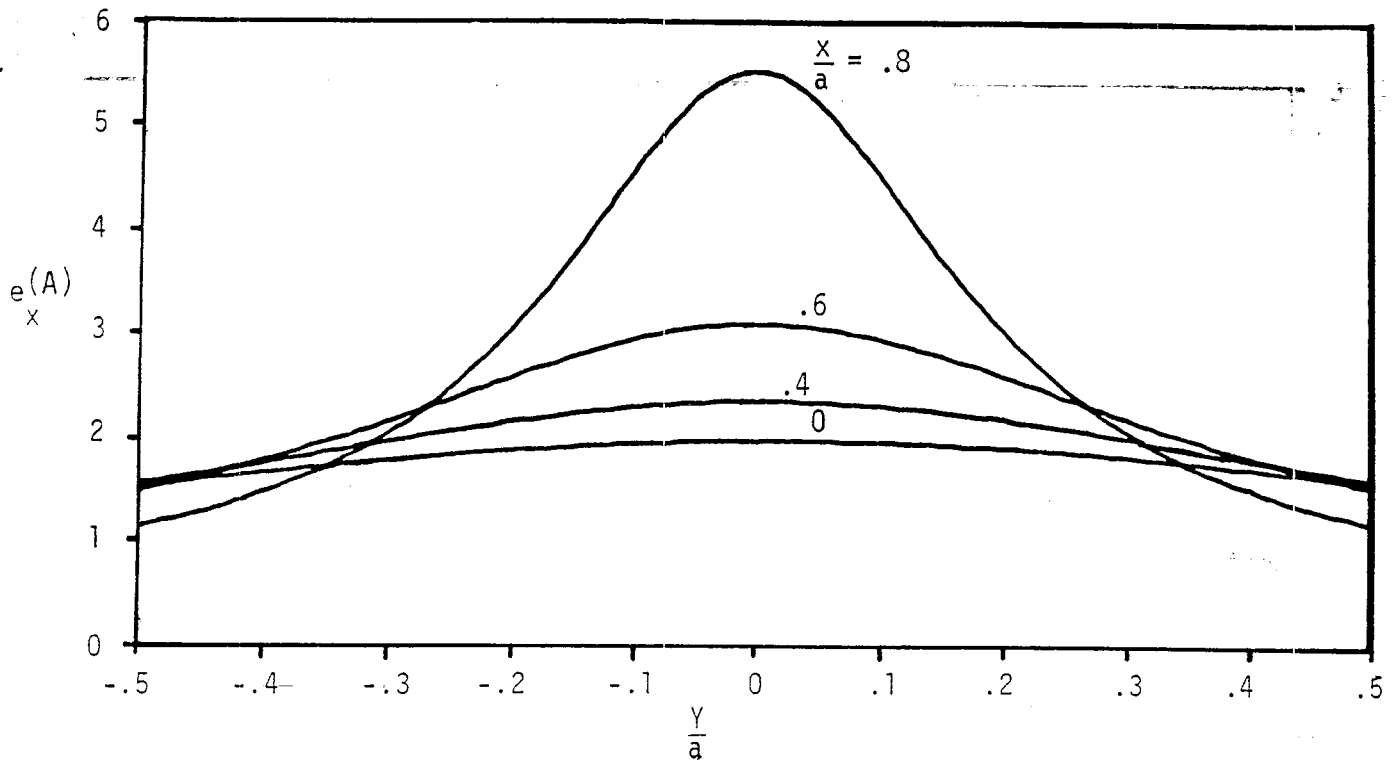
A. $e_x^{(A)}$ IN THE X DIRECTION WITH $\frac{x}{a}$ AS A PARAMETER
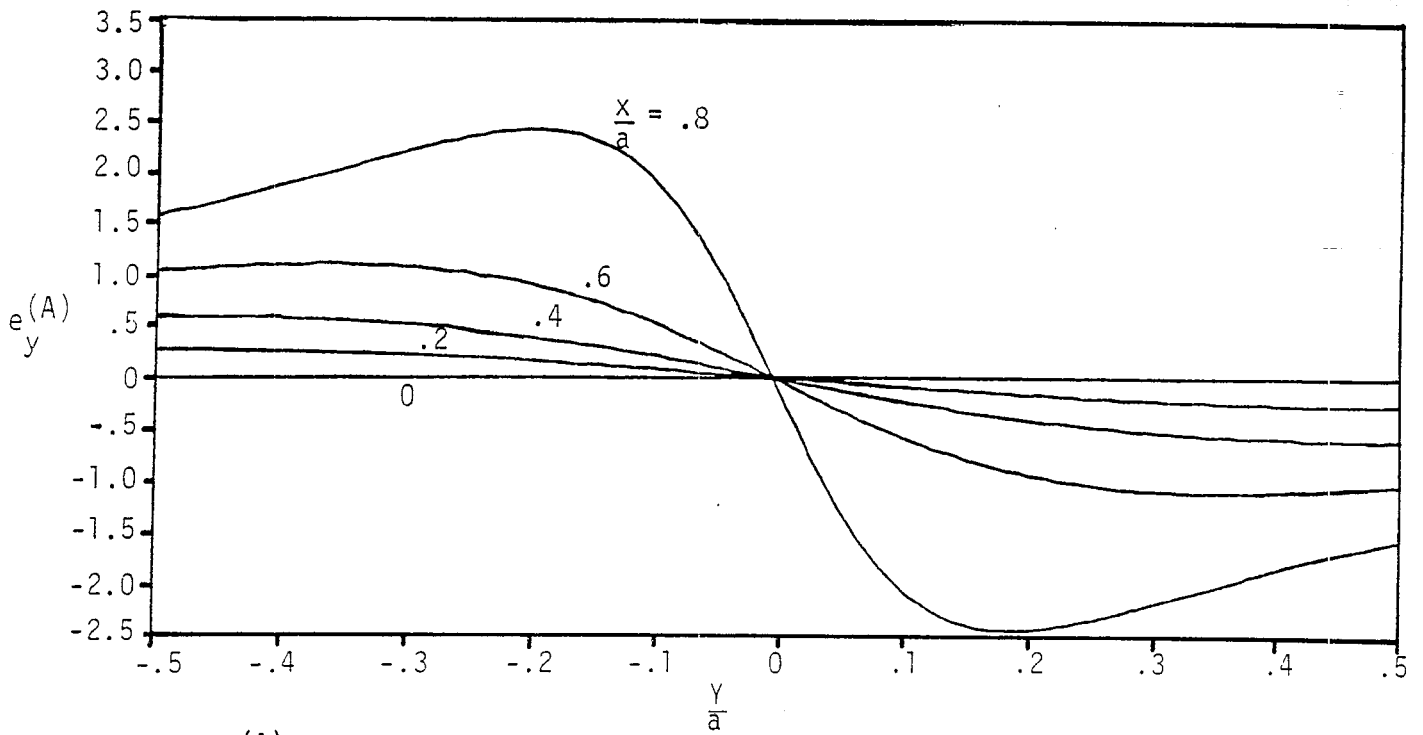
B. $e_y^{(A)}$ IN THE Y DIRECTION WITH $\frac{x}{a}$ AS A PARAMETER

FIGURE 11. NORMALIZED ELECTRIC FIELD FOR $\frac{b}{a} \to \infty$
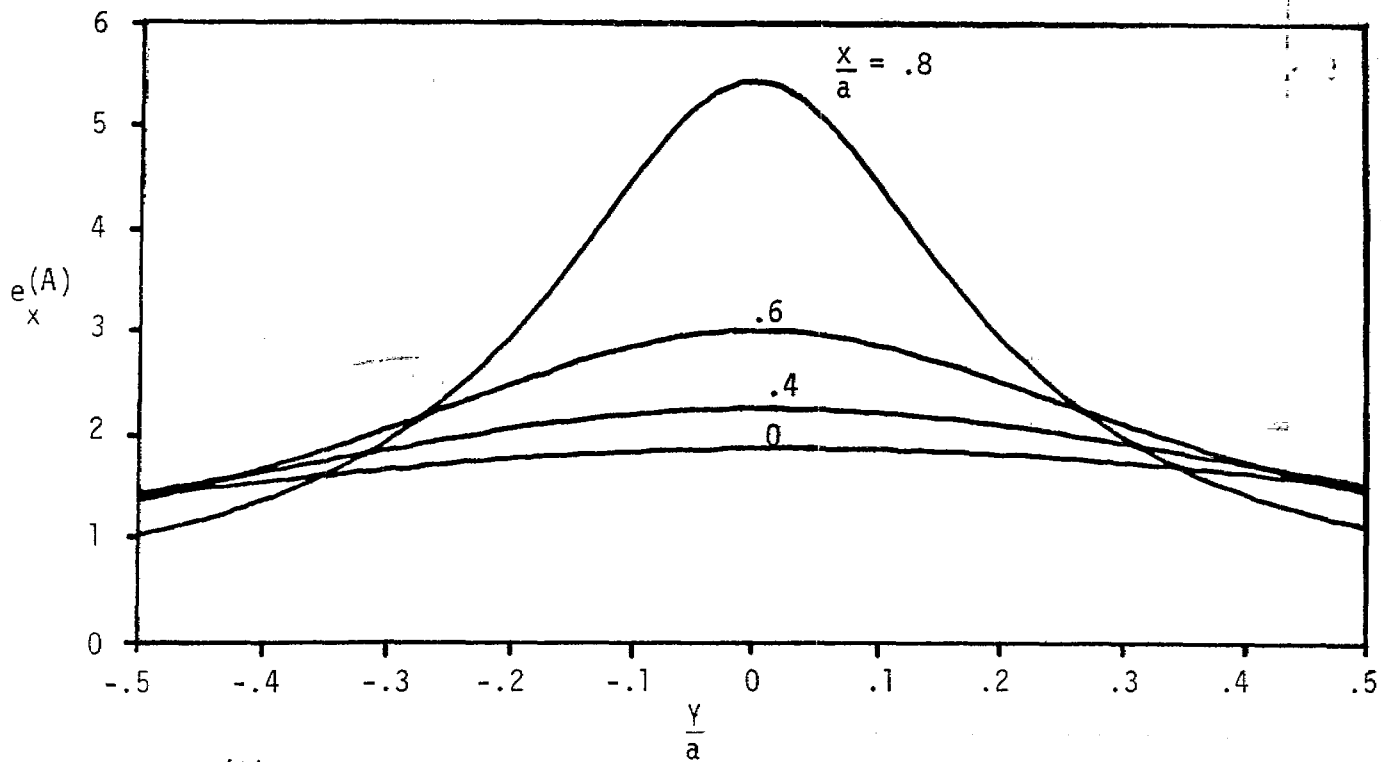
A. $e_x^{(A)}$ IN THE X DIRECTION WITH $\frac{x}{a}$ AS A PARAMETER
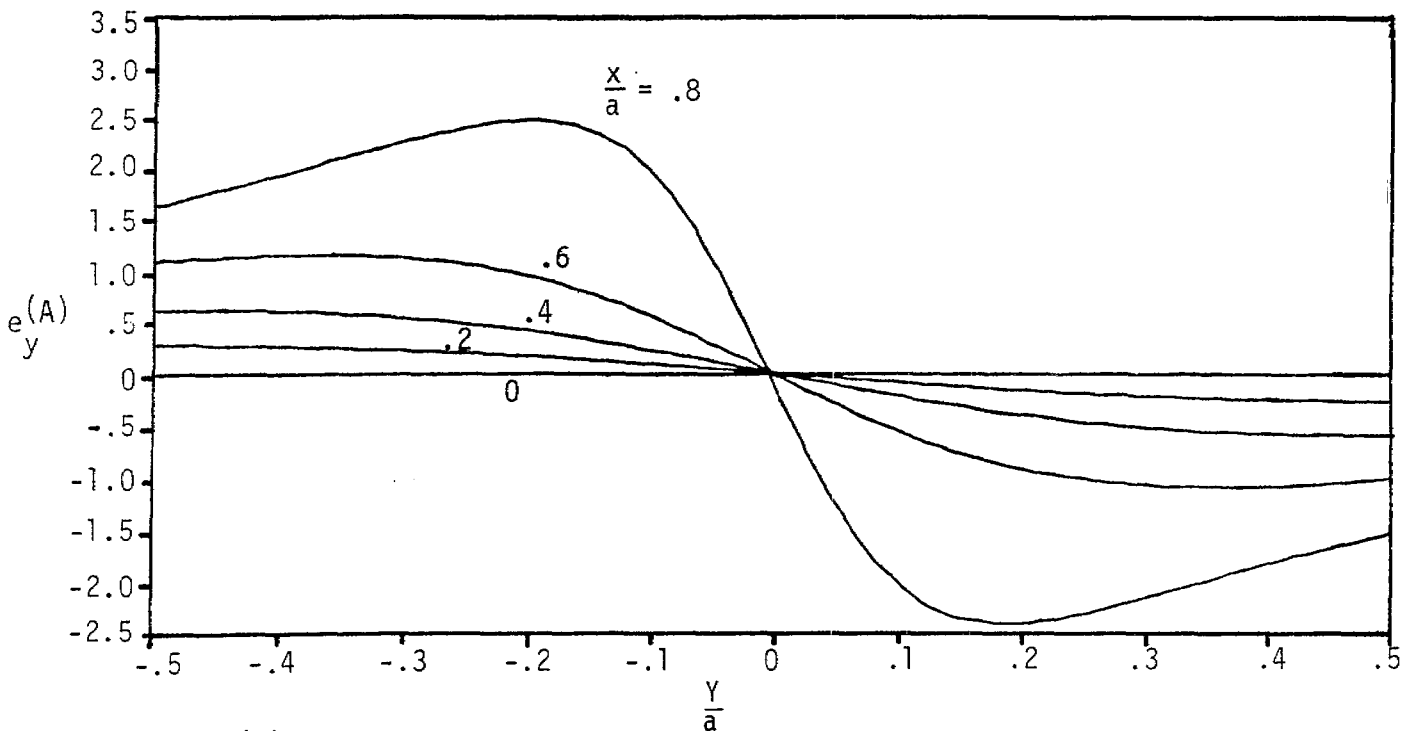
B. $e_y^{(A)}$ IN THE Y DIRECTION WITH $\frac{x}{a}$ AS A PARAMETER

FIGURE 12. NORMALIZED ELECTRIC FIELD FOR $\frac{b}{a} = 2$
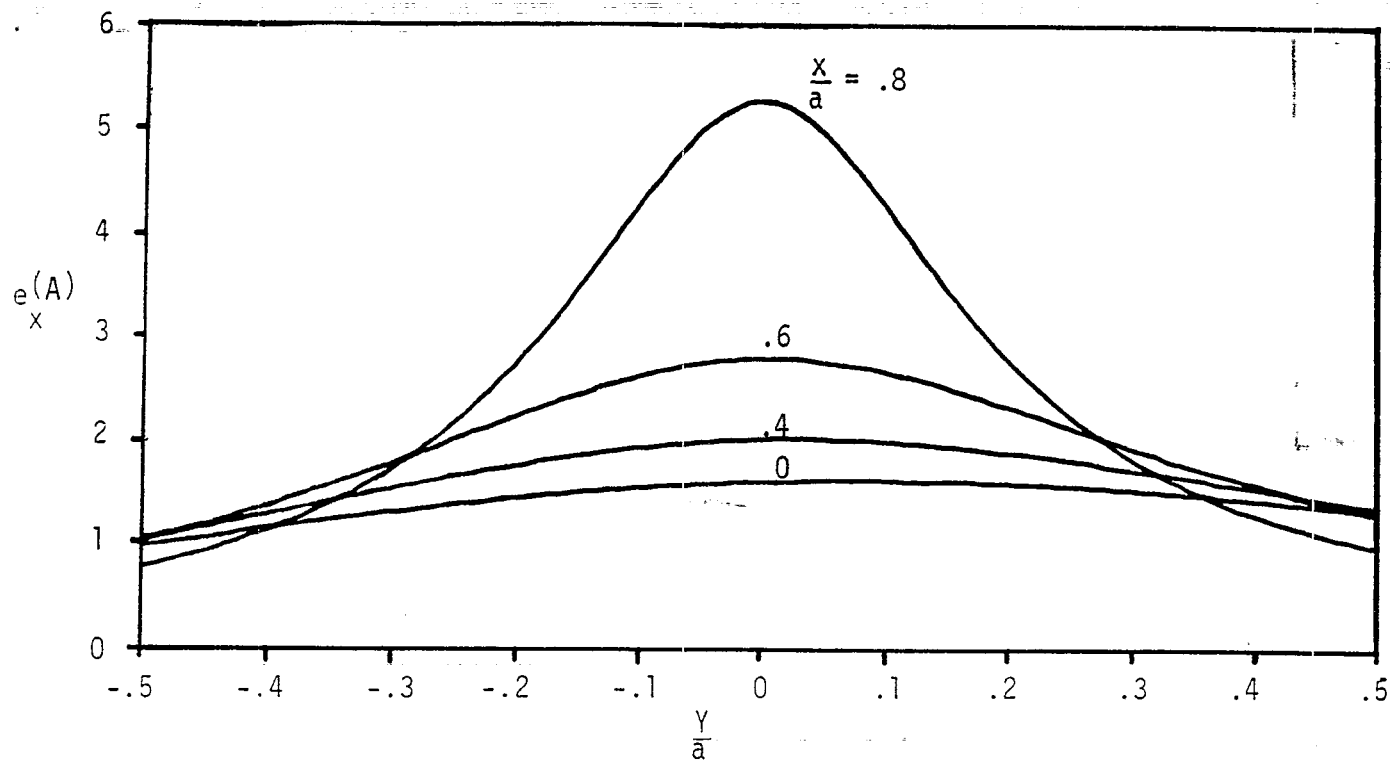
A. $e^{(A)}$ IN THE X DIRECTION WITH $\frac{X}{a}$ AS A PARAMETER
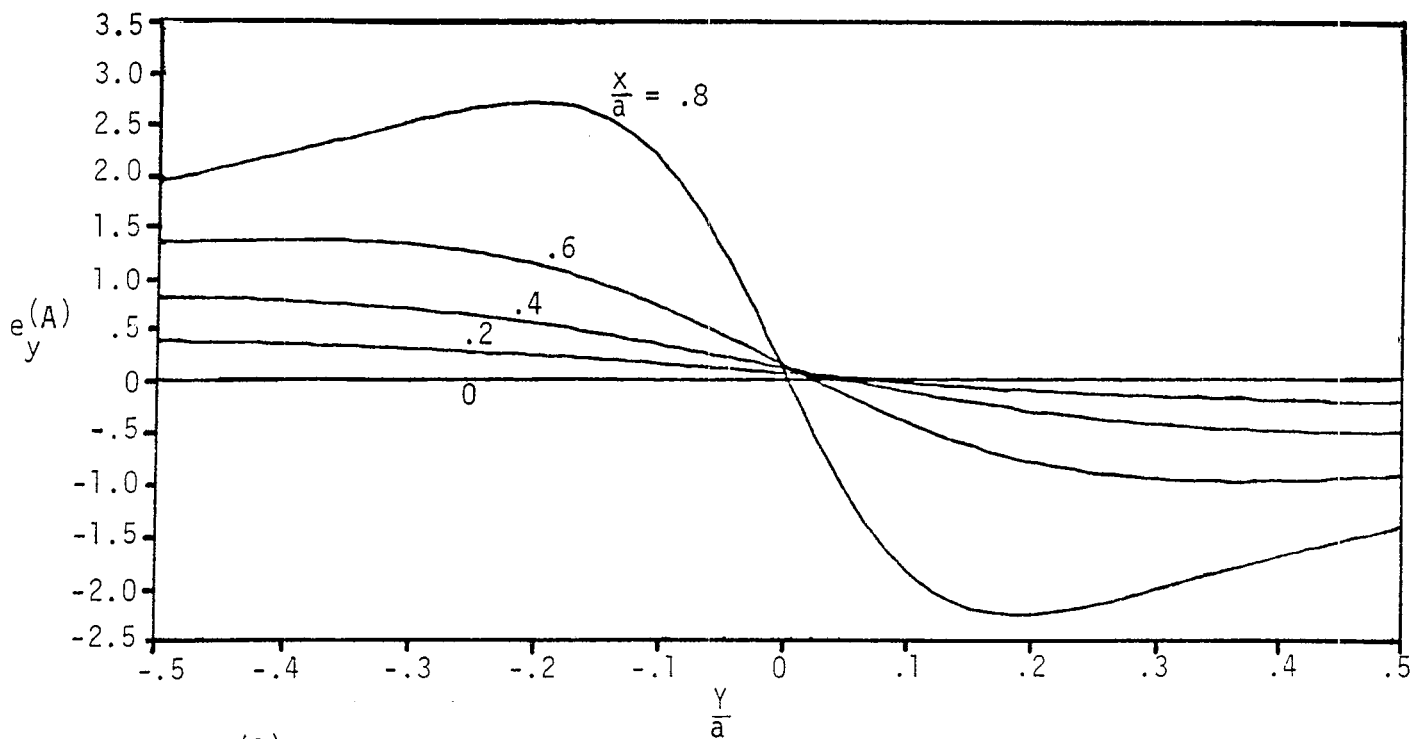
B. $e^{(A)}$ IN THE Y DIRECTION WITH $\frac{X}{a}$ AS A PARAMETER

FIGURE 13. NORMALIZED ELECTRIC FIELD FOR $\frac{b}{a} = 1$
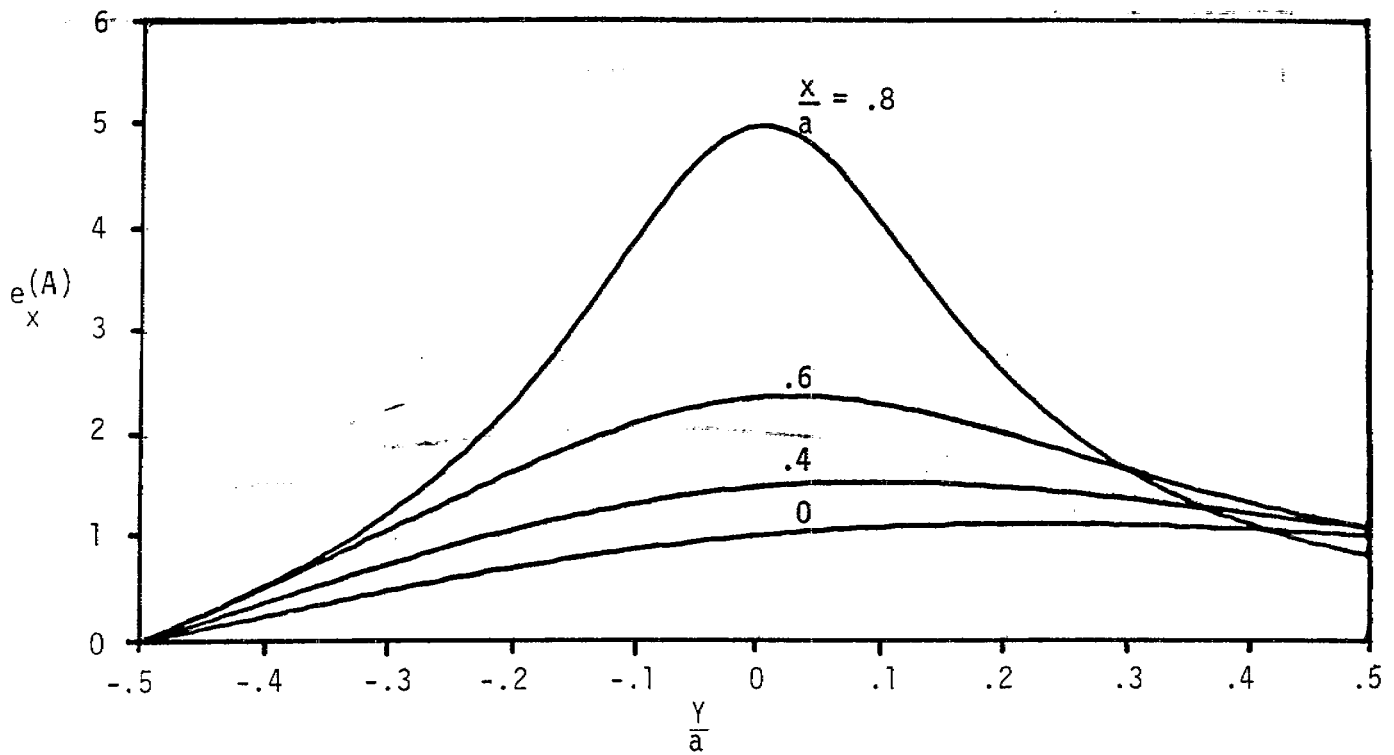
31

A. $e^{(A)}$ IN THE X DIRECTION WITH $\frac{X}{a}$ AS A PARAMETER
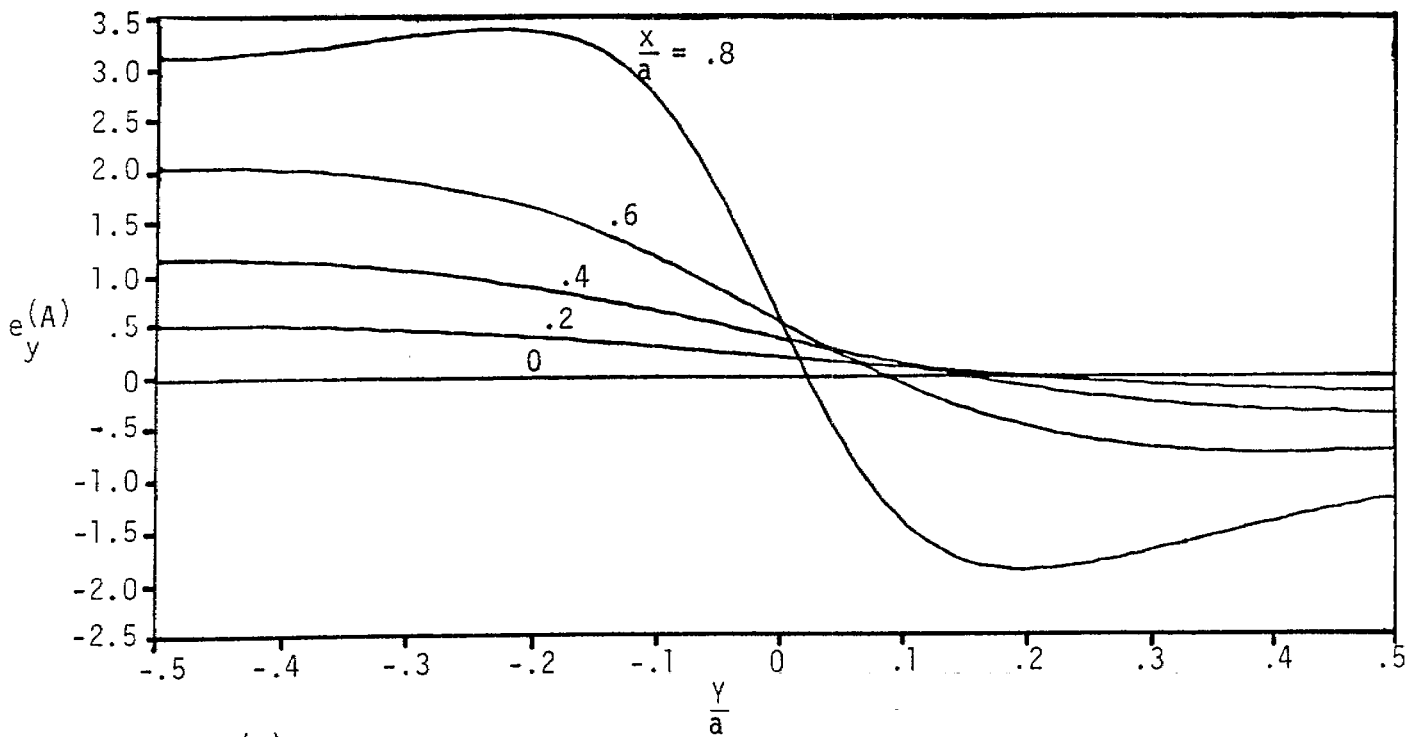
B. $e^{(A)}$ IN THE Y DIRECTION WITH $\frac{X}{a}$ AS A PARAMETER

FIGURE 14.   NORMALIZED ELECTRIC FIELD FOR $\frac{b}{a} = .5$
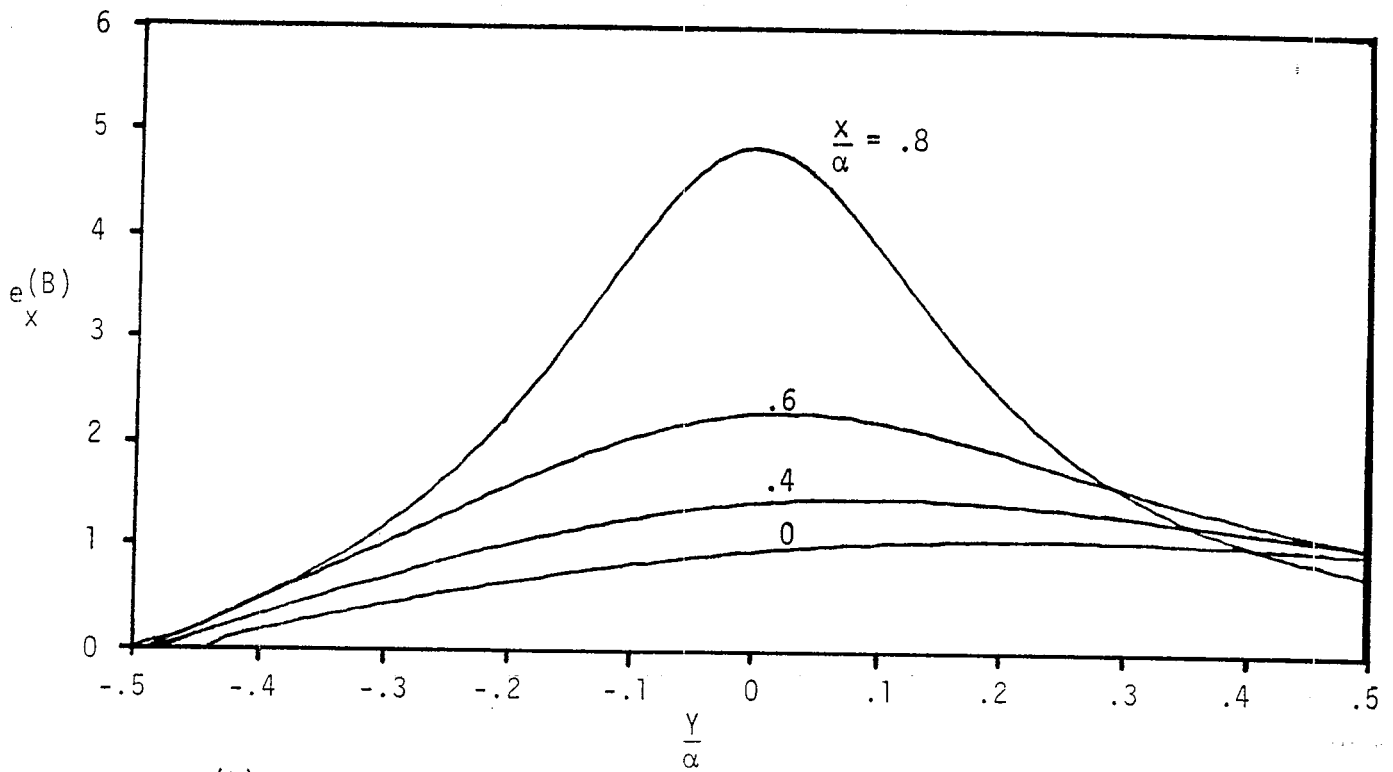
A. $e^{(B)}$ IN THE X DIRECTION WITH $\frac{X}{\alpha}$ AS A PARAMETER
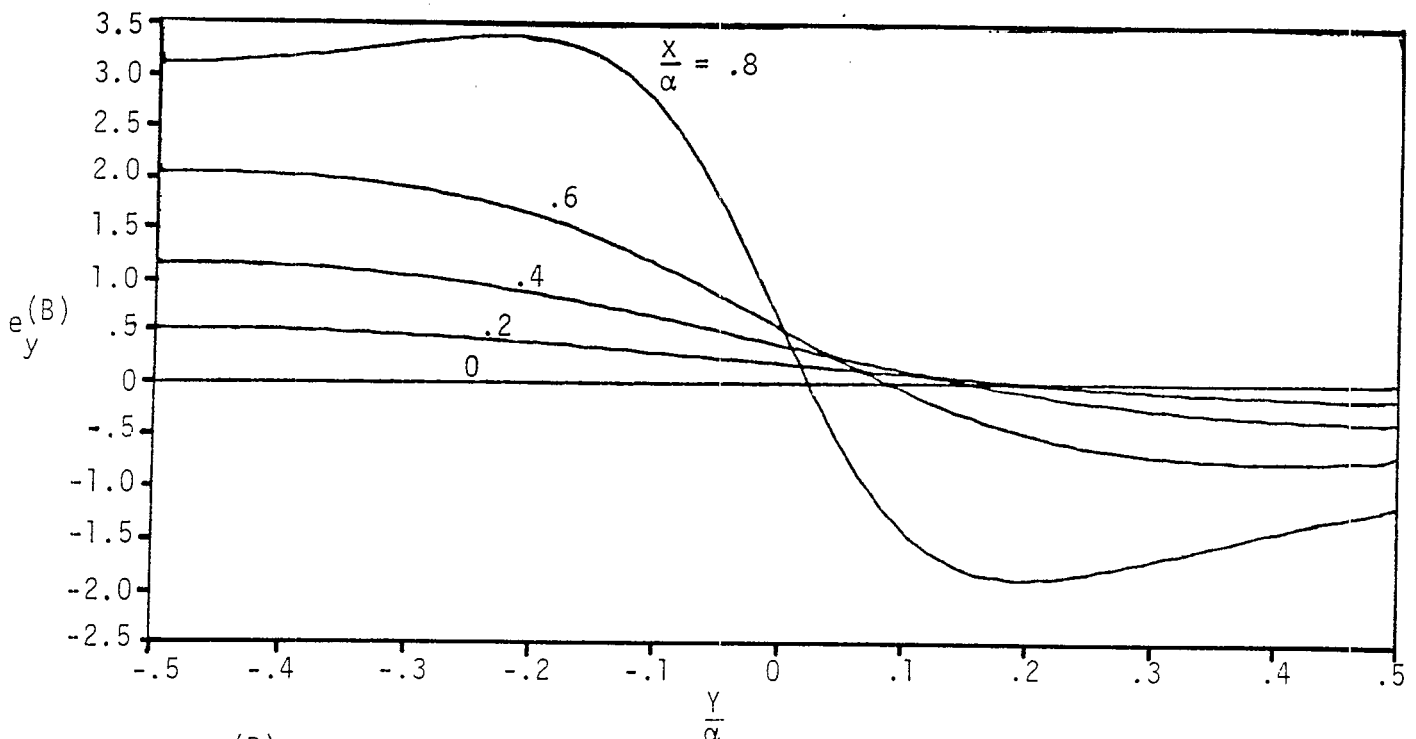
B. $e^{(B)}$ IN THE Y DIRECTION WITH $\frac{X}{\alpha}$ AS A PARAMETER

FIGURE 15. NORMALIZED ELECTRIC FIELD FOR $\frac{X}{\alpha} = .05$, $\frac{\beta}{\alpha} = .5$
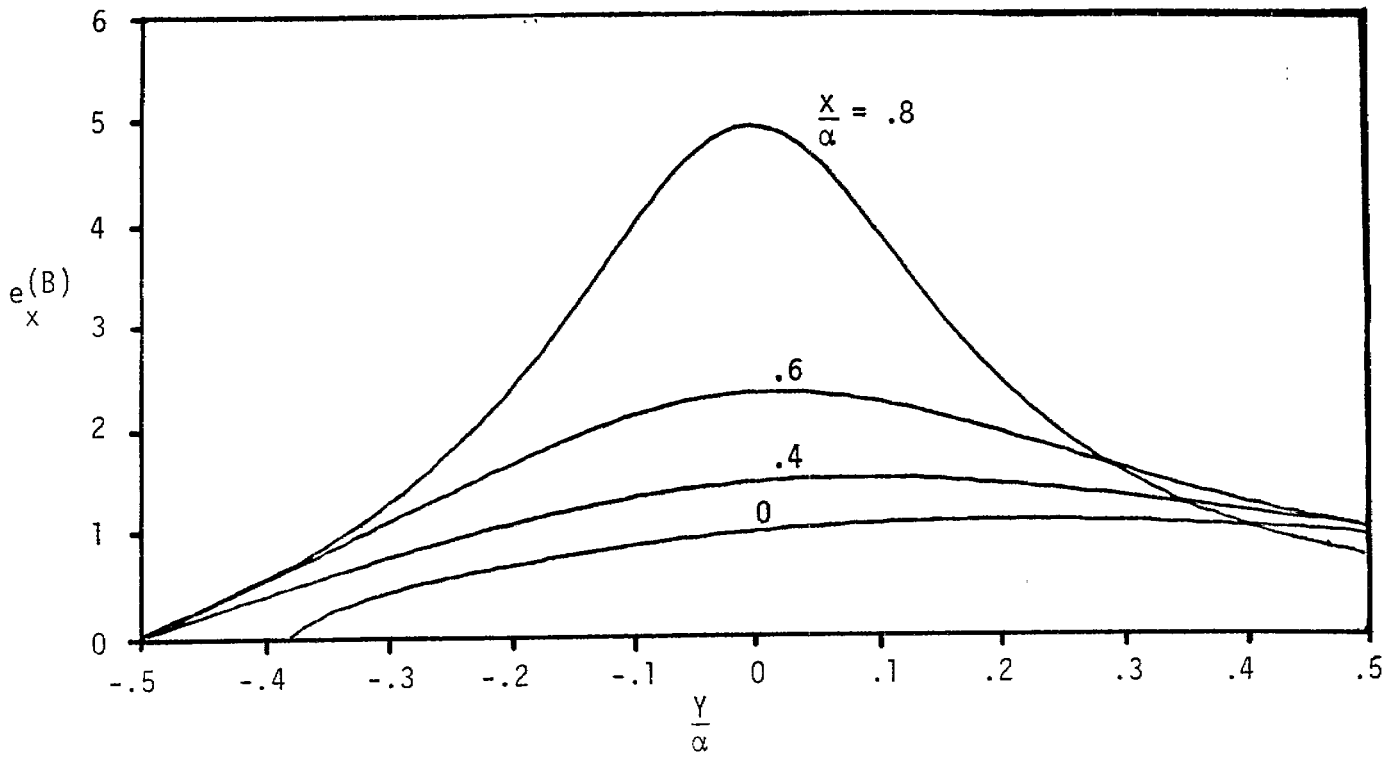
33

A. $e^{(B)}$ IN THE X DIRECTION WITH $\frac{X}{\alpha}$ AS A PARAMETER
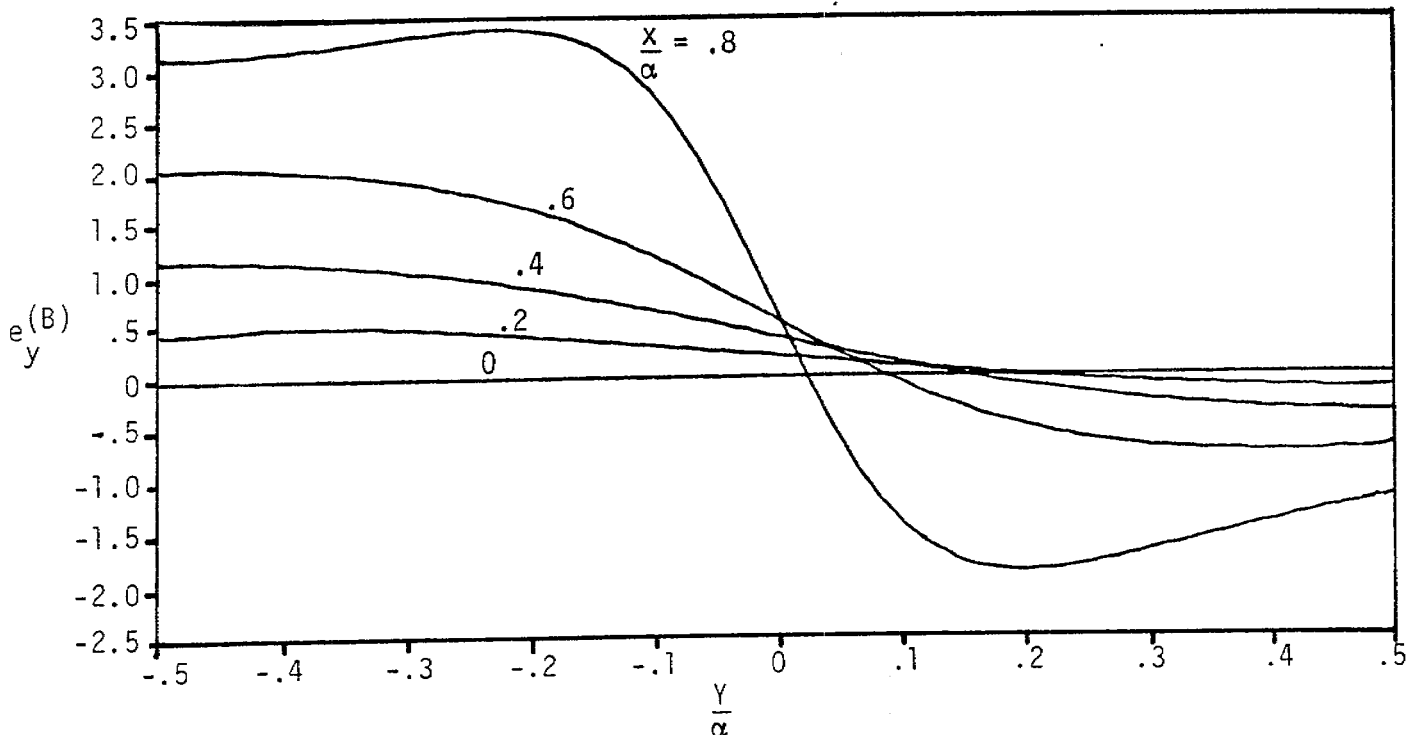
B. $e^{(B)}$ IN THE Y DIRECTION WITH $\frac{X}{\alpha}$ AS A PARAMETER

FIGURE 16.   NORMALIZED ELECTRIC FIELD FOR $\frac{X}{\alpha} = .125$, $\frac{\beta}{\alpha} = .5$
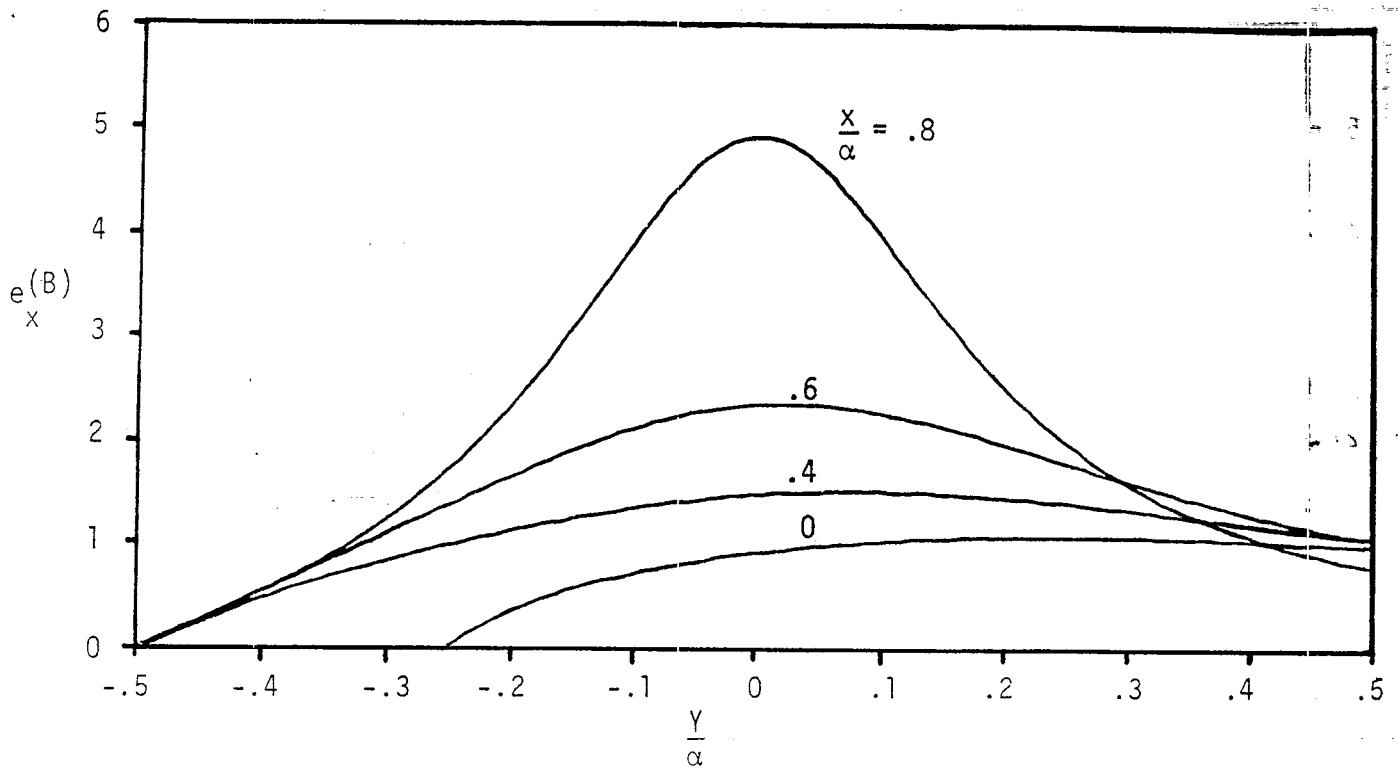
34

A. $e^{(B)}$ IN THE X DIRECTION WITH $\frac{x}{\alpha}$ AS A PARAMETER
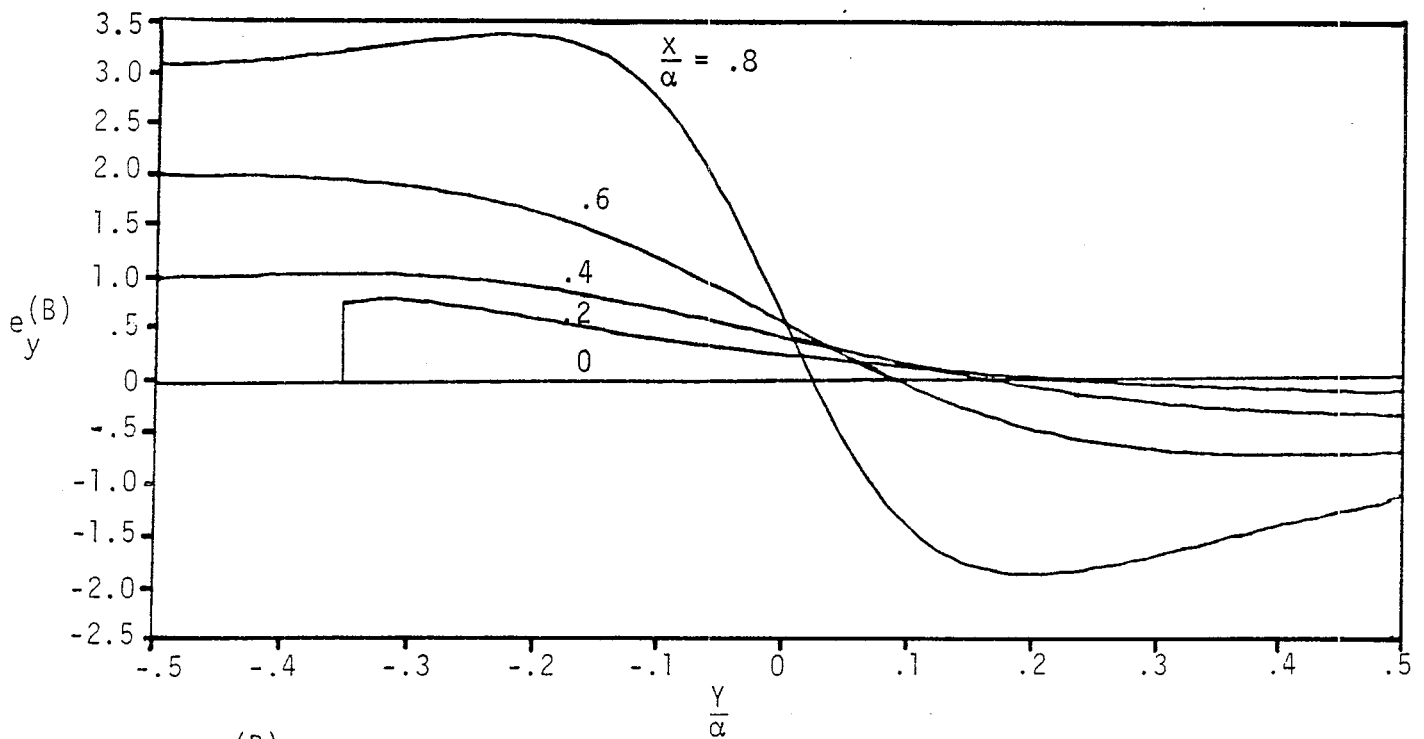
B. $e^{(B)}$ IN THE Y DIRECTION WITH $\frac{x}{\alpha}$ AS A PARAMETER

FIGURE 17. NORMALIZED ELECTRIC FIELD FOR $\frac{x}{\alpha} = .25$, $\frac{\beta}{\alpha} = .5$
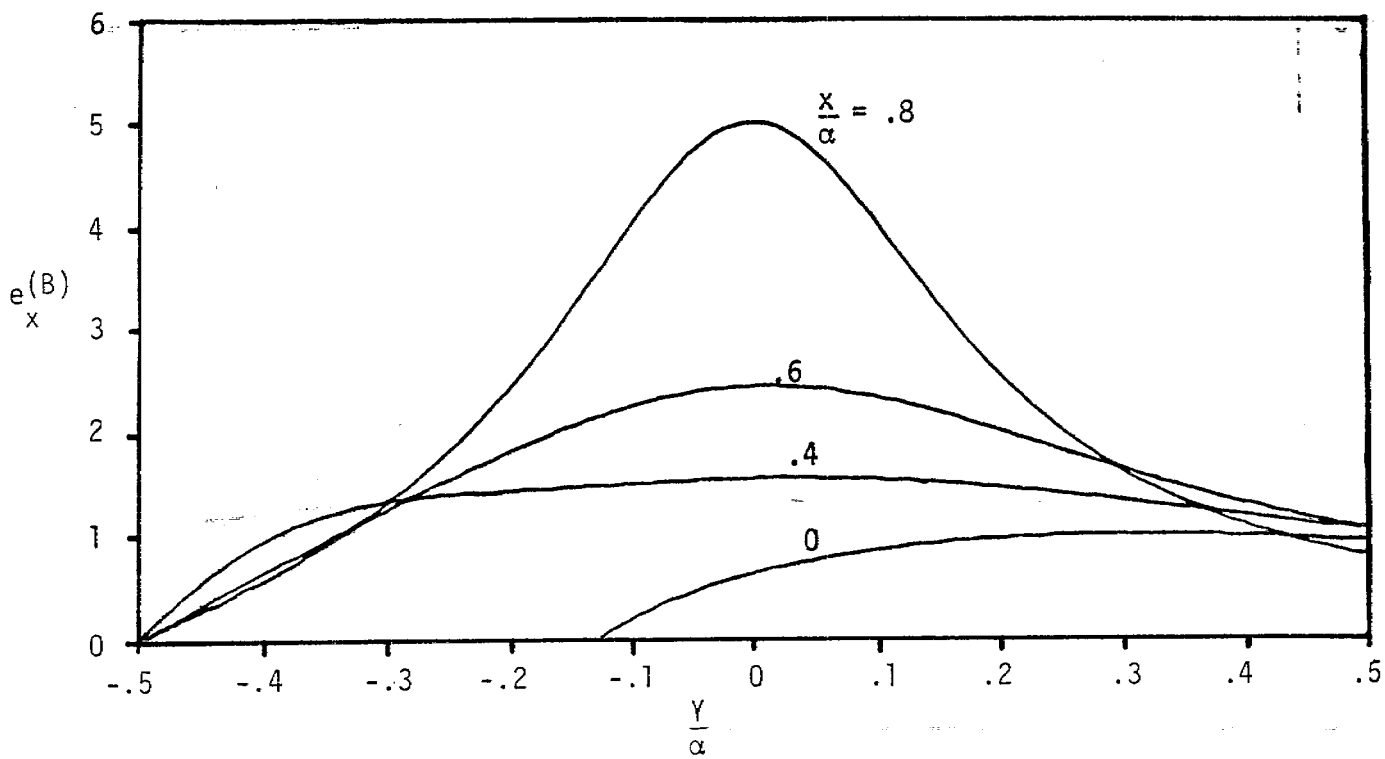
35

A. $e_x^{(B)}$ IN THE X DIRECTION WITH $\frac{X}{\alpha}$ AS A PARAMETER
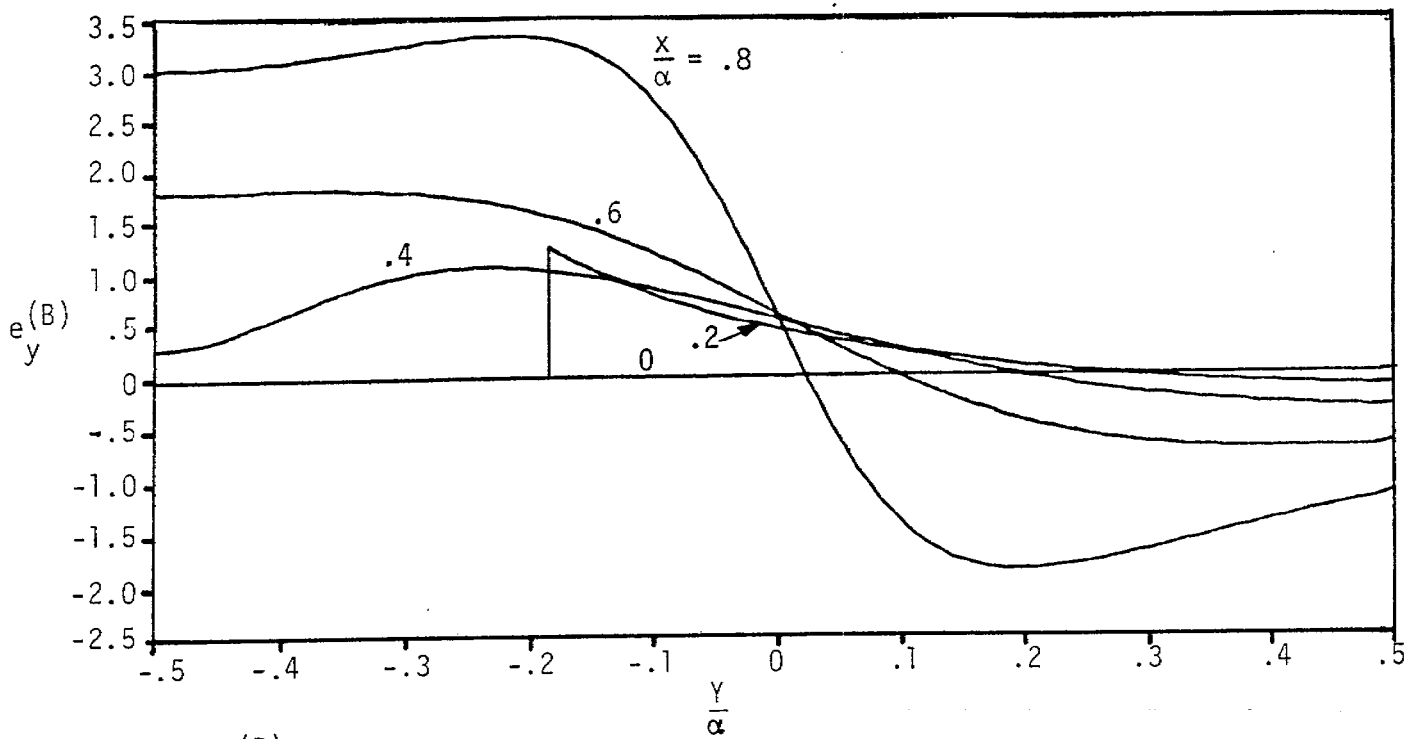
B. $e_y^{(B)}$ IN THE Y DIRECTION WITH $\frac{X}{\alpha}$ AS A PARAMETER

FIGURE 18. NORMALIZED ELECTRIC FIELD FOR $\frac{X}{\alpha} = .375$, $\frac{\beta}{\alpha} = .5$
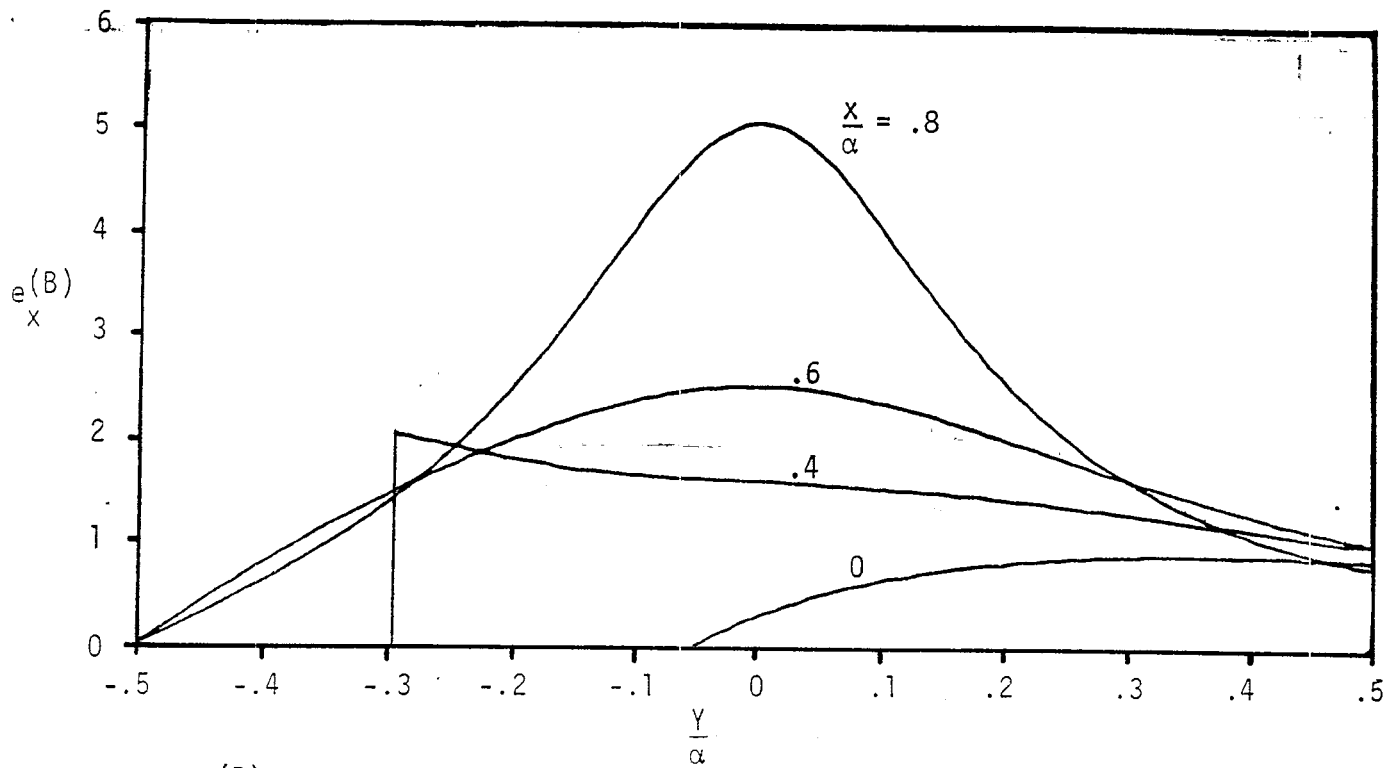
A. $e_x^{(B)}$ IN THE X DIRECTION WITH $\frac{X}{\alpha}$ AS A PARAMETER
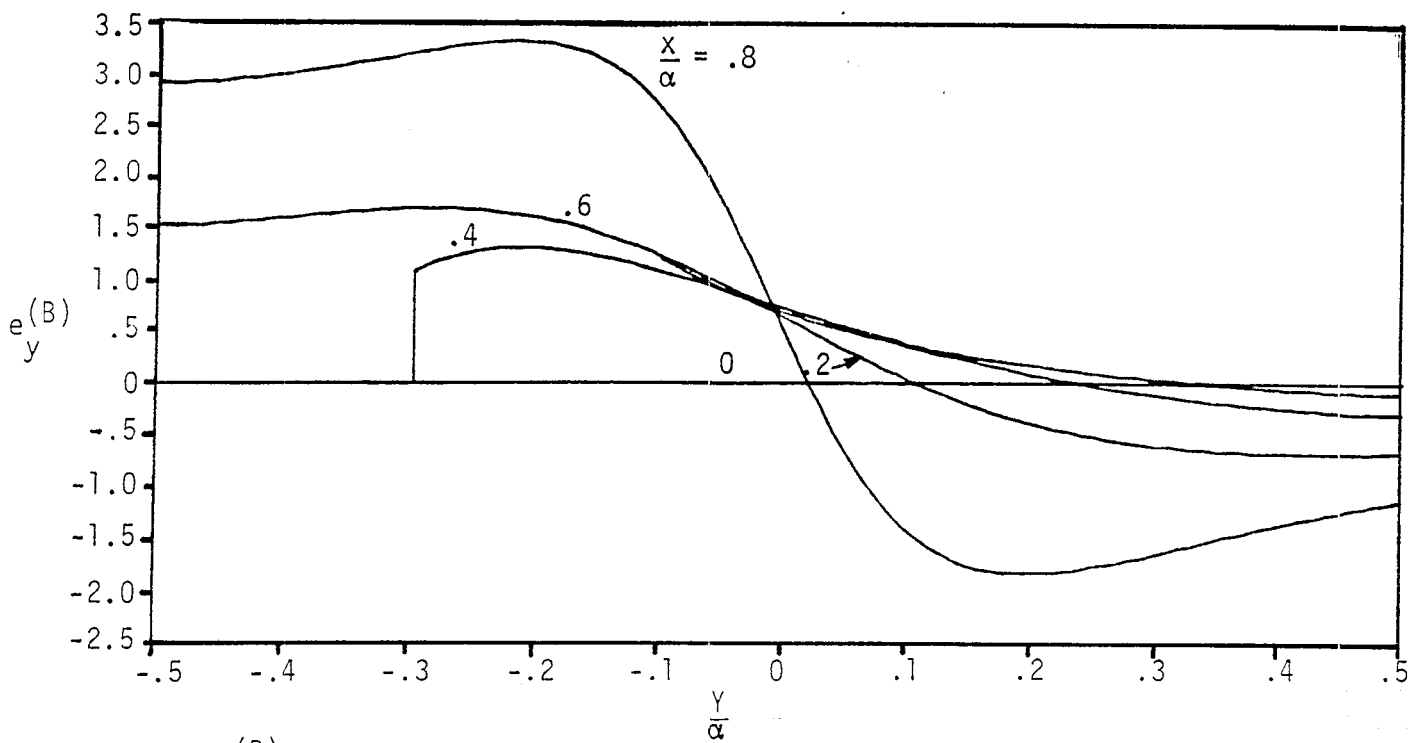
B. $e_y^{(B)}$ IN THE Y DIRECTION WITH $\frac{X}{\alpha}$ AS A PARAMETER

FIGURE 19. NORMALIZED ELECTRIC FIELD FOR $\frac{X}{\alpha} = .45$, $\frac{\beta}{\alpha} = .5$
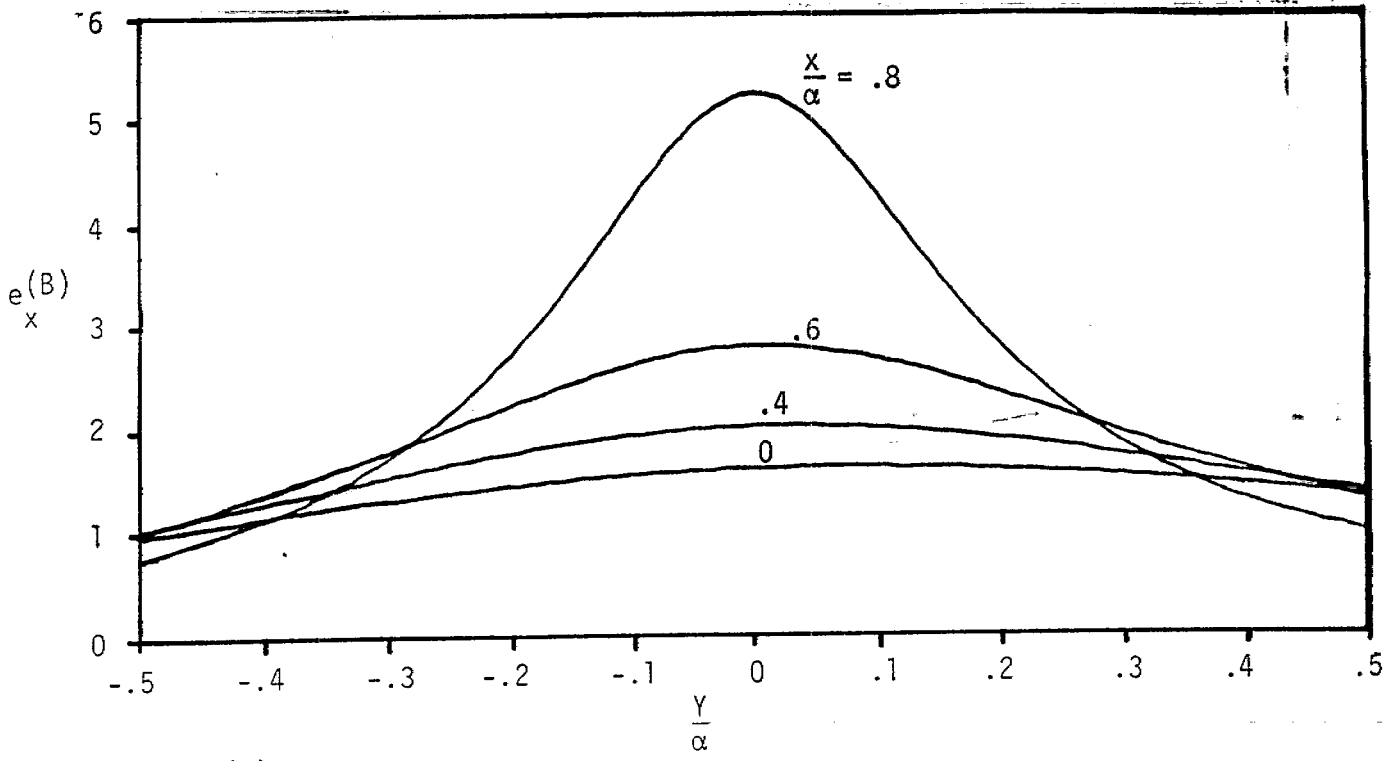
A. $e_x^{(B)}$ IN THE X DIRECTION WITH $\frac{X}{\alpha}$ AS A PARAMETER
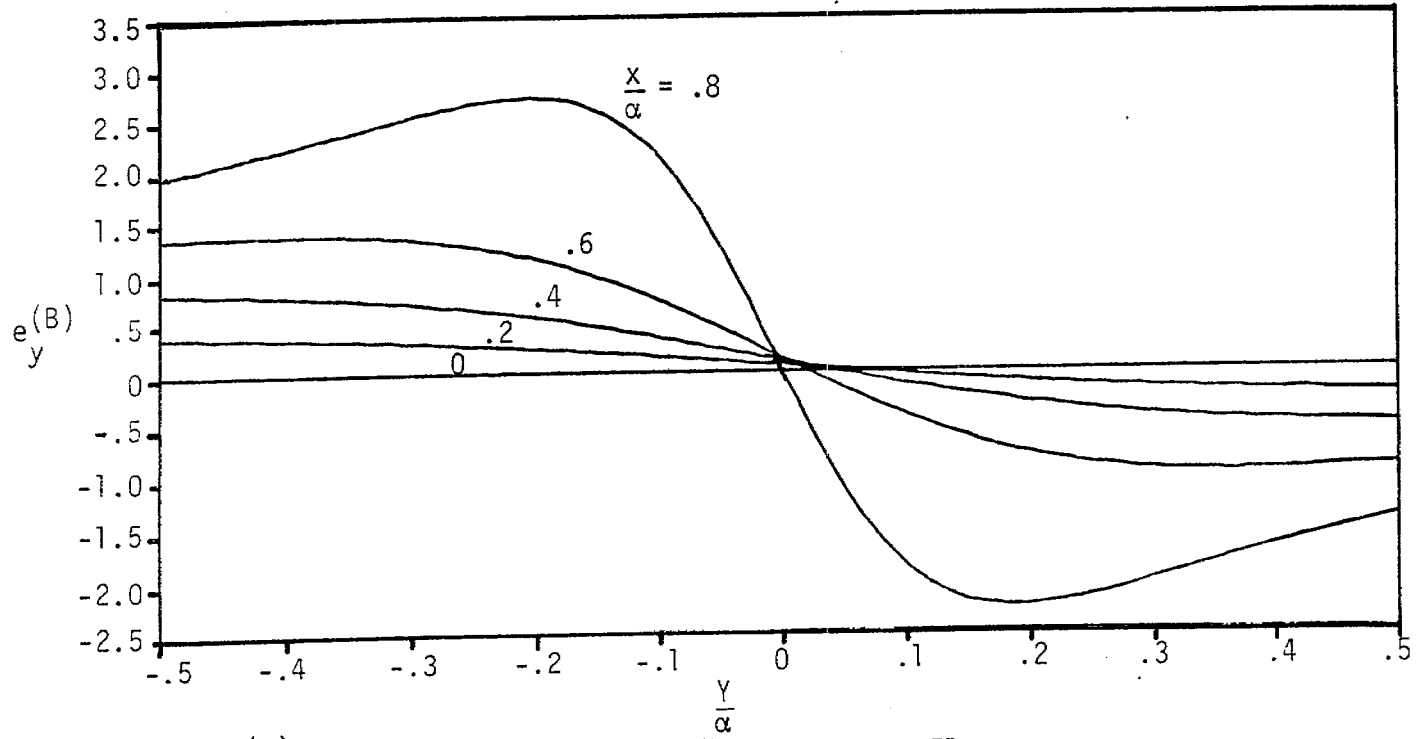
B. $e_y^{(B)}$ IN THE Y DIRECTION WITH $\frac{X}{\alpha}$ AS A PARAMETER

FIGURE 20. NORMALIZED ELECTRIC FIELD FOR $\frac{X}{\alpha} = .1$, $\frac{\beta}{\alpha} = 1$
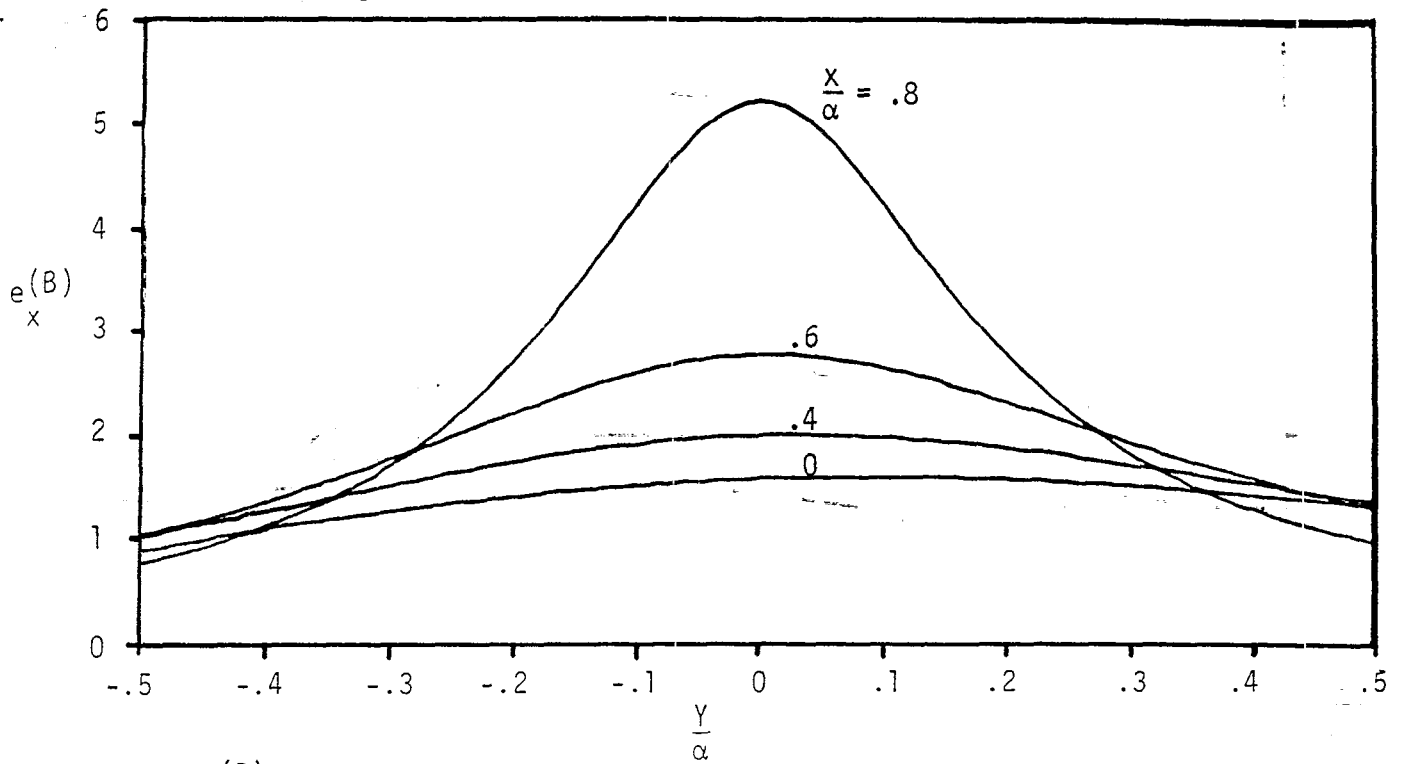
A. $e_x^{(B)}$ IN THE X DIRECTION WITH $\frac{X}{\alpha}$ AS A PARAMETER
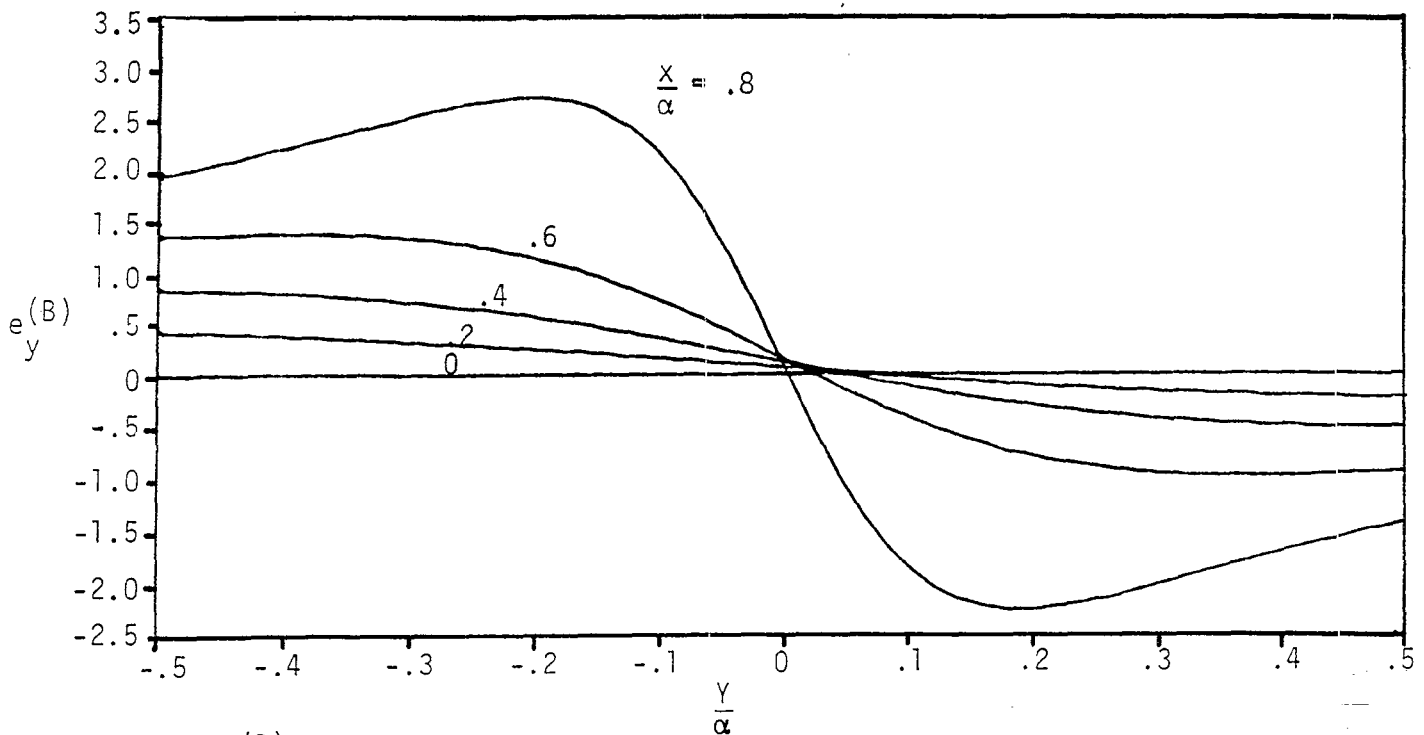
B. $e_y^{(B)}$ IN THE Y DIRECTION WITH $\frac{X}{\alpha}$ AS A PARAMETER

FIGURE 21. NORMALIZED ELECTRIC FIELD FOR $\frac{X}{\alpha} = .25$, $\frac{\beta}{\alpha} = 1$
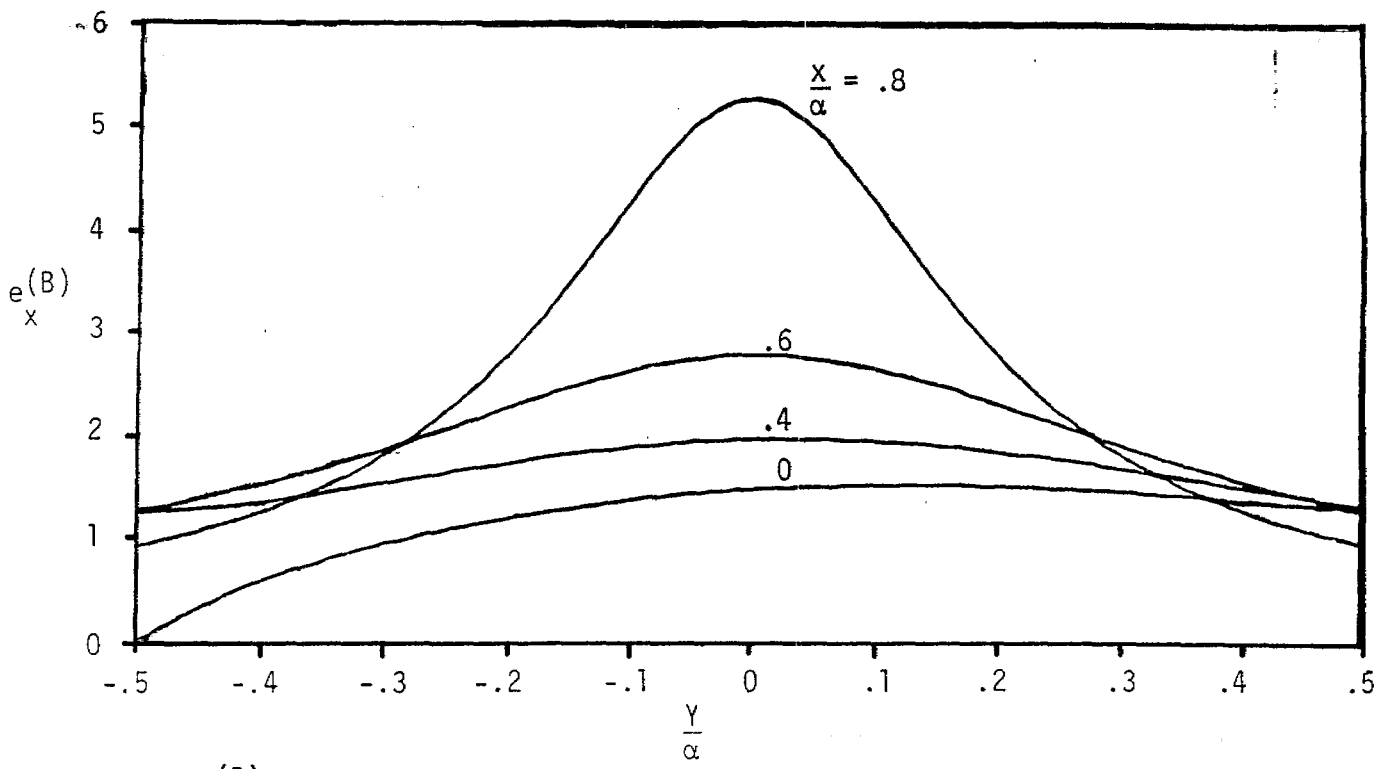
A. $e_x^{(B)}$ IN THE X DIRECTION WITH $\frac{X}{\alpha}$ AS A PARAMETER
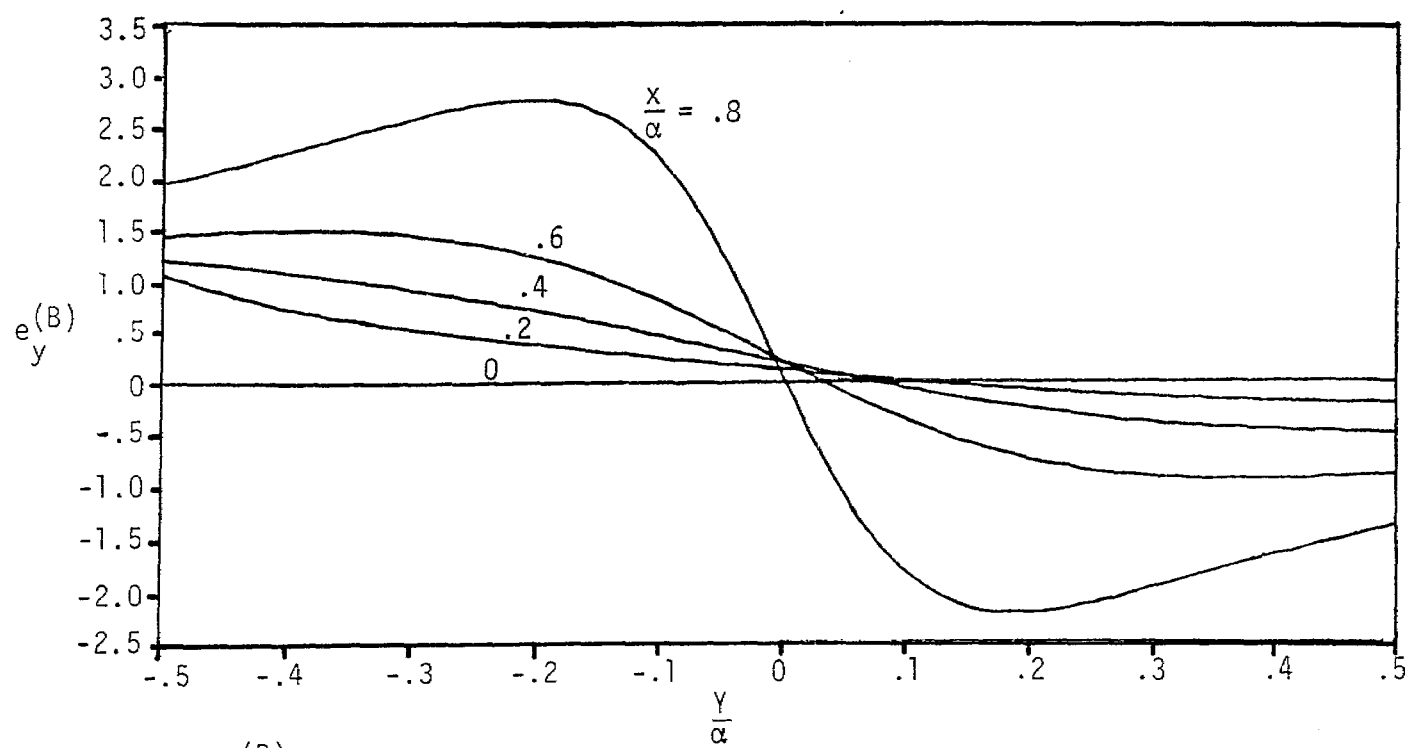
B. $e_y^{(B)}$ IN THE Y DIRECTION WITH $\frac{X}{\alpha}$ AS A PARAMETER

FIGURE 22. NORMALIZED ELECTRIC FIELD FOR $\frac{X}{\alpha} = .5$, $\frac{\beta}{\alpha} = 1$
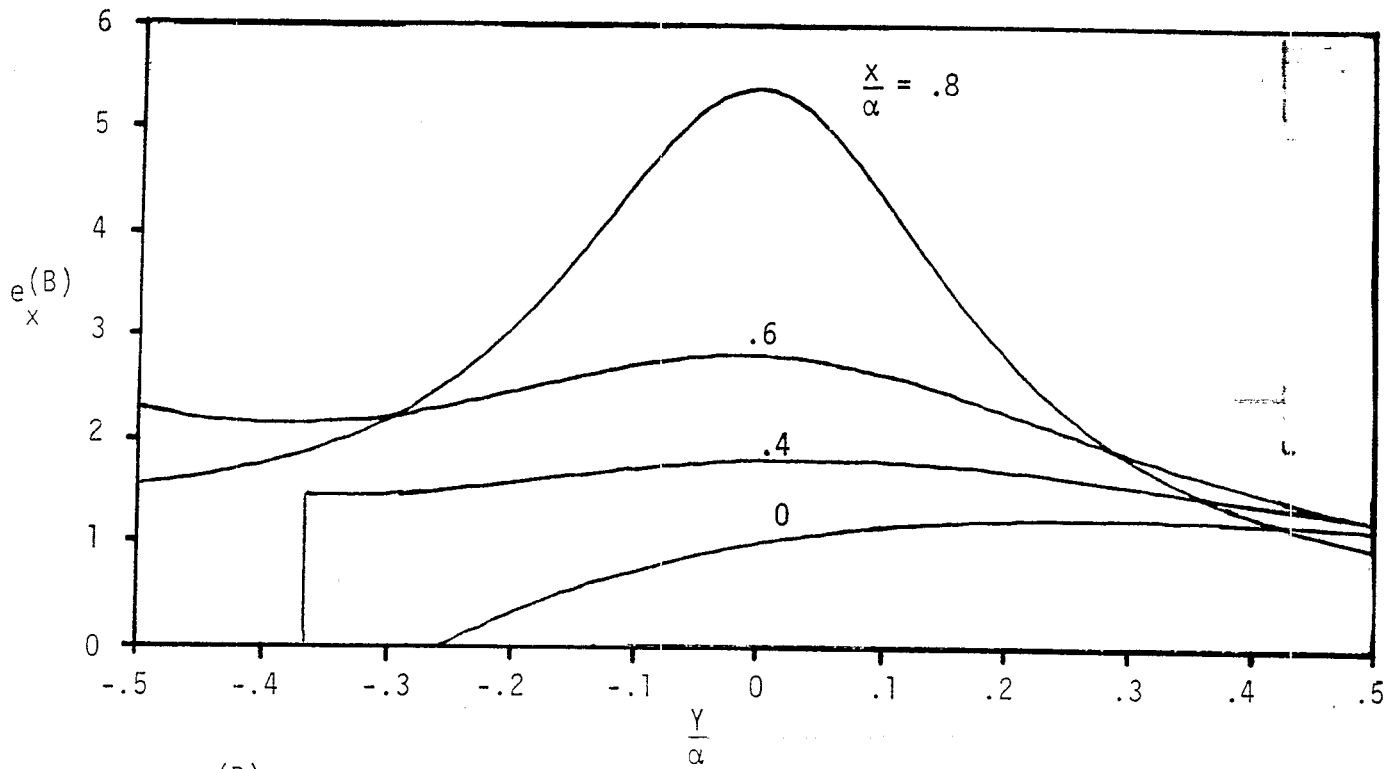
A. $e^{(B)}$ IN THE X DIRECTION WITH $\frac{X}{\alpha}$ AS A PARAMETER
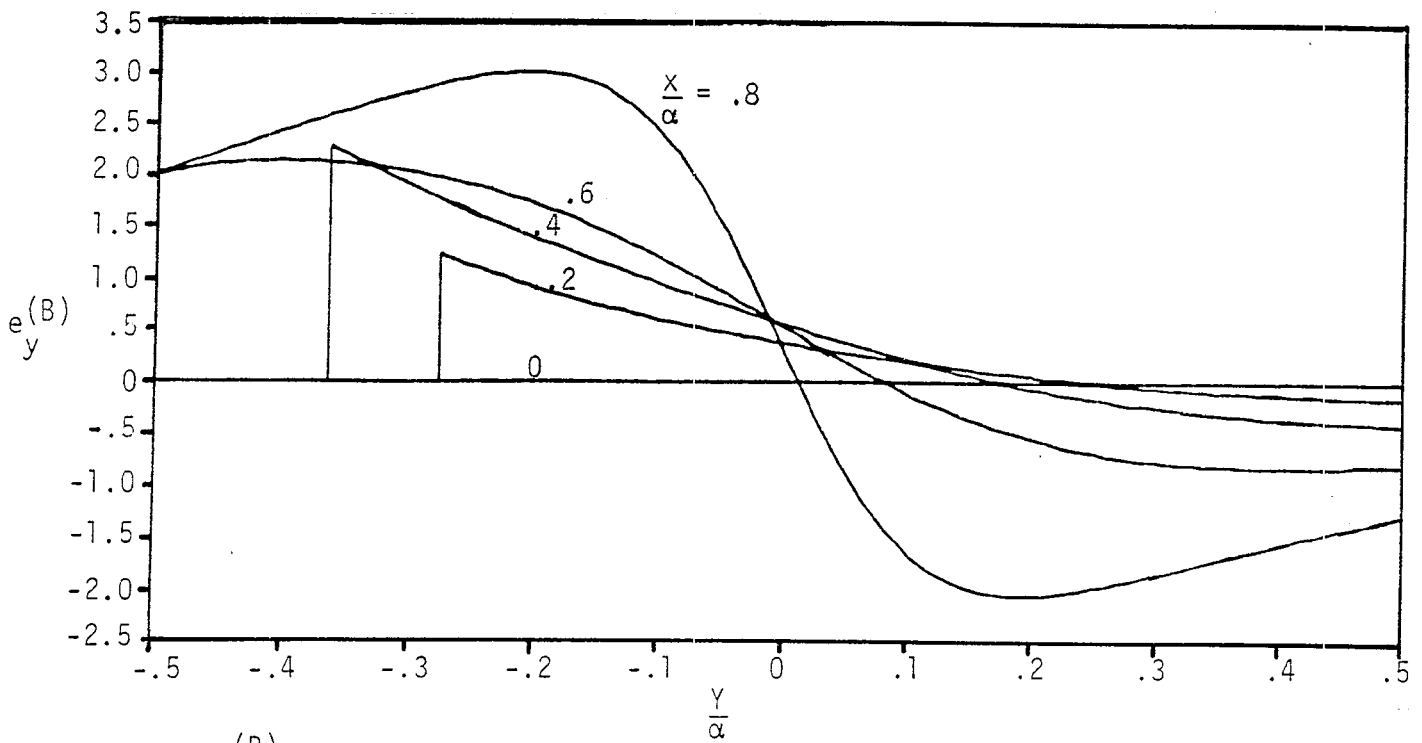
B. $e^{(B)}$ IN THE Y DIRECTION WITH $\frac{X}{\alpha}$ AS A PARAMETER

FIGURE 23. NORMALIZED ELECTRIC FIELD FOR $\frac{X}{\alpha} = .75$, $\frac{\beta}{\alpha} = 1$
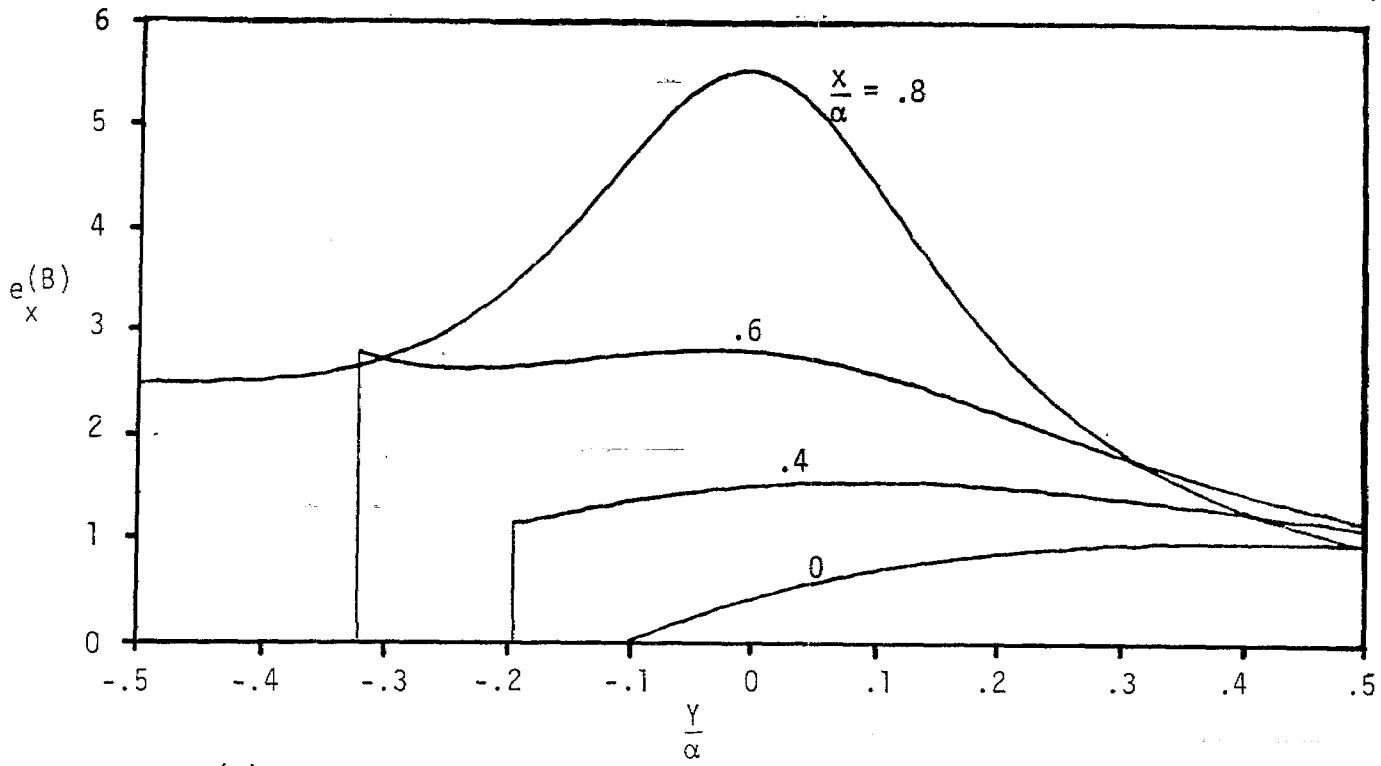
41

A. $e_x^{(B)}$ IN THE X DIRECTION WITH $\frac{X}{\alpha}$ AS A PARAMETER
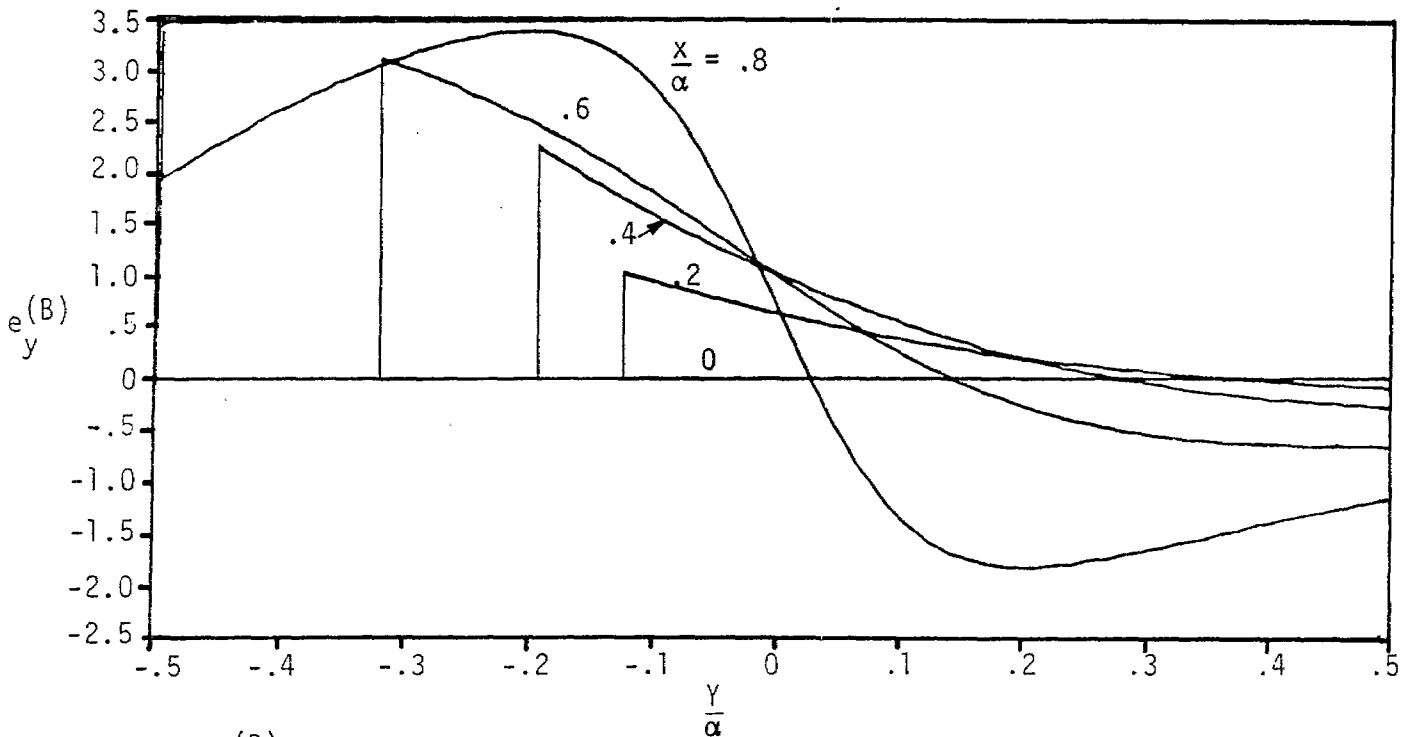
B. $e_y^{(B)}$ IN THE Y DIRECTION WITH $\frac{X}{\alpha}$ AS A PARAMETER

FIGURE 24. NORMALIZED ELECTRIC FIELD FOR $\frac{X}{\alpha} = .9$, $\frac{\beta}{\alpha} = 1$
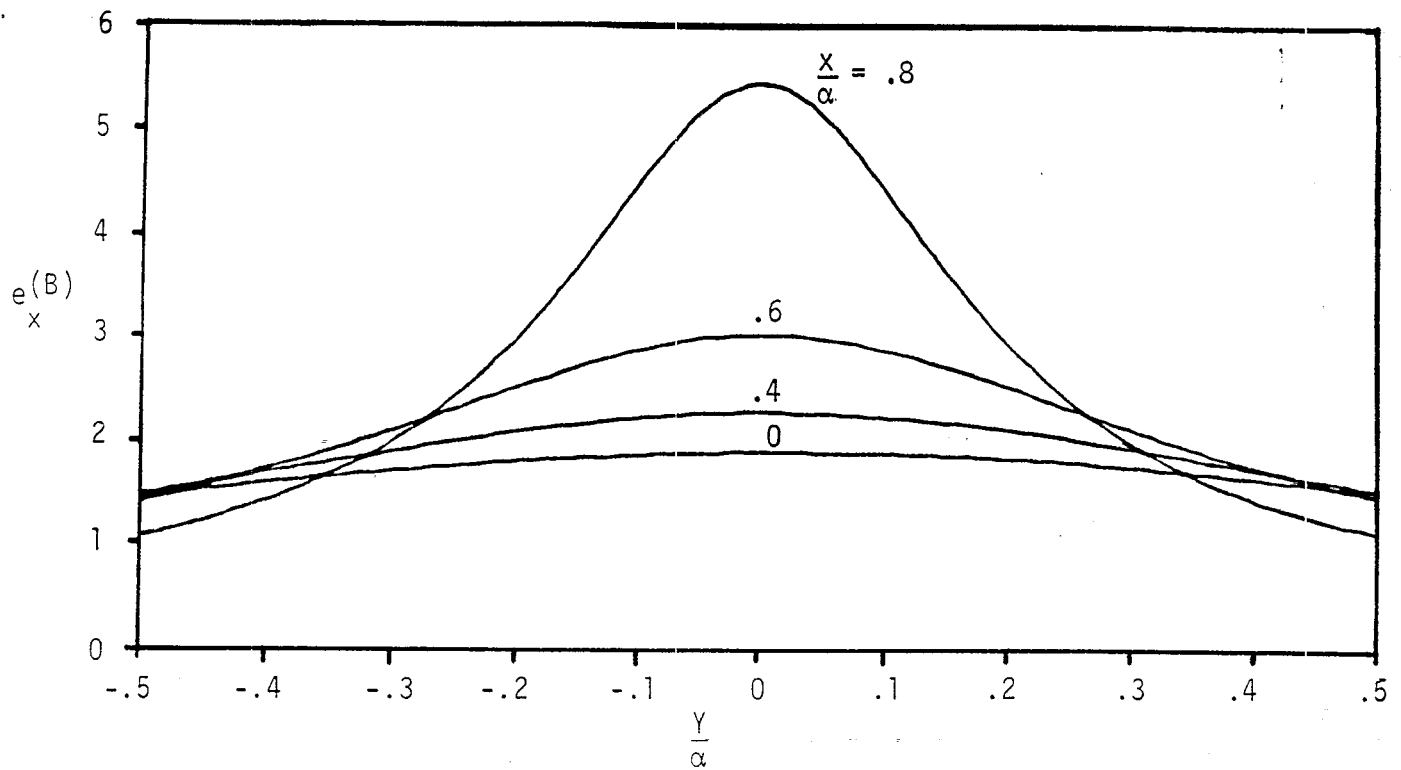
A. $e^{(B)}$ IN THE X DIRECTION WITH $\frac{X}{\alpha}$ AS A PARAMETER
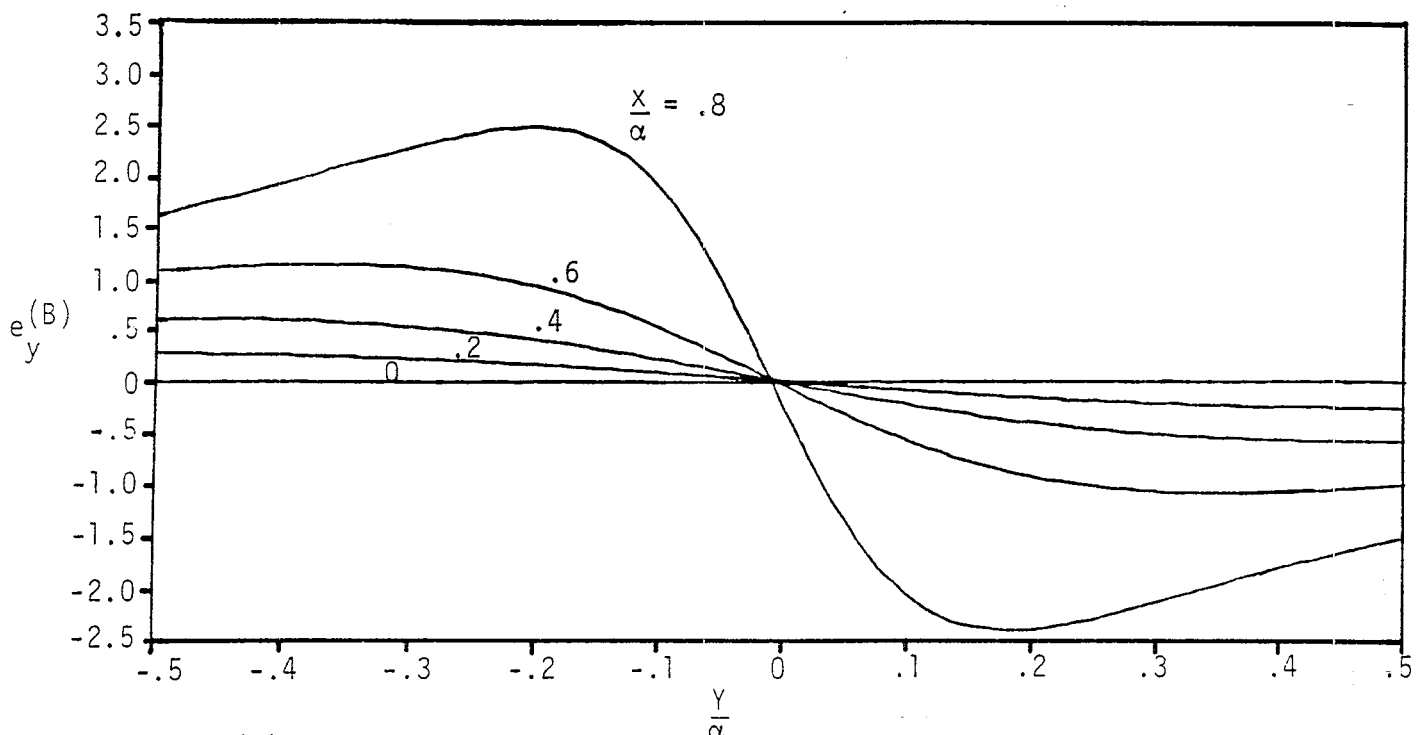
B. $e^{(B)}$ IN THE Y DIRECTION WITH $\frac{X}{\alpha}$ AS A PARAMETER

FIGURE 25. NORMALIZED ELECTRIC FIELD FOR $\frac{X}{\alpha} = .2$, $\frac{\beta}{\alpha} = 2$
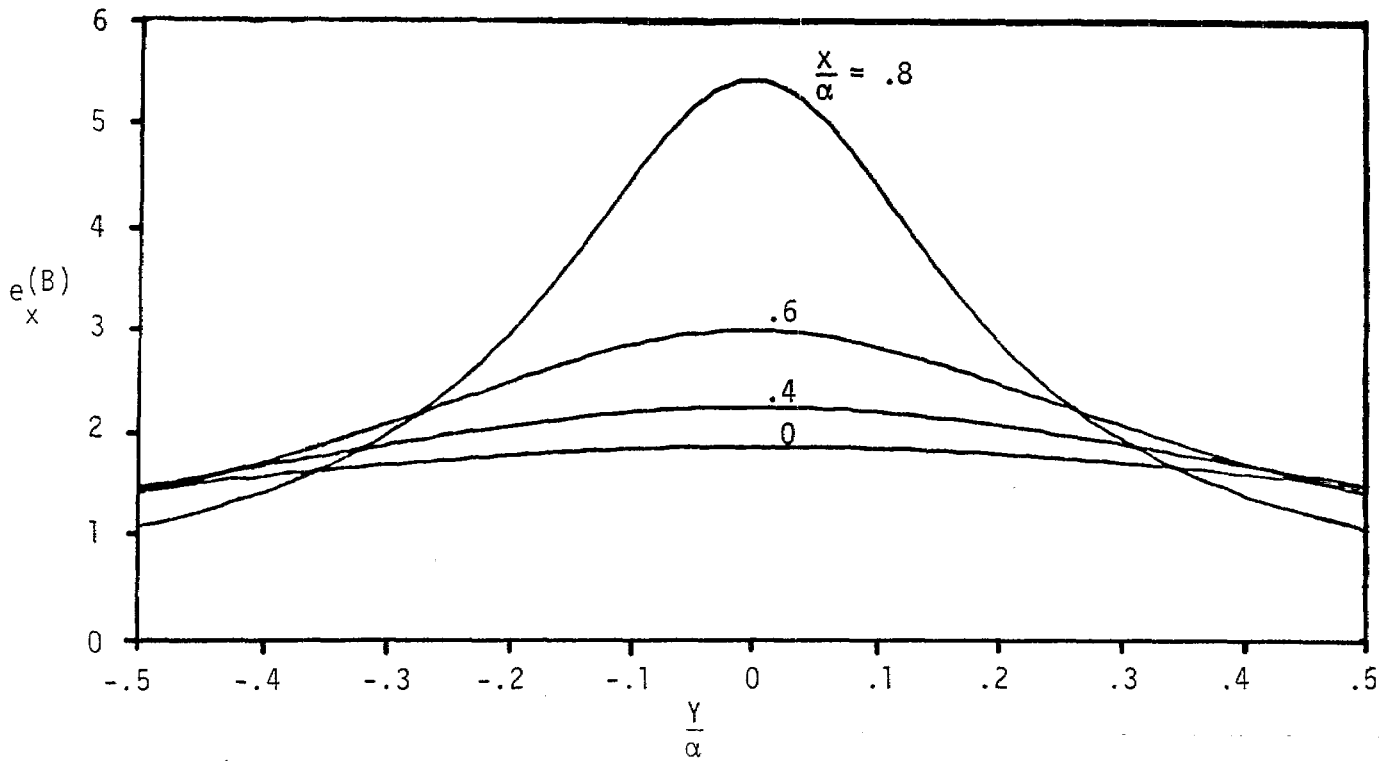
A. $e_x^{(B)}$ IN THE X DIRECTION WITH $\frac{X}{\alpha}$ AS A PARAMETER
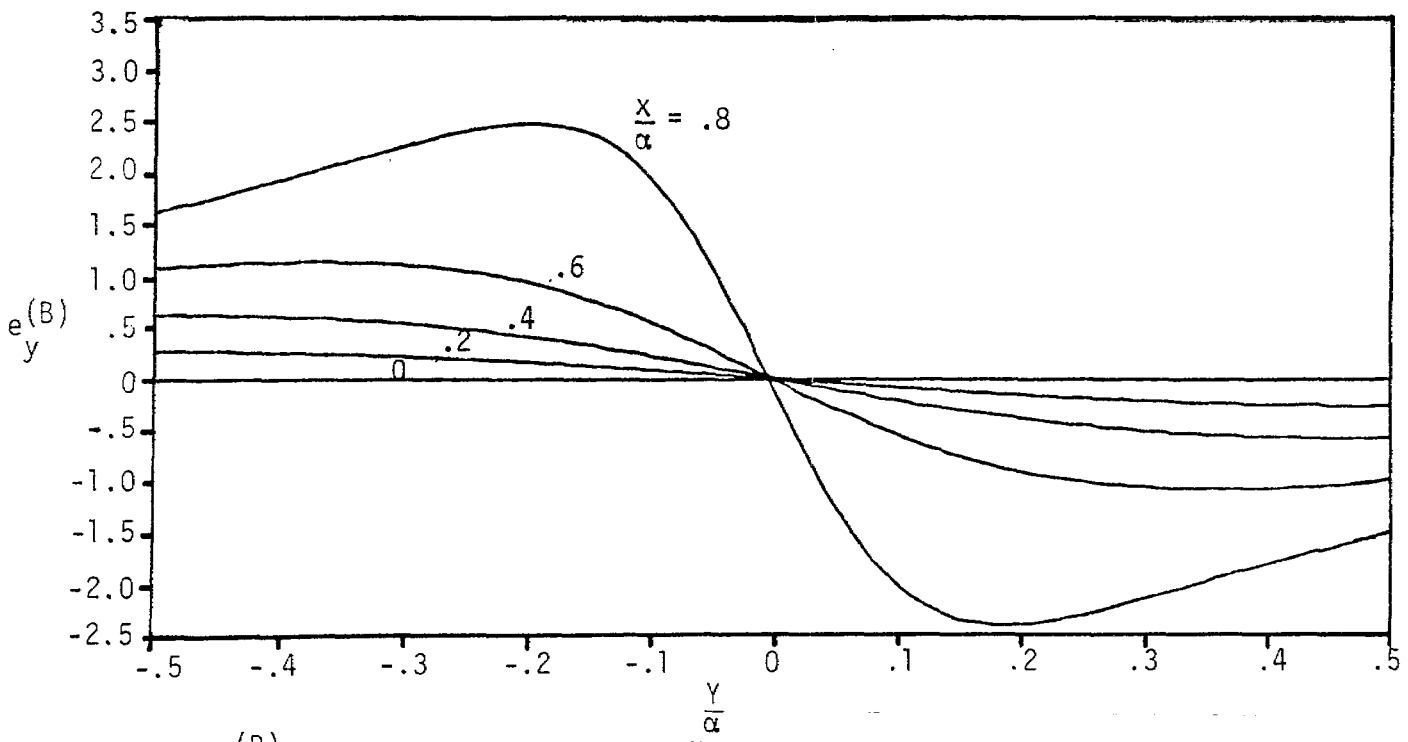
B. $e_y^{(B)}$ IN THE Y DIRECTION WITH $\frac{X}{\alpha}$ AS A PARAMETER

FIGURE 26. NORMALIZED ELECTRIC FIELD FOR $\frac{X}{\alpha} = .5$, $\frac{\beta}{\alpha} = 2$
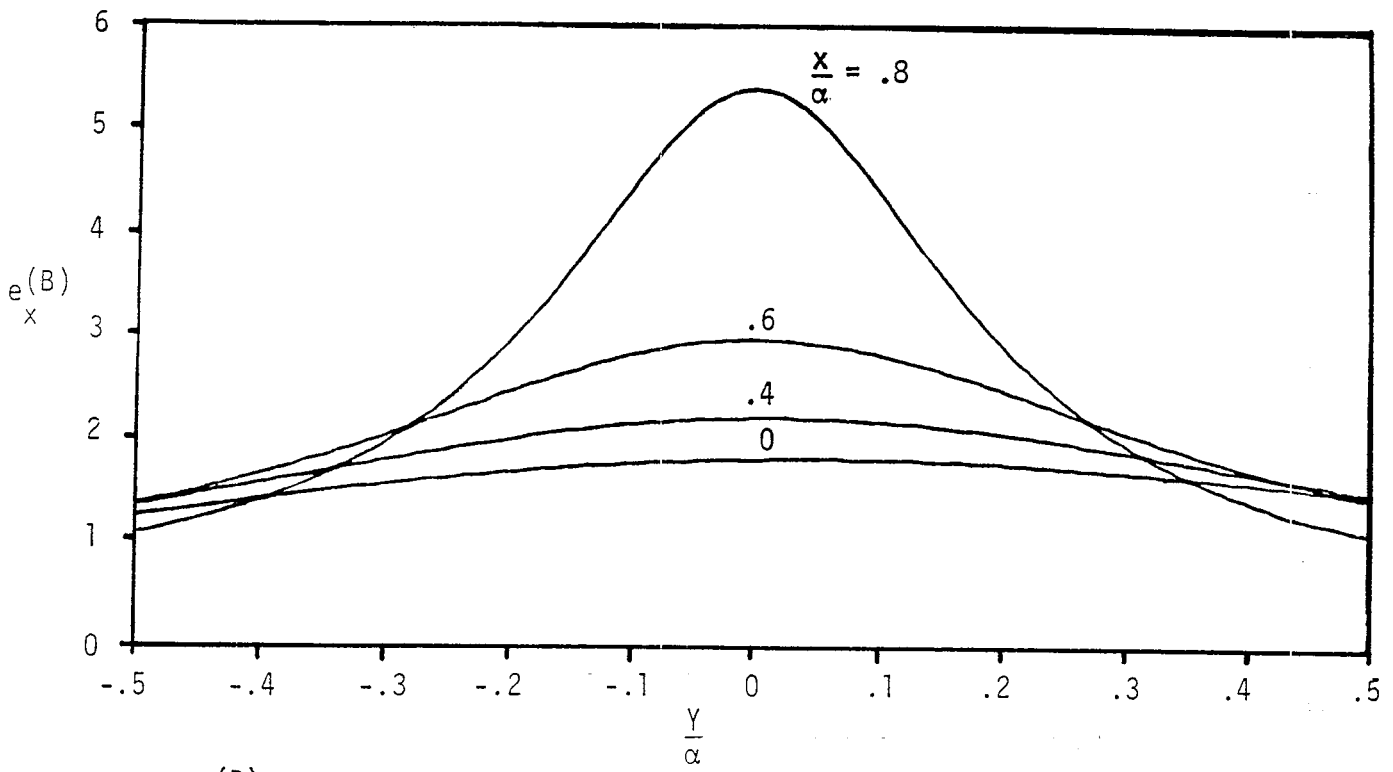
44

A. $e_x^{(B)}$ IN THE X DIRECTION WITH $\frac{X}{\alpha}$ AS A PARAMETER
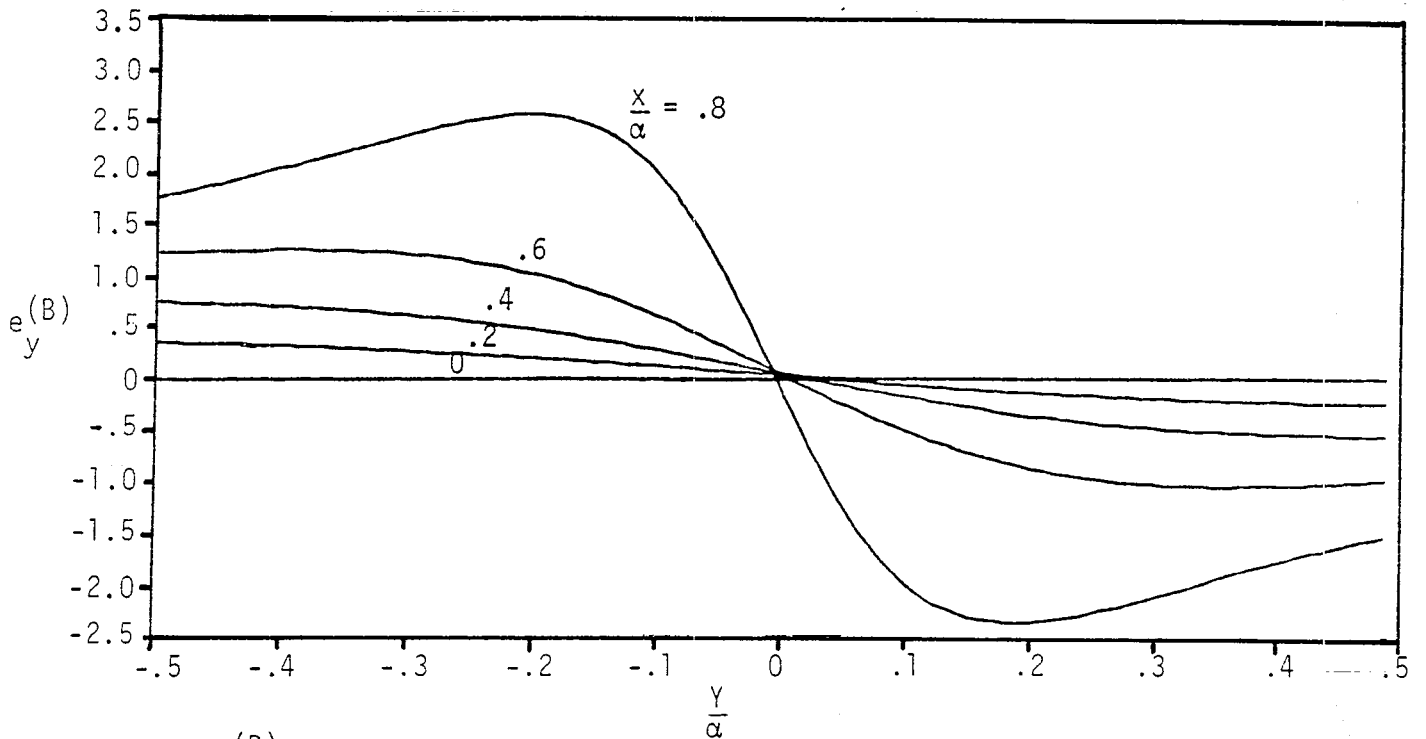
B. $e_y^{(B)}$ IN THE Y DIRECTION WITH $\frac{X}{\alpha}$ AS A PARAMETER

FIGURE 27.   NORMALIZED ELECTRIC FIELD FOR $\frac{X}{\alpha} = 1$, $\frac{\beta}{\alpha} = 2$
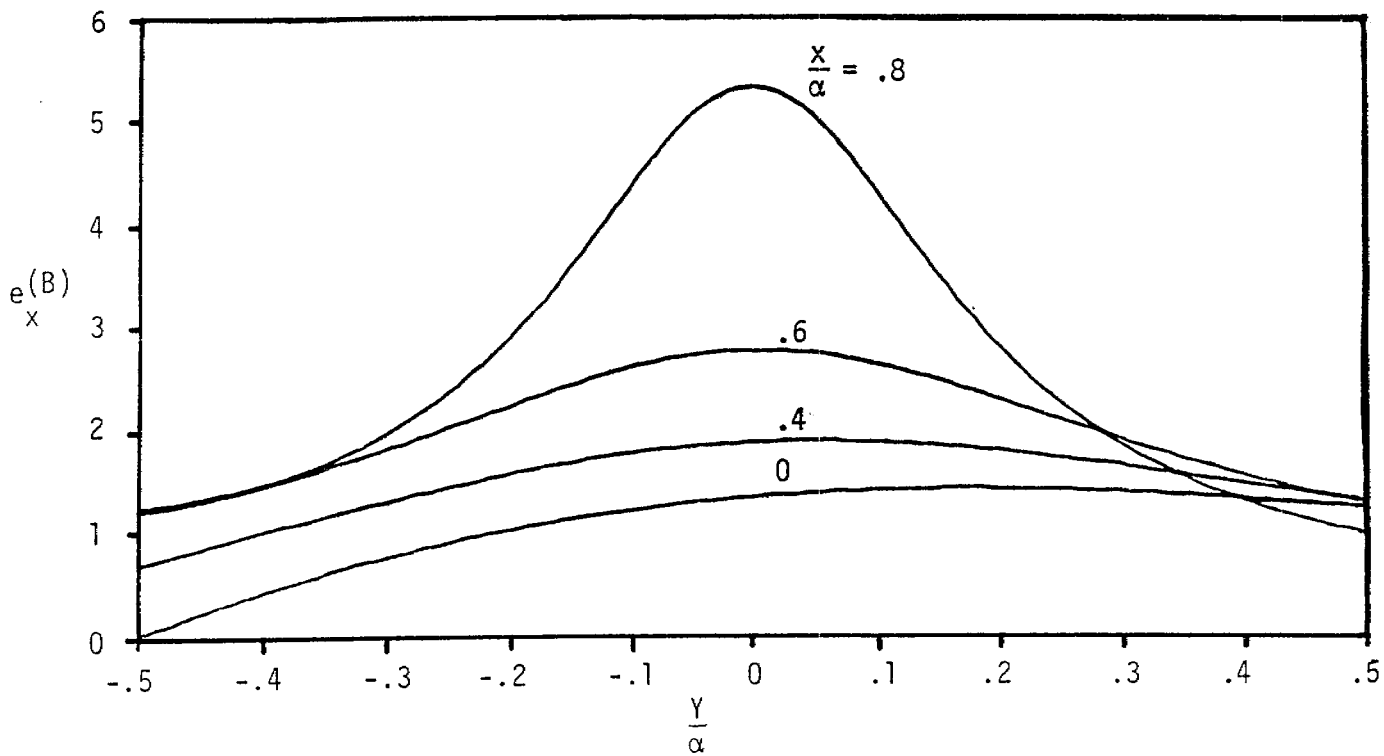
A. $e_x^{(B)}$ IN THE X DIRECTION WITH $\frac{X}{\alpha}$ AS A PARAMETER
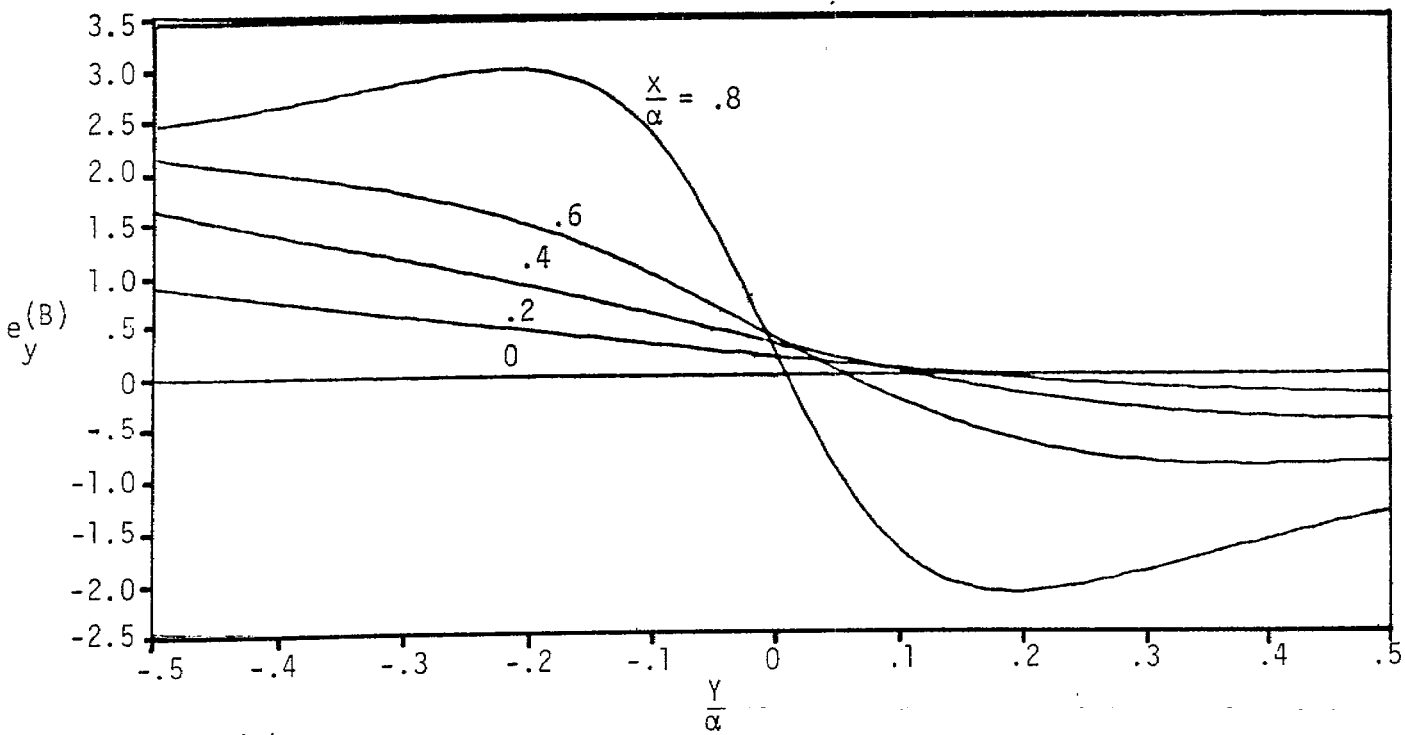
B. $e_y^{(B)}$ IN THE Y DIRECTION WITH $\frac{X}{\alpha}$ AS A PARAMETER

FIGURE 28. NORMALIZED ELECTRIC FIELD FOR $\frac{X}{\alpha} = 1.5$, $\frac{\beta}{\alpha} = 2$
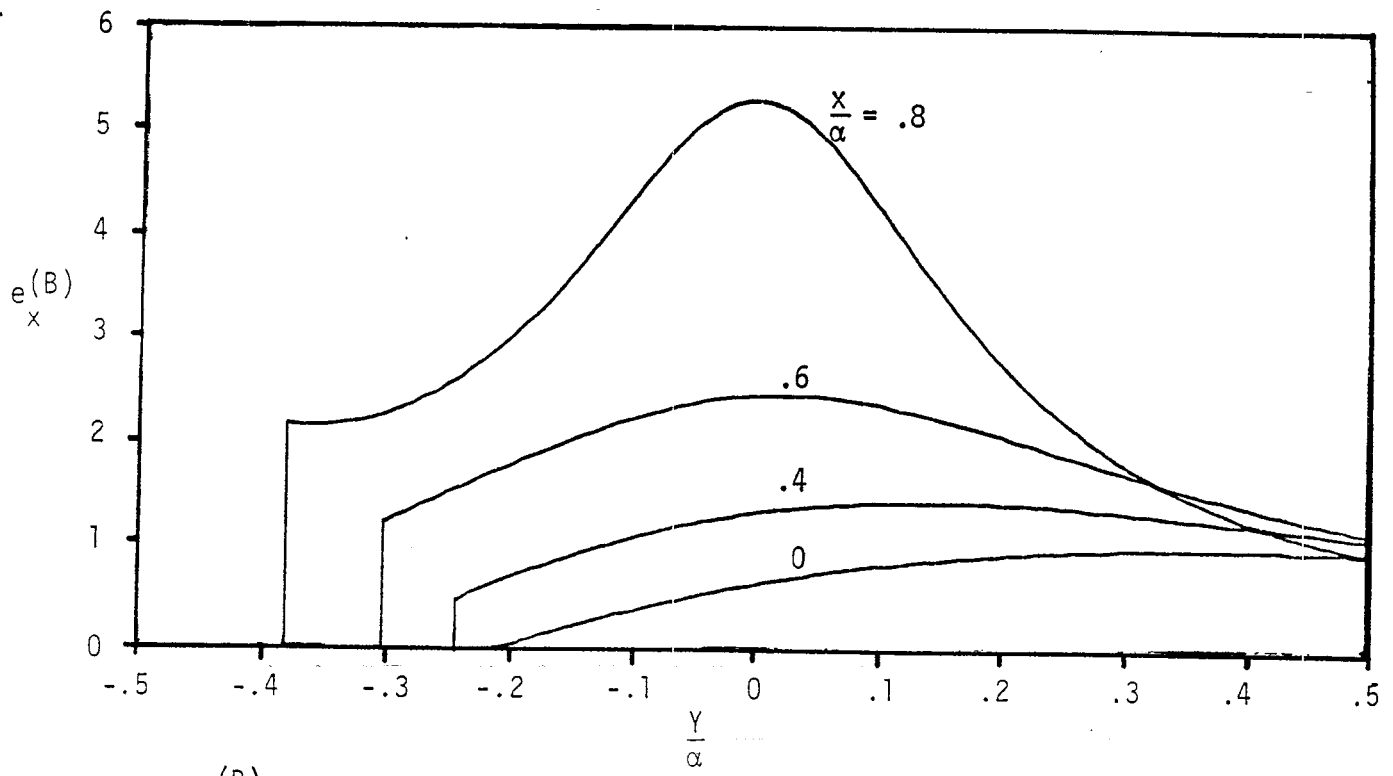
A. $e^{(B)}$ IN THE X DIRECTION WITH $\frac{x}{\alpha}$ AS A PARAMETER
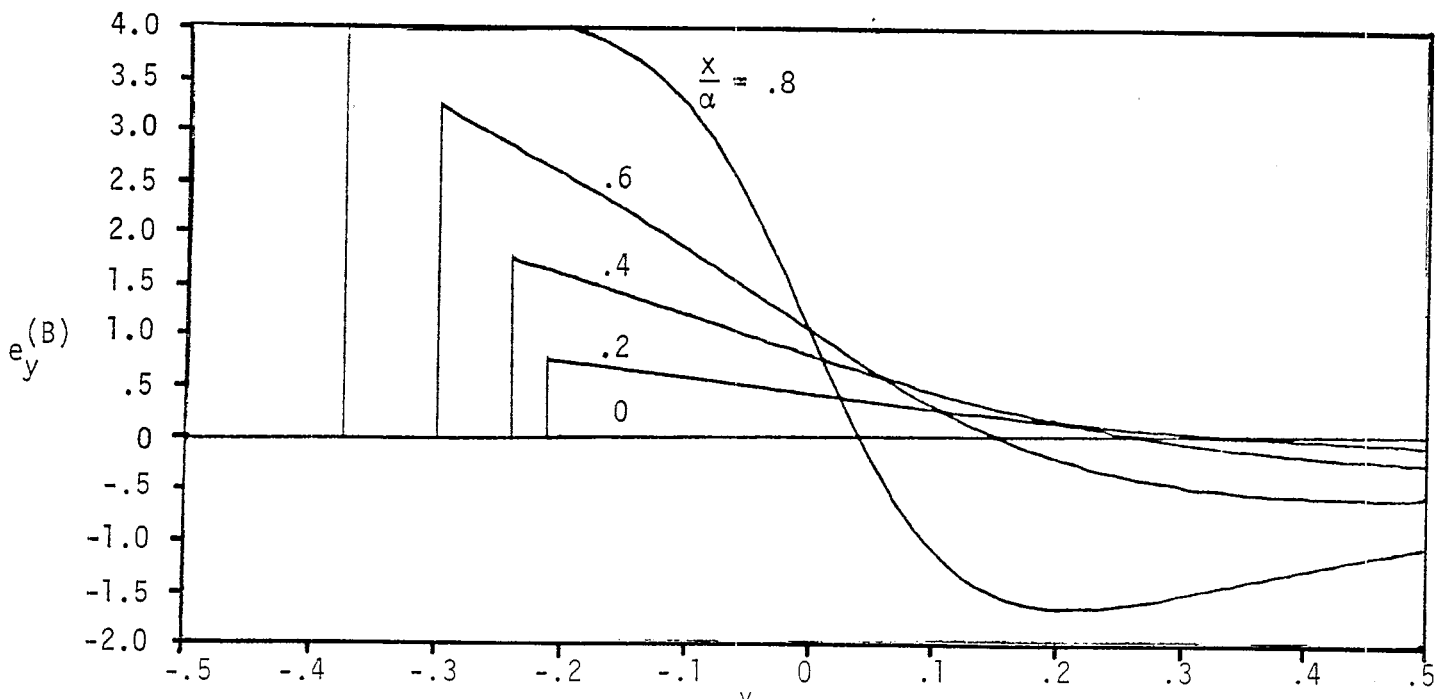
B. $e^{(B)}$ IN THE Y DIRECTION WITH $\frac{x}{\alpha}$ AS A PARAMETER

FIGURE 29.   NORMALIZED ELECTRIC FIELD FOR $\frac{x}{\alpha}$ = 1.8, $\frac{\beta}{\alpha}$ = 2
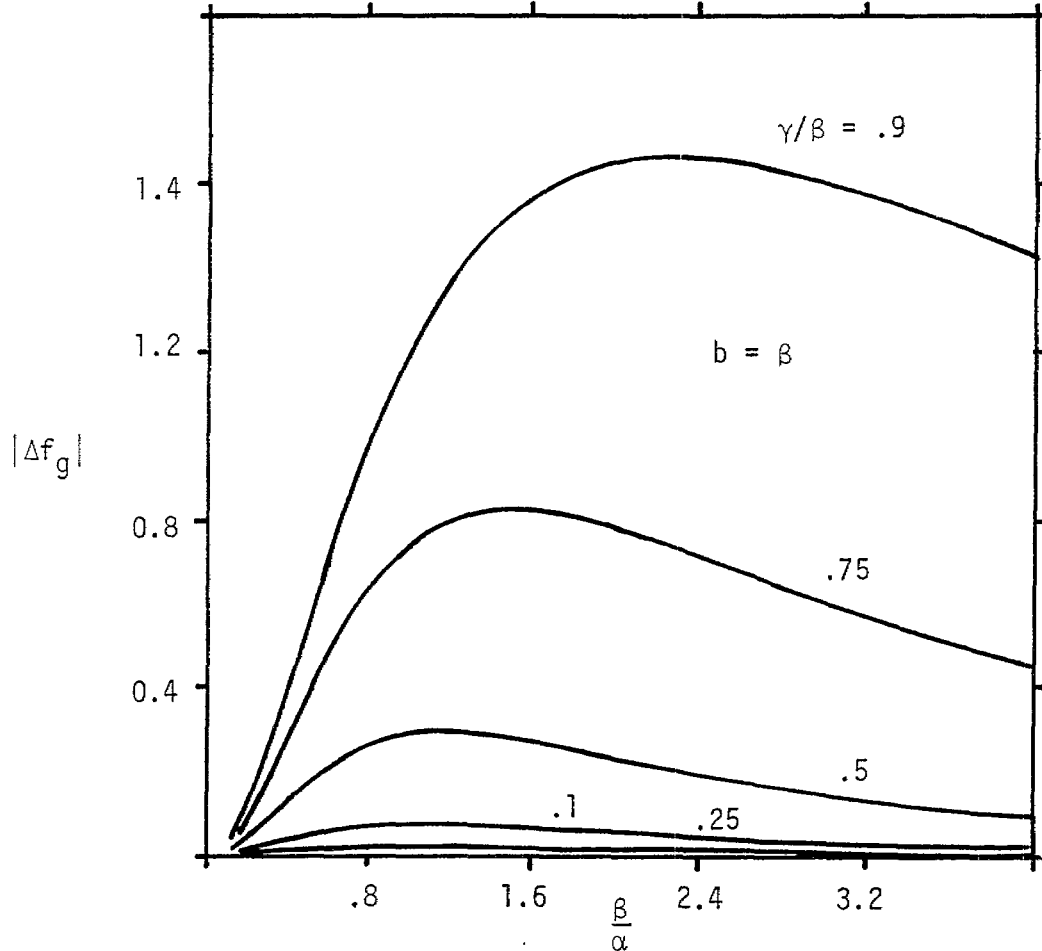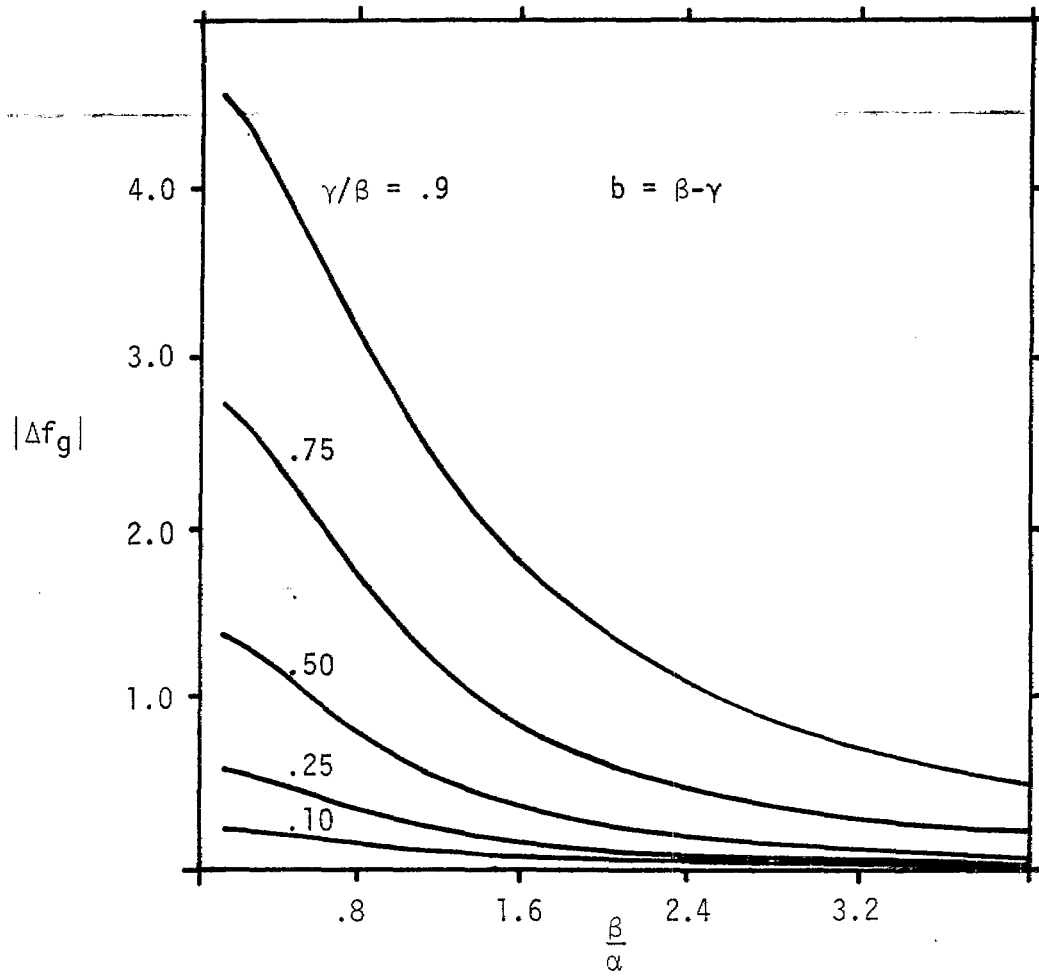
FIGURE 30. CHANGE IN GEOMETRICAL FACTOR DUE TO GROUND CONTOURING
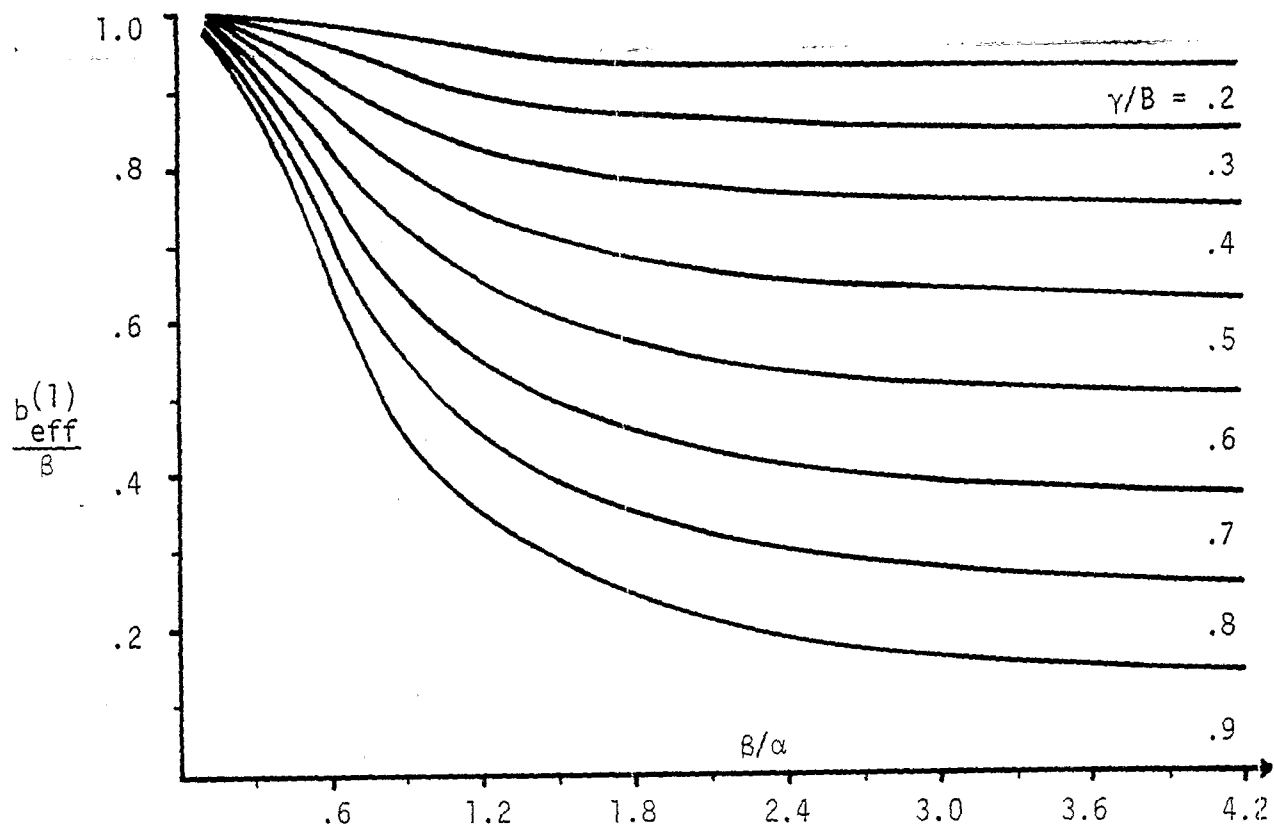
A. $b_{eff}^{(1)}$
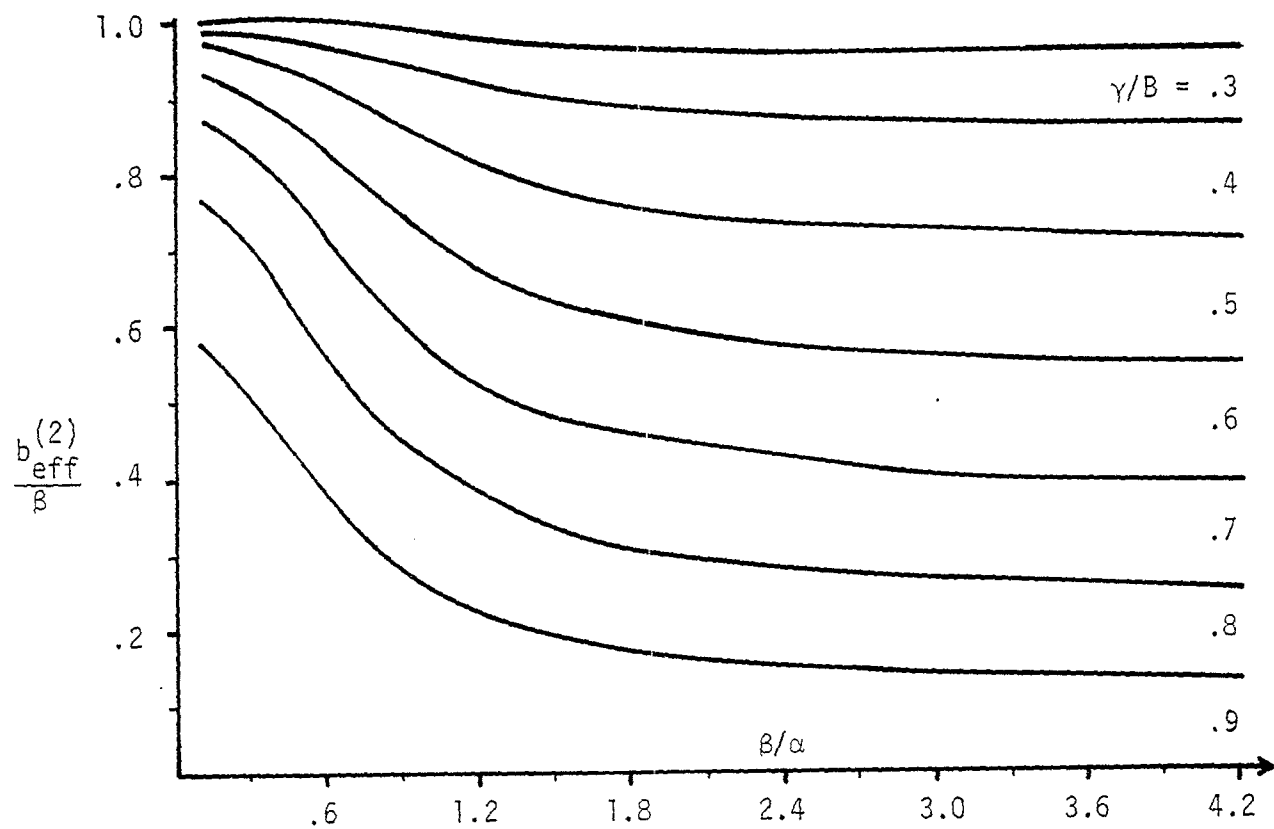
B. $b_{eff}^{(2)}$

FIGURE 31. DISTANCE TO EQUIVALENT PLANAR GROUND, b_{eff}, AS A FUNCTION OF β WITH γ A PARAMETER

49
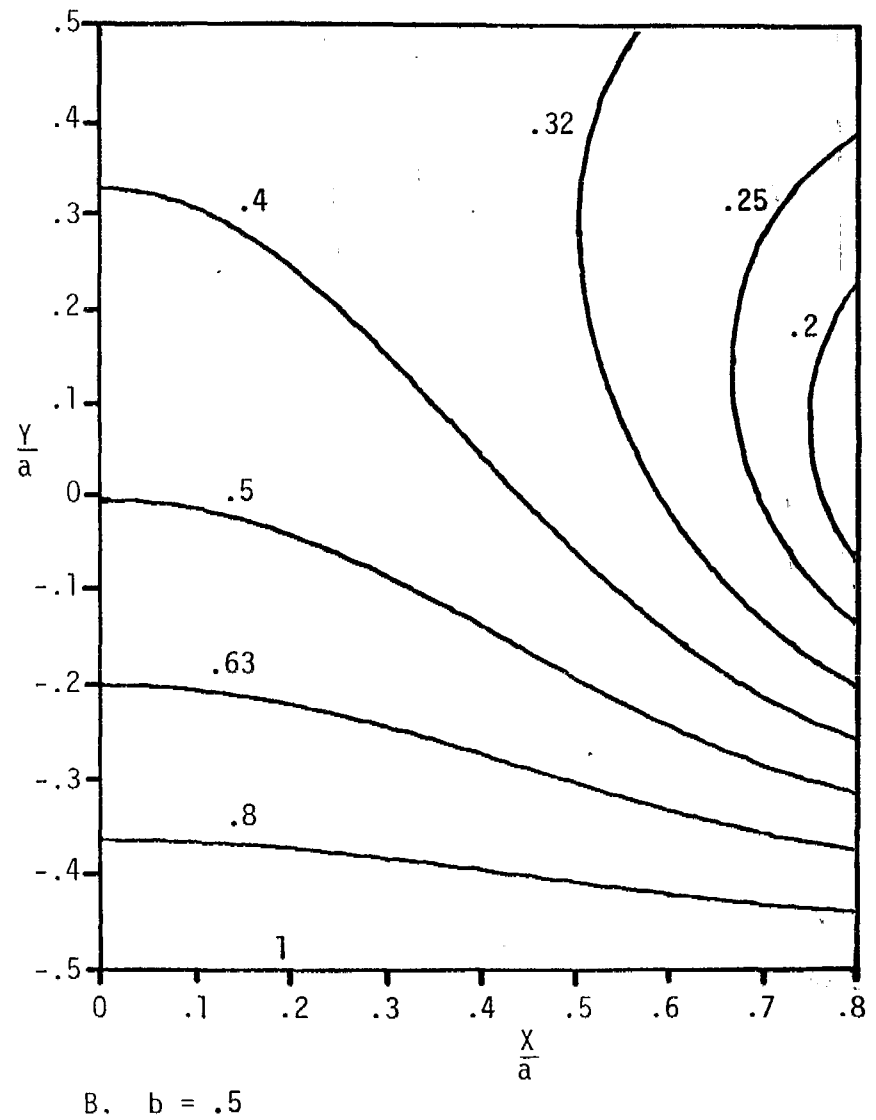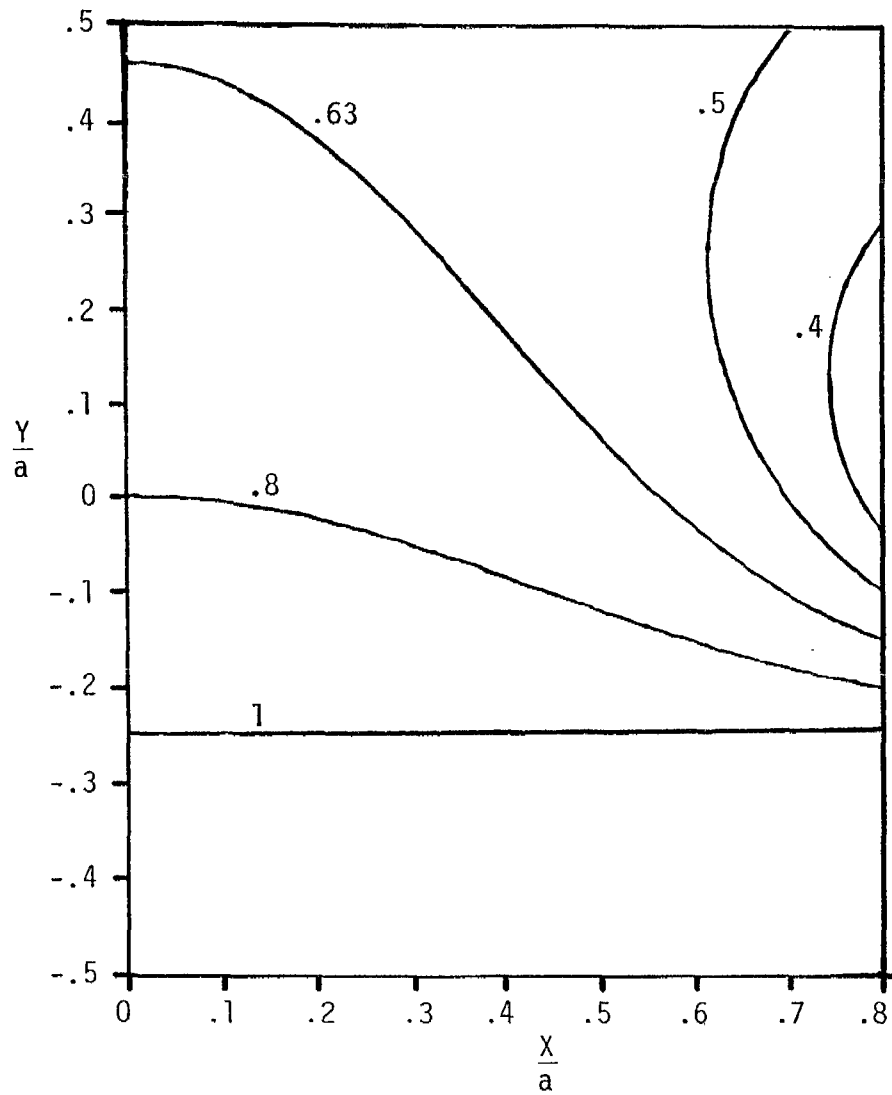
FIGURE 32. ERROR CONTOUR OF FIELD DEVIATION FOR $\Delta e^{(A)}$

A. b = .25

B. b = .5

A. b = 1.0

B. b = 2.0
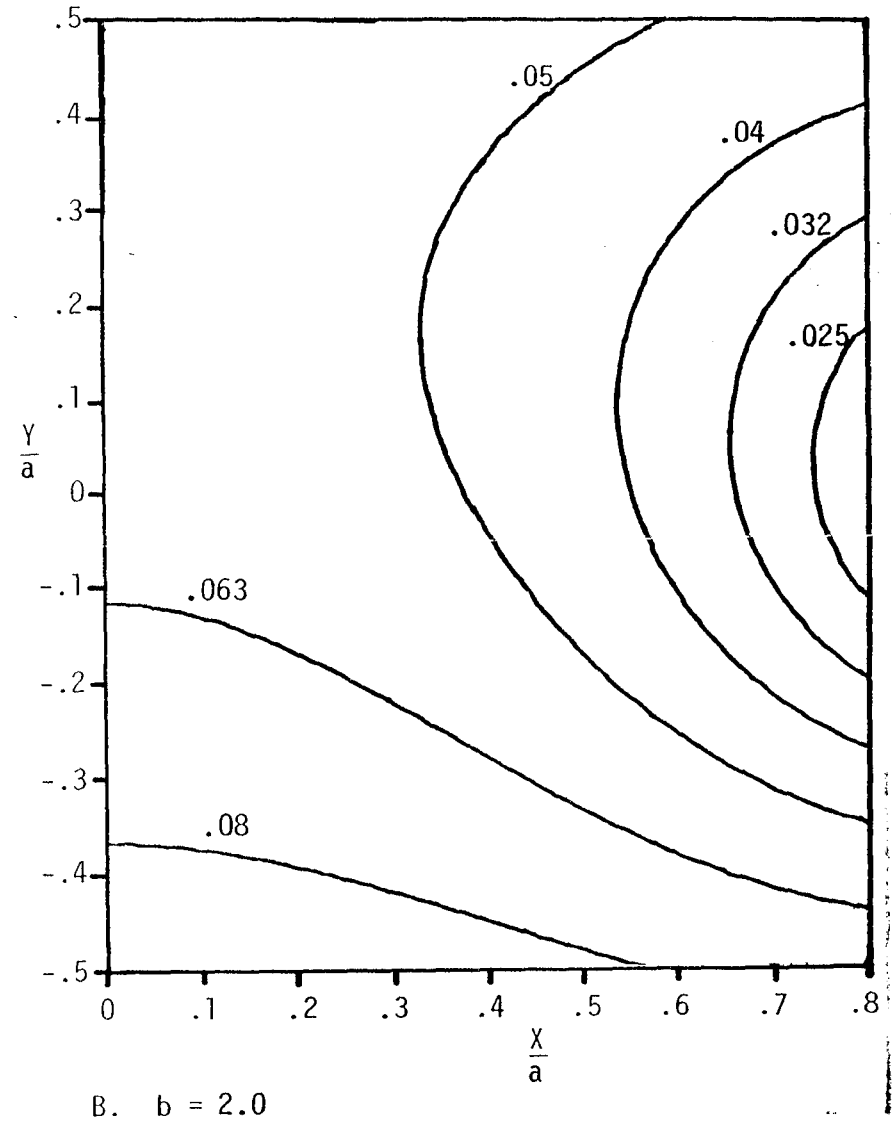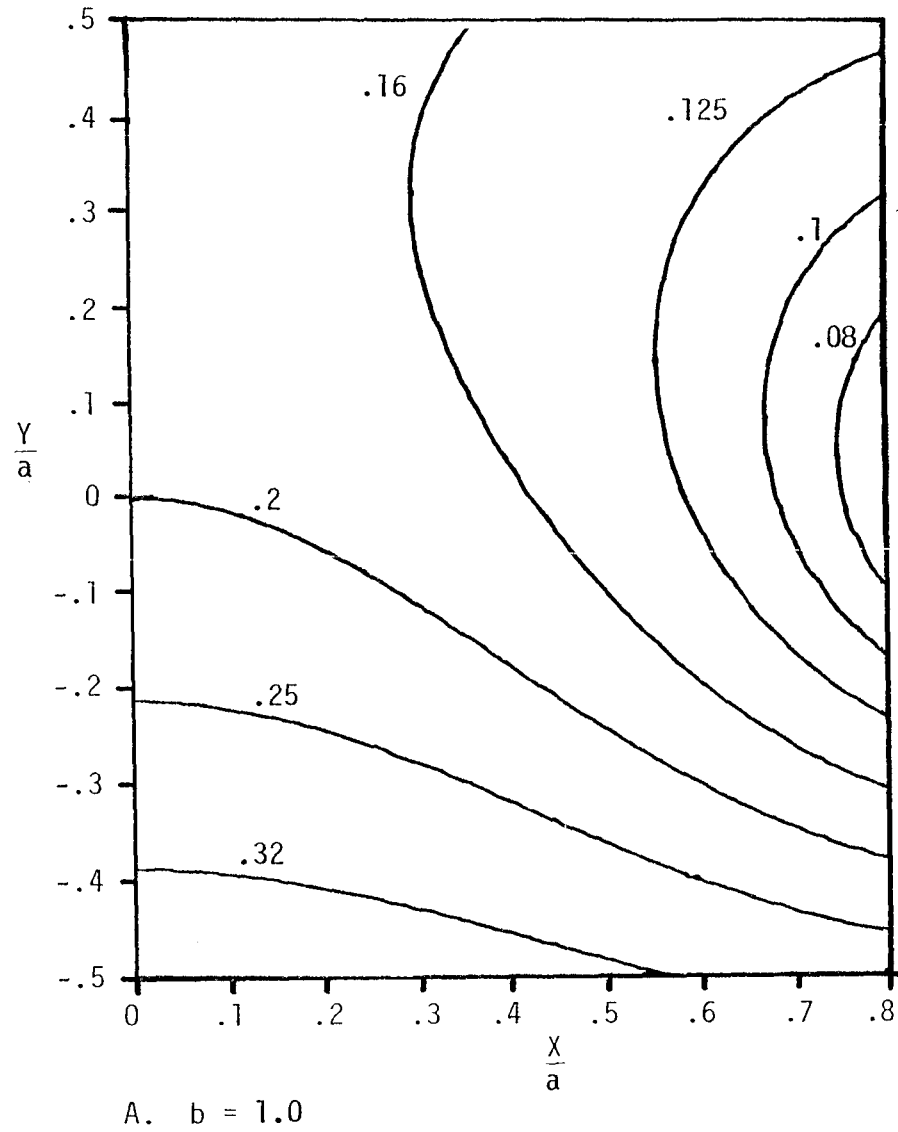
FIGURE 33. ERROR CONTOUR OF FIELD DEVIATION FOR $\Delta e^{(A)}$
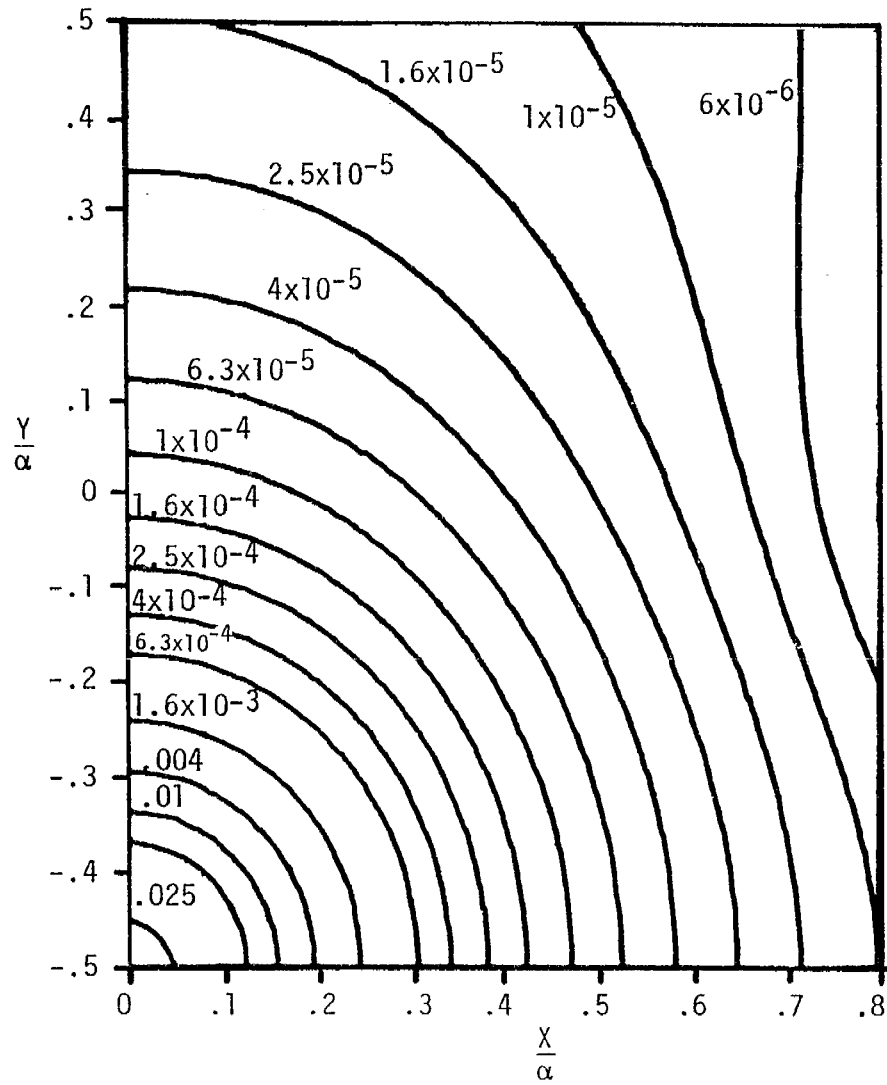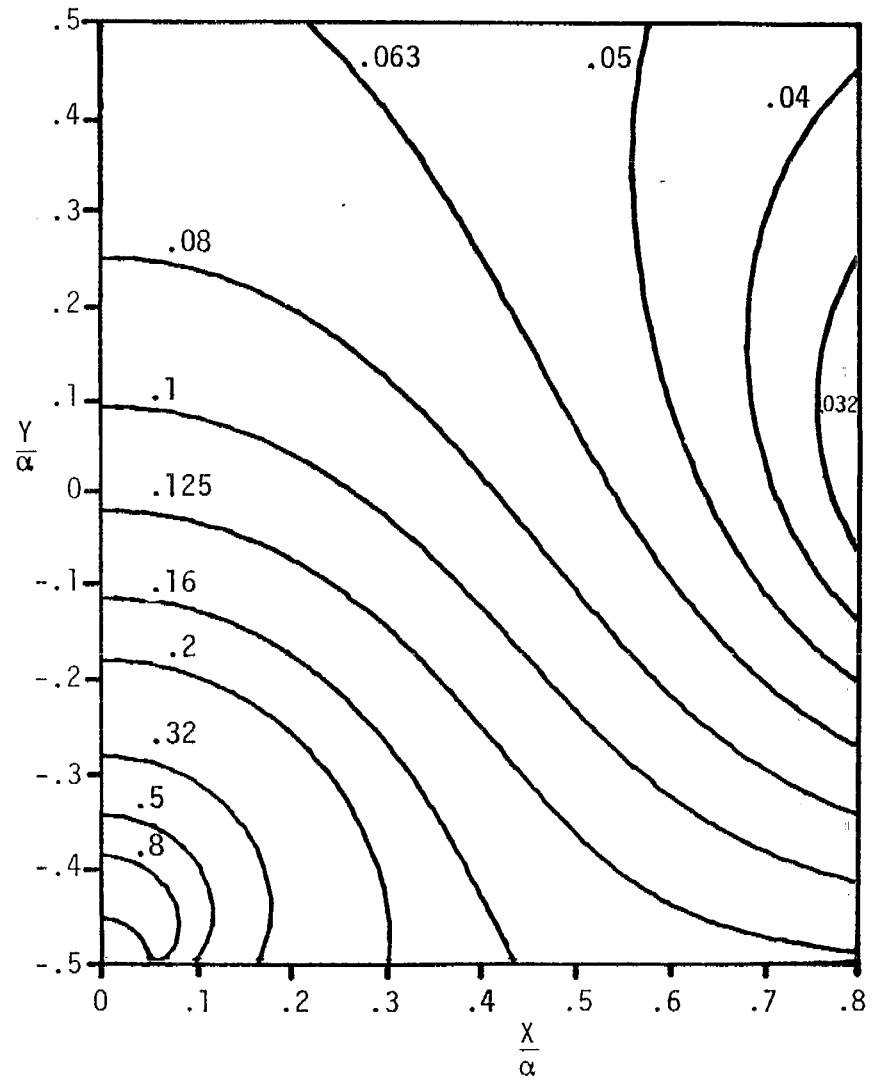
FIGURE 34. ERROR CONTOUR OF FIELD DEVIATION FOR $\Delta e^{(B)}$ $\qquad$ $\frac{\beta}{\alpha} = .5$ $\qquad$ $\frac{\gamma}{\beta} = .1$
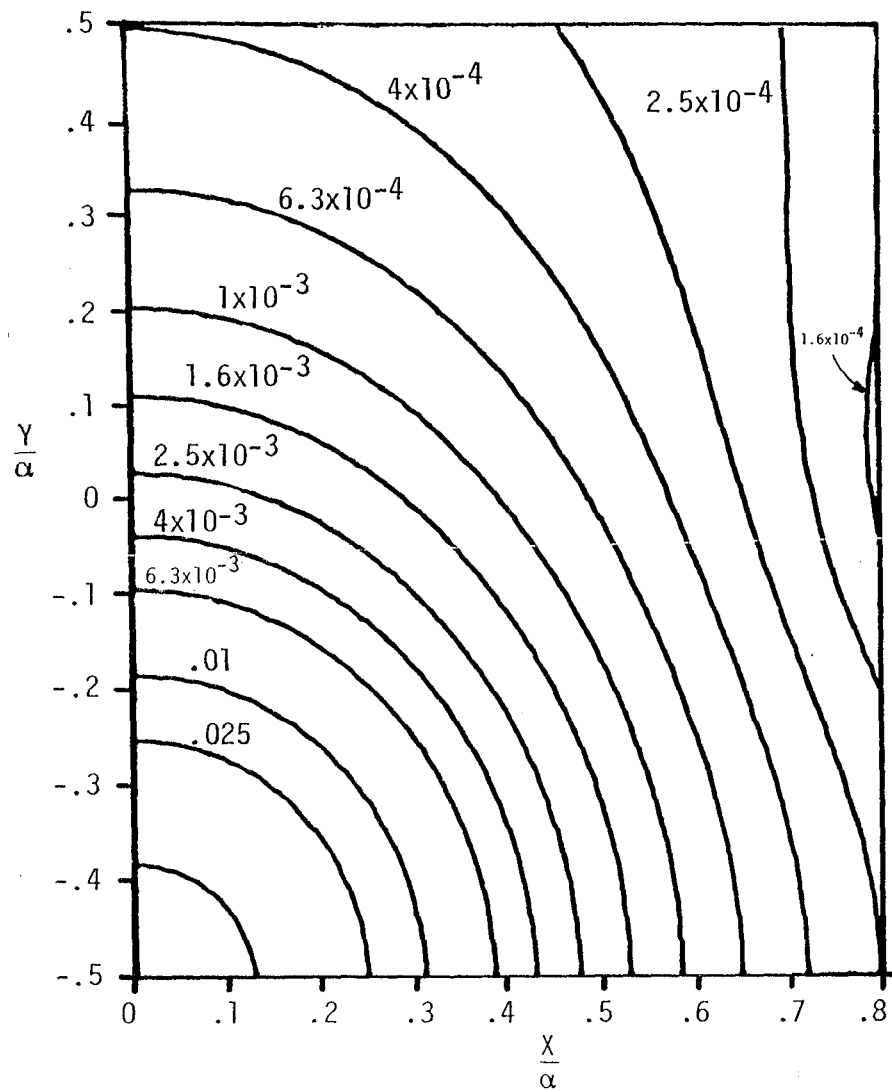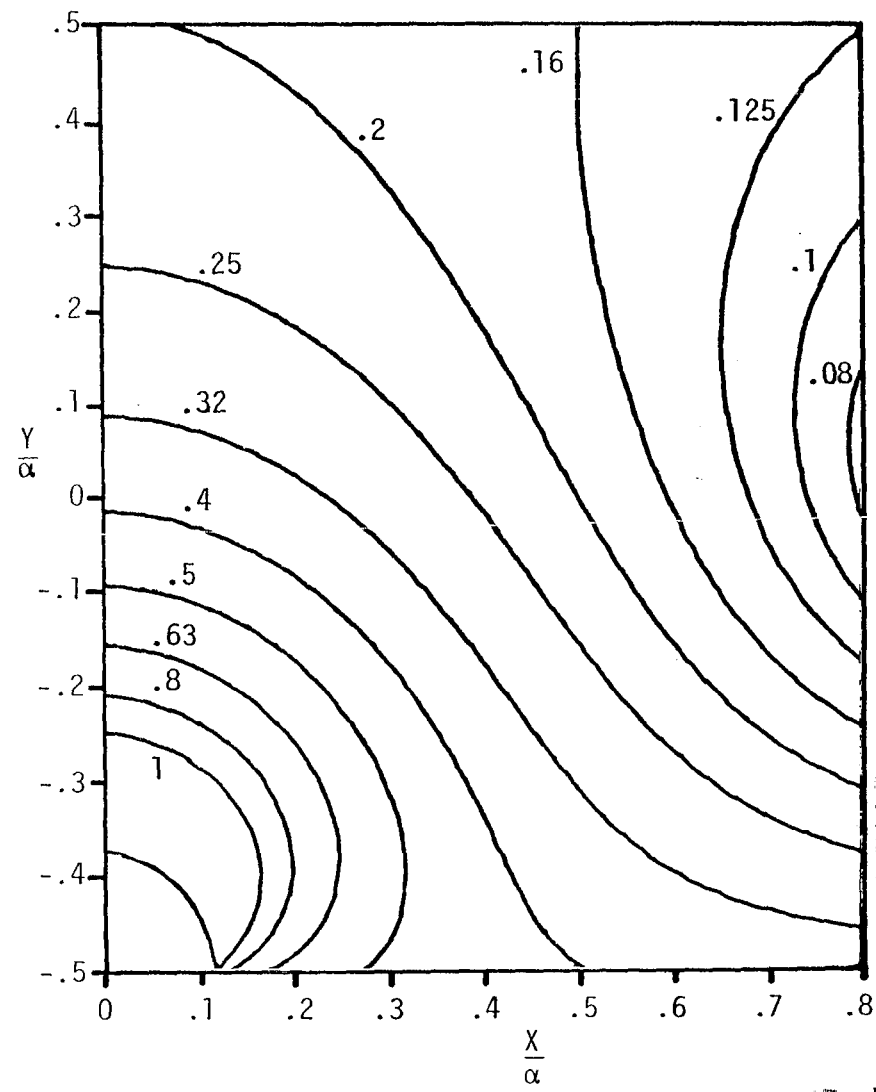
FIGURE 35. ERROR CONTOUR OF FIELD DEVIATION FOR $\Delta e^{(B)}$ $\frac{\beta}{\alpha} = .5$ $\frac{\gamma}{\beta} = .25$

A. $b = \beta$

B. $b = \beta - \gamma$

53

54
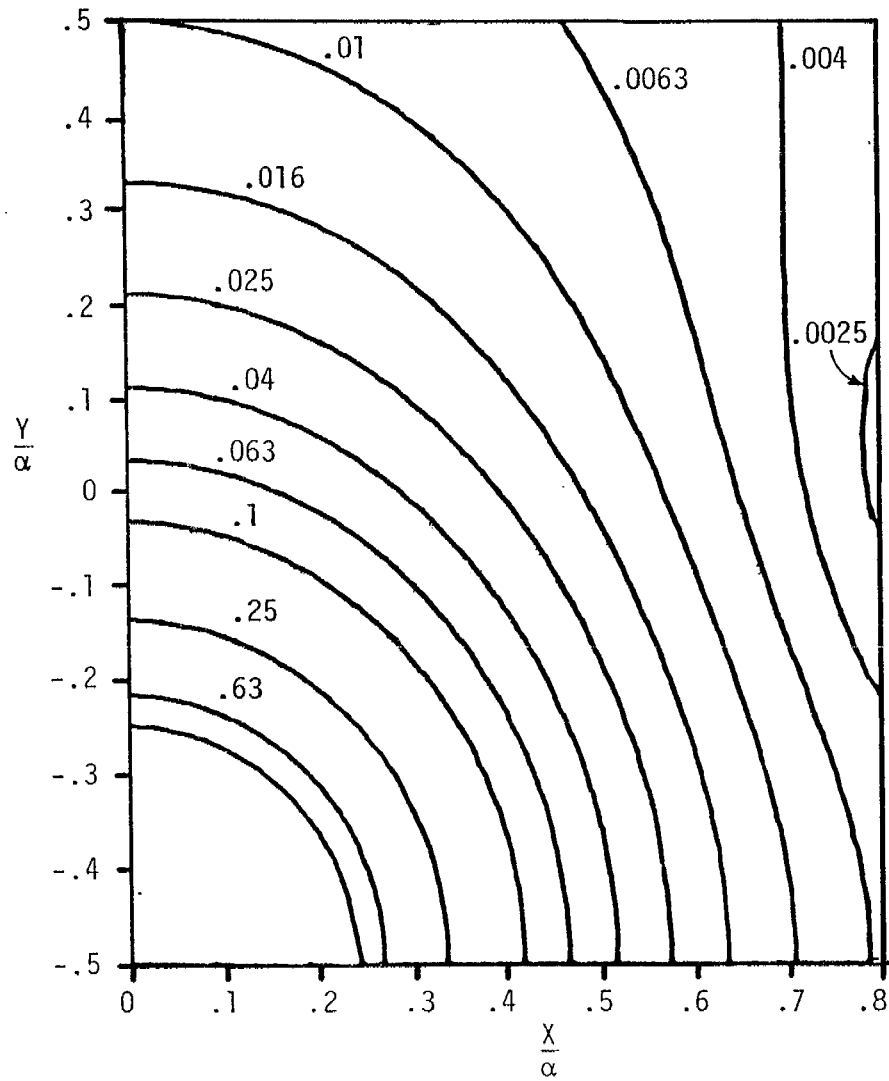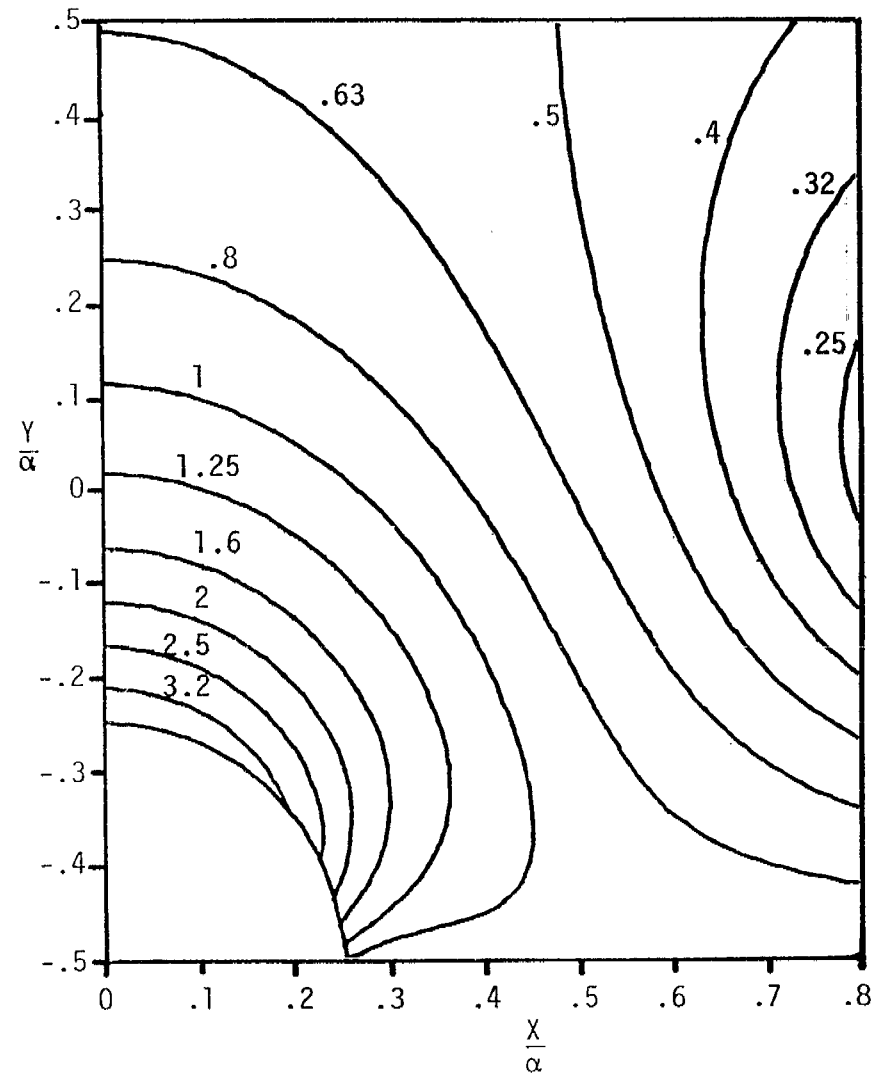
FIGURE 36. ERROR CONTOUR OF FIELD DEVIATION FOR $\Delta e^{(B)}$ $\quad \frac{\beta}{\alpha} = .5 \quad \frac{\gamma}{\beta} = .5$
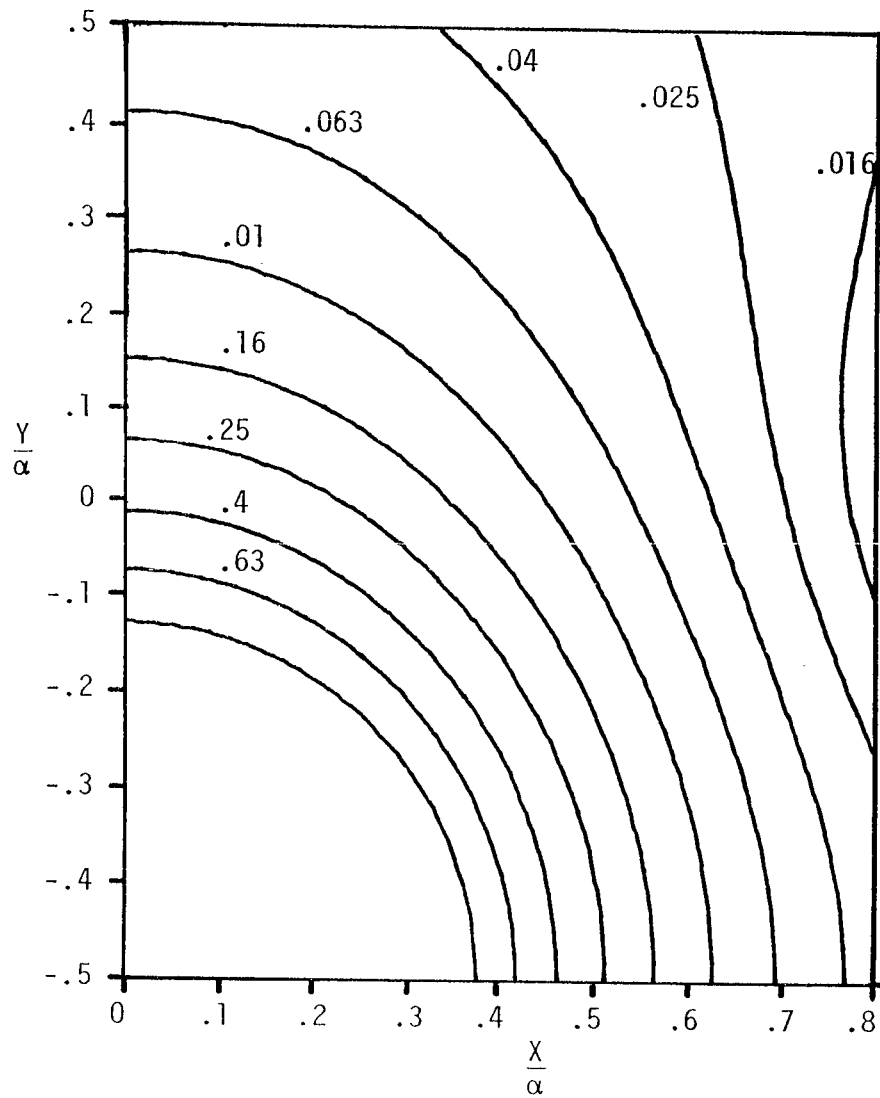
A. $b = \beta$
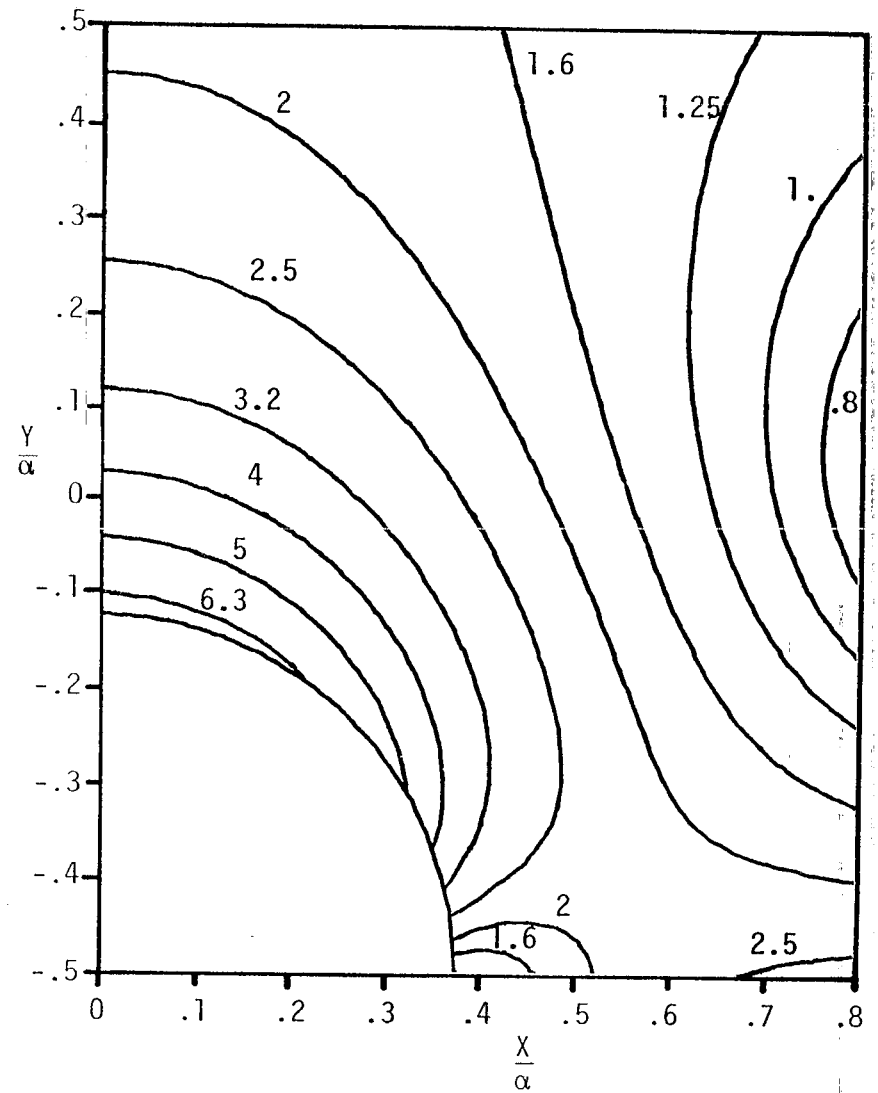
B. $b = \beta - \gamma$

FIGURE 37.   ERROR CONTOUR OF FIELD DEVIATION FOR $\Delta e^{(B)}$ $\frac{\beta}{\alpha} = .5$ $\frac{\gamma}{\beta} = .75$

A.   b = β

B.   b = β-γ

A. b = β

B. b = β-γ
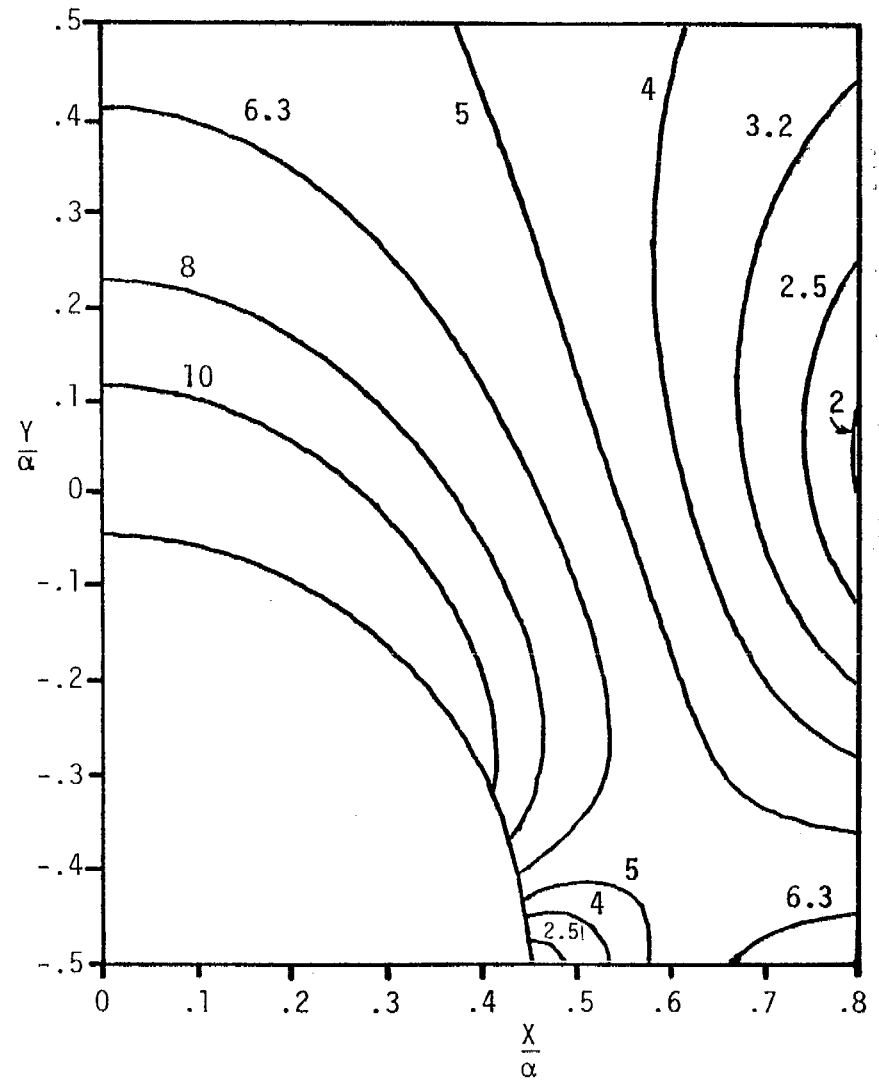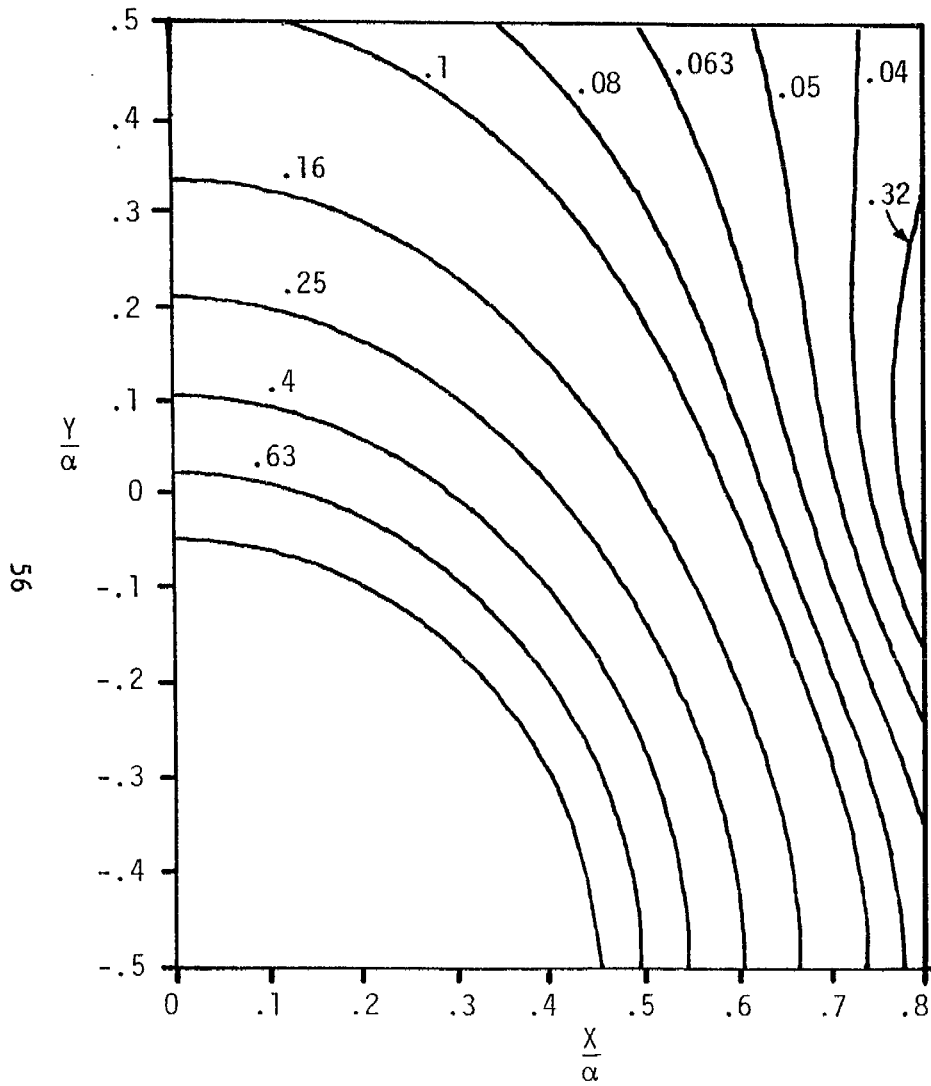
FIGURE 38. ERROR CONTOUR OF FIELD DEVIATION FOR $\Delta e^{(B)}$ $\frac{\beta}{\alpha} = .5$ $\frac{\gamma}{\beta} = .9$

A. b = β

B. b = β-γ
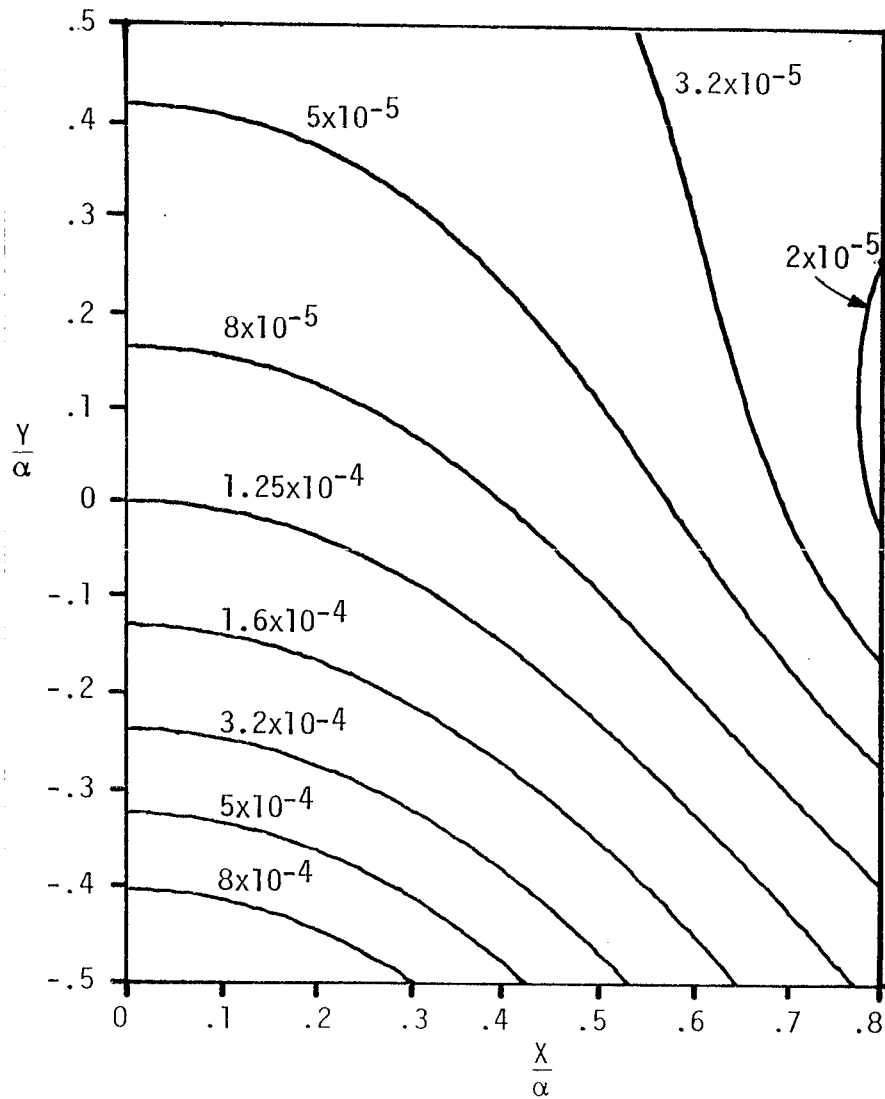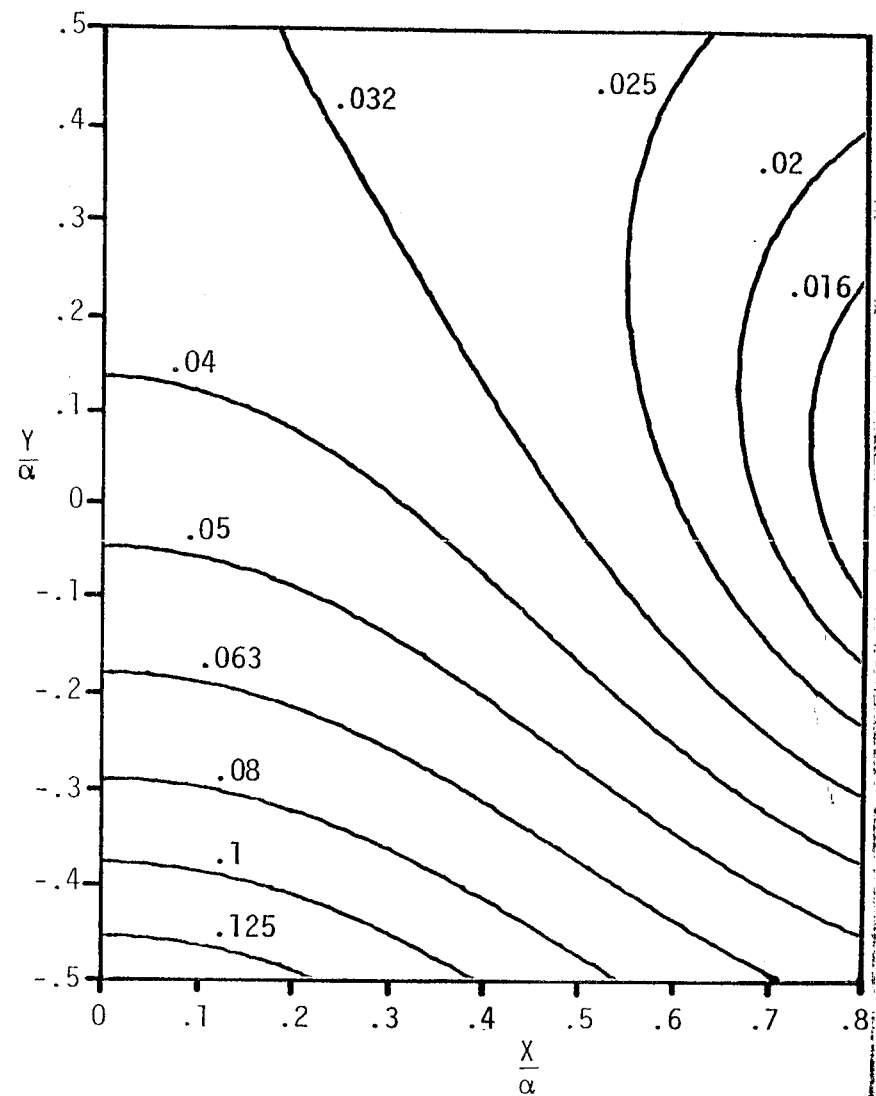
FIGURE 39.   ERROR CONTOUR OF FIELD DEVIATION FOR $\Delta e^{(B)}$ $\frac{\beta}{\alpha} = 1$ $\frac{\gamma}{\beta} = .1$
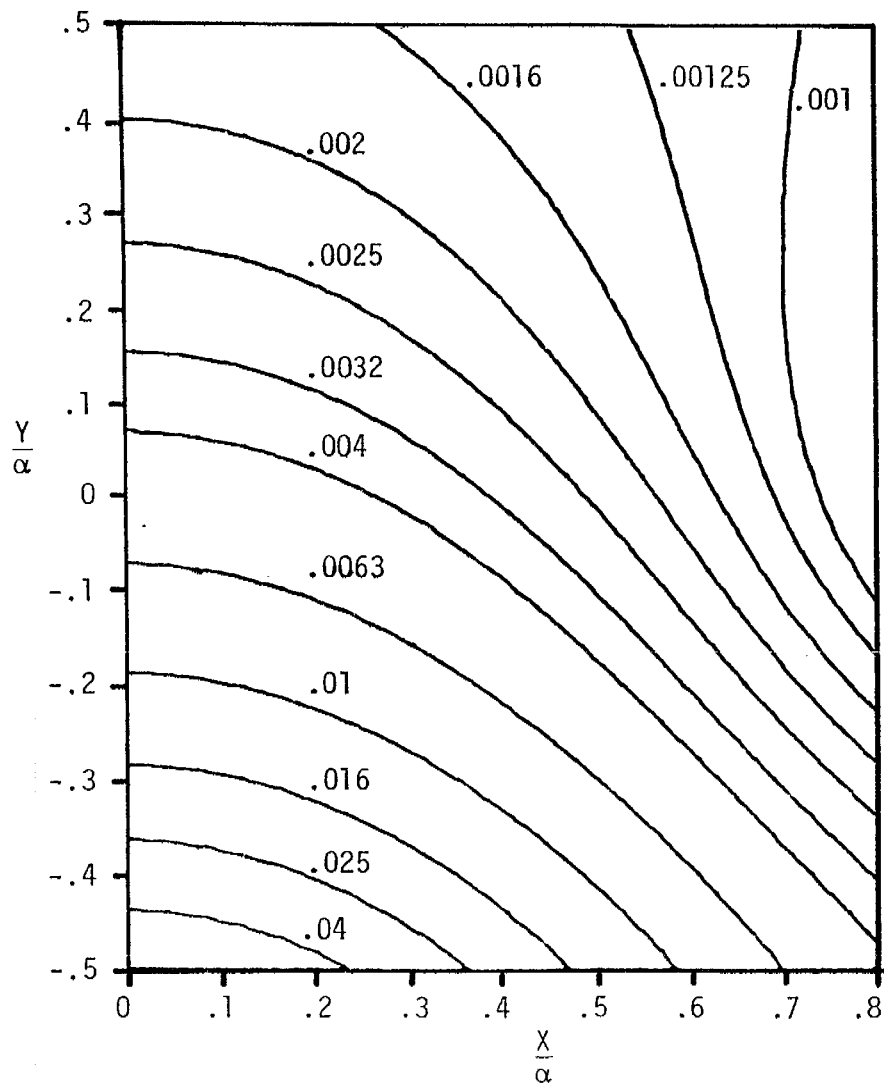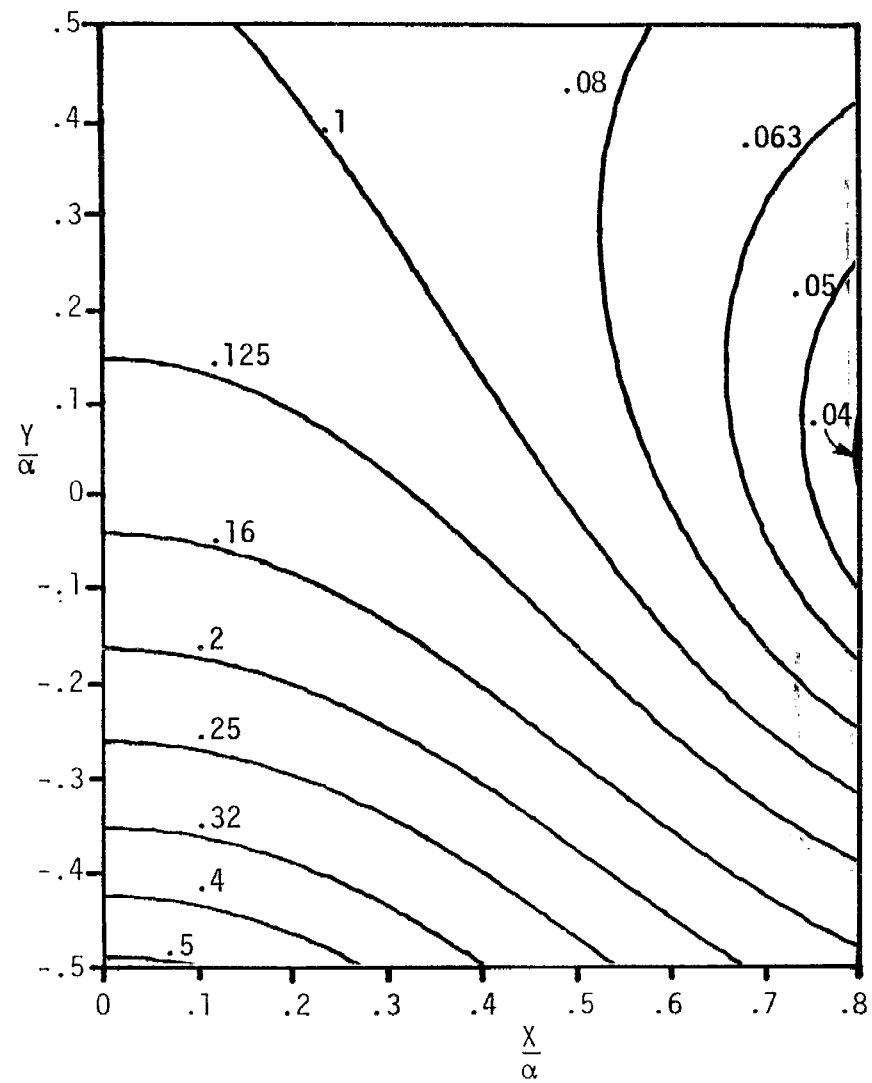
FIGURE 40. ERROR CONTOUR OF FIELD DEVIATION FOR $\Delta e^{(B)}$ $\quad \frac{\beta}{\alpha} = 1 \quad \frac{\gamma}{\beta} = .25$

A. $b = \beta$

B. $b = \beta - \gamma$

A. b = β

B. b = β-γ
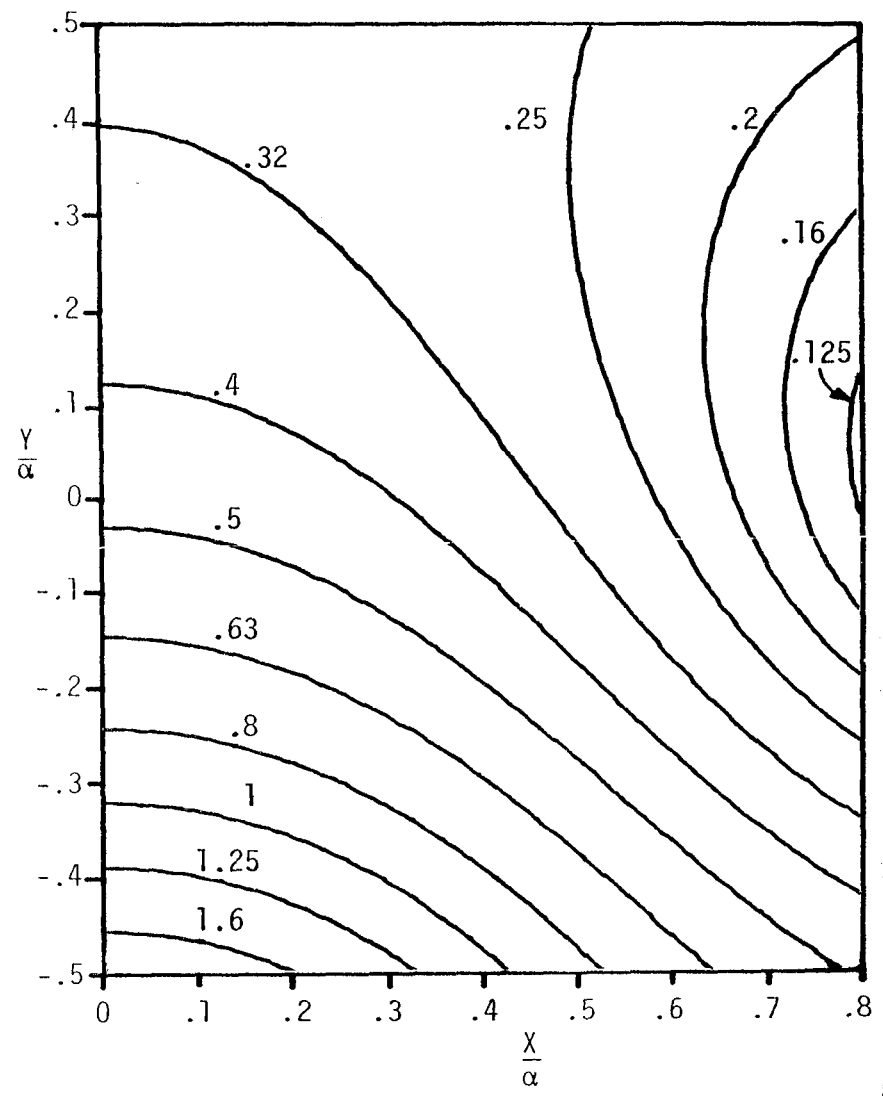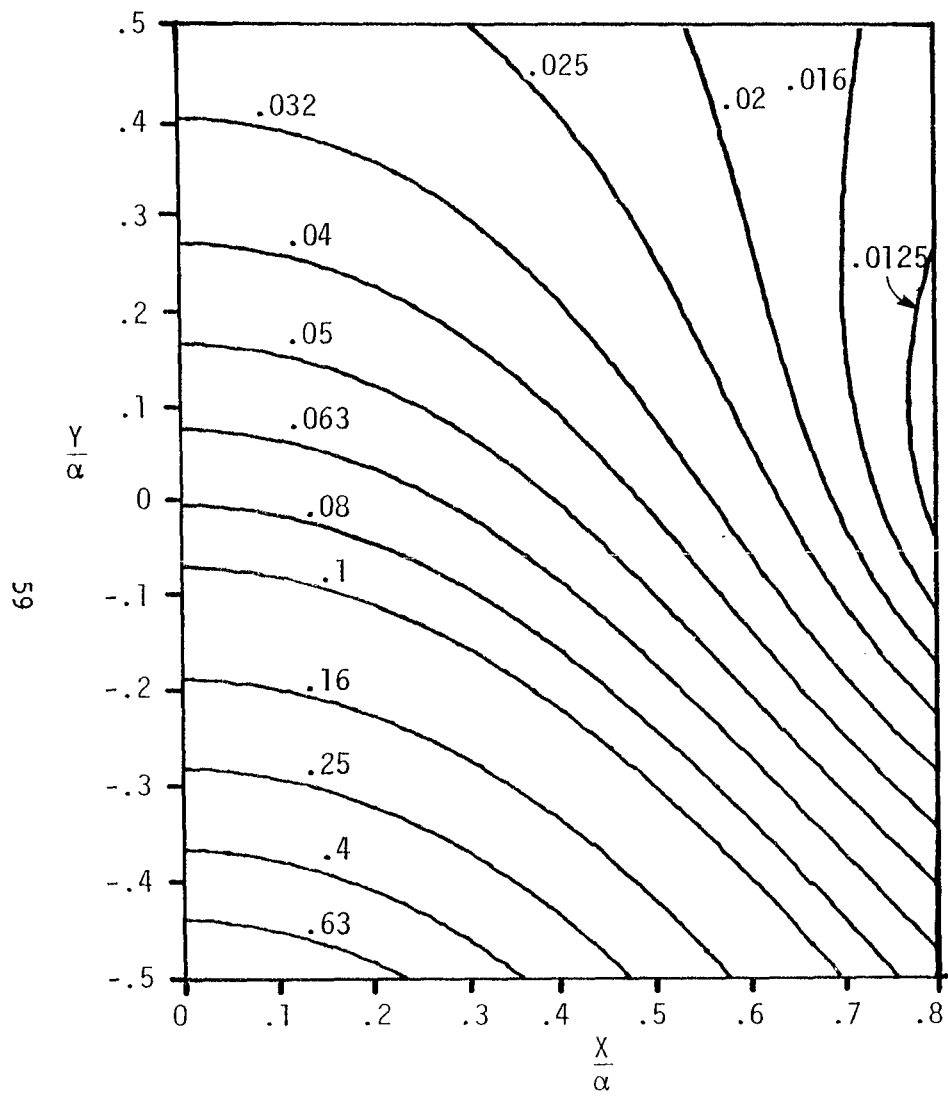
FIGURE 41.   ERROR CONTOUR OF FIELD DEVIATION FOR $\Delta e^{(B)}$ $\frac{\beta}{\alpha} = 1$ $\frac{\gamma}{\beta} = .5$

59
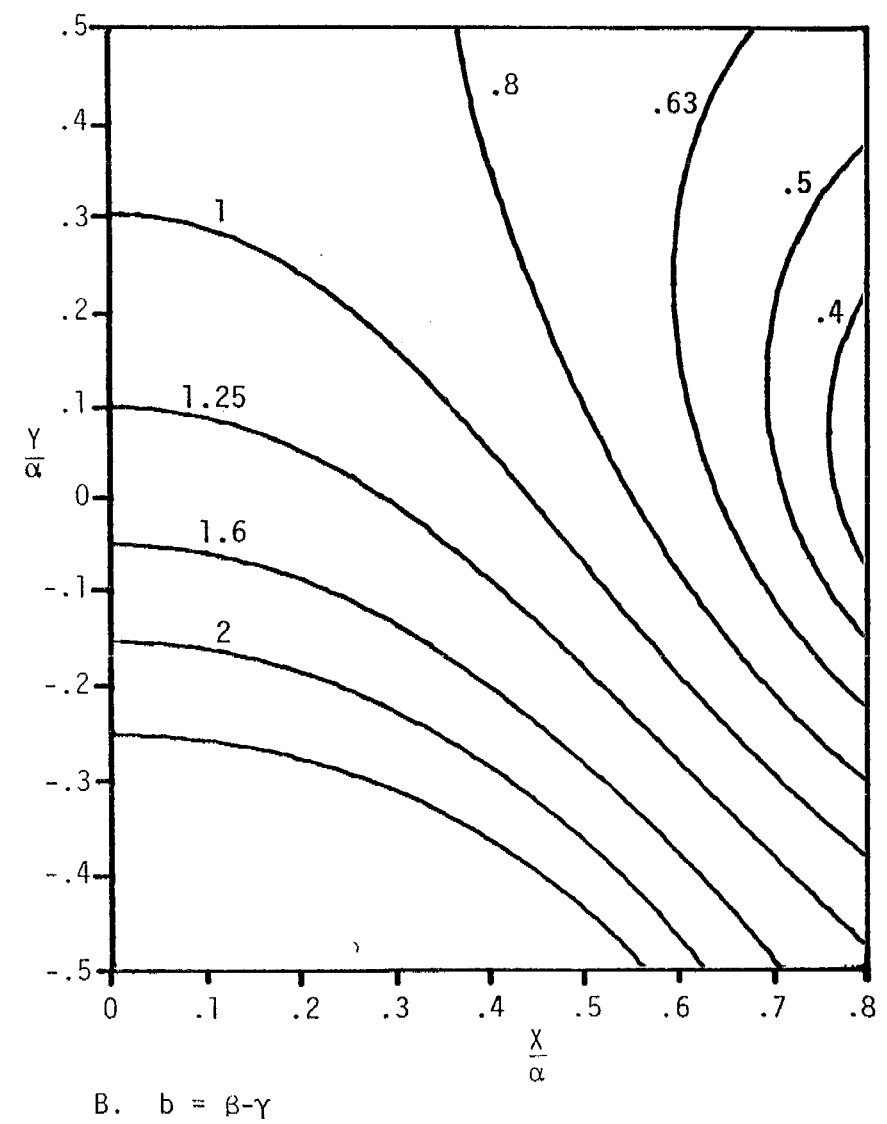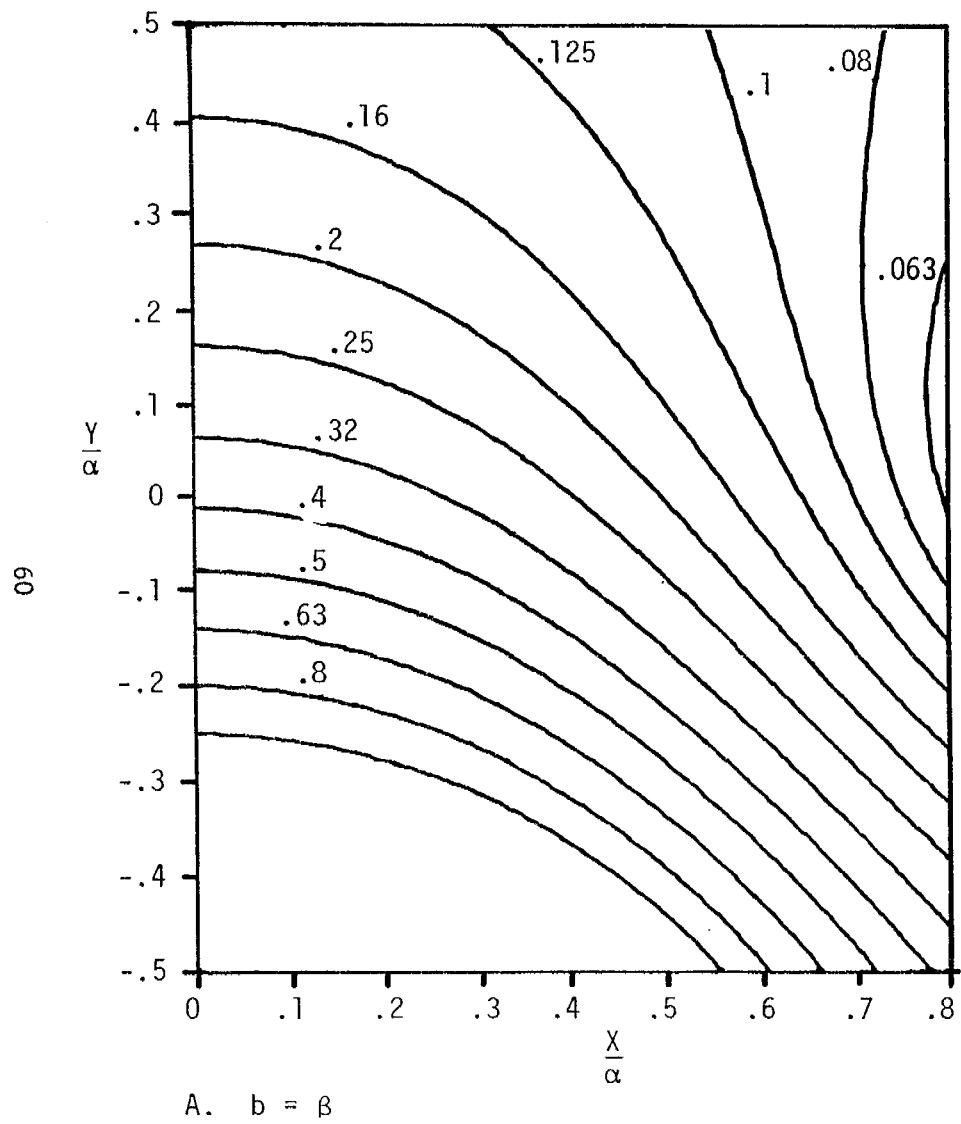
FIGURE 42. ERROR CONTOUR OF FIELD DEVIATION FOR $\Delta e^{(B)}$ $\frac{\beta}{\alpha} = 1$ $\frac{\gamma}{\beta} = .75$

A. $b = \beta$

B. $b = \beta - \gamma$
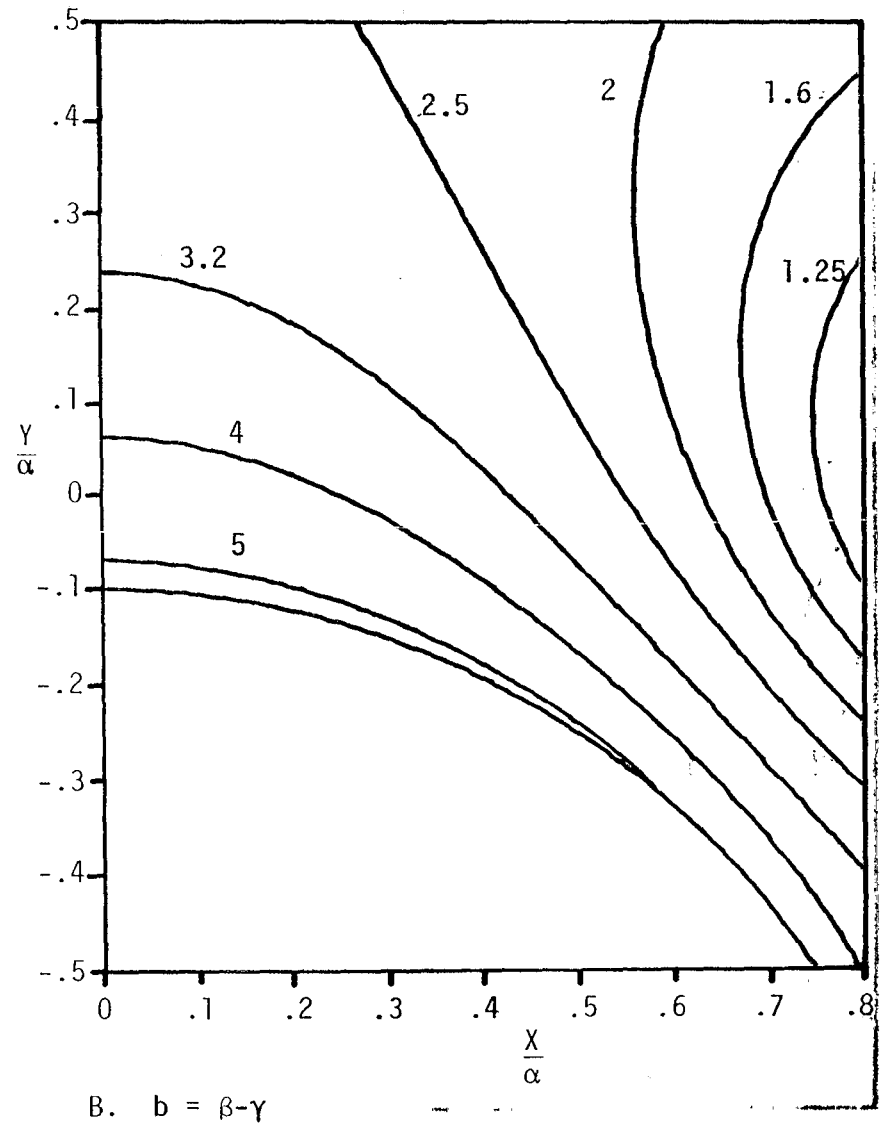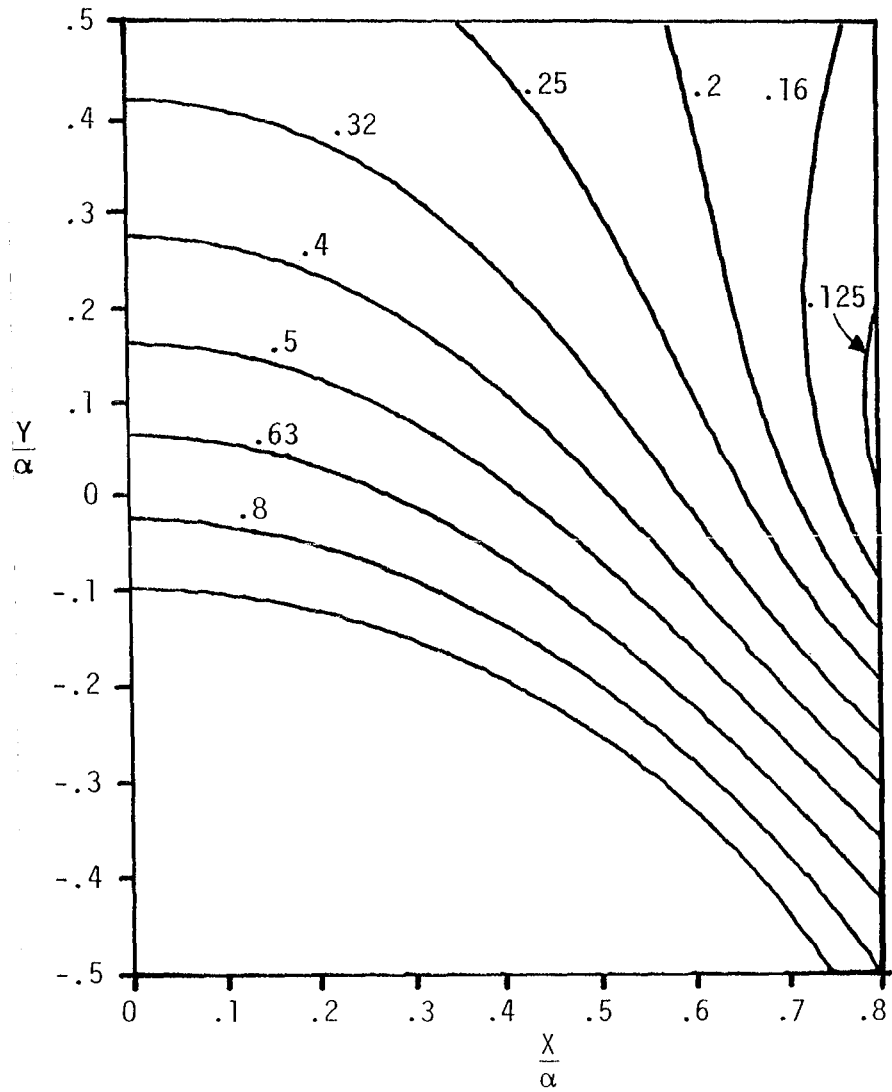
FIGURE 43. ERROR CONTOUR OF FIELD DEVIATION FOR $\Delta e^{(B)}$ $\frac{\beta}{\alpha} = 1$ $\frac{\gamma}{\beta} = .9$
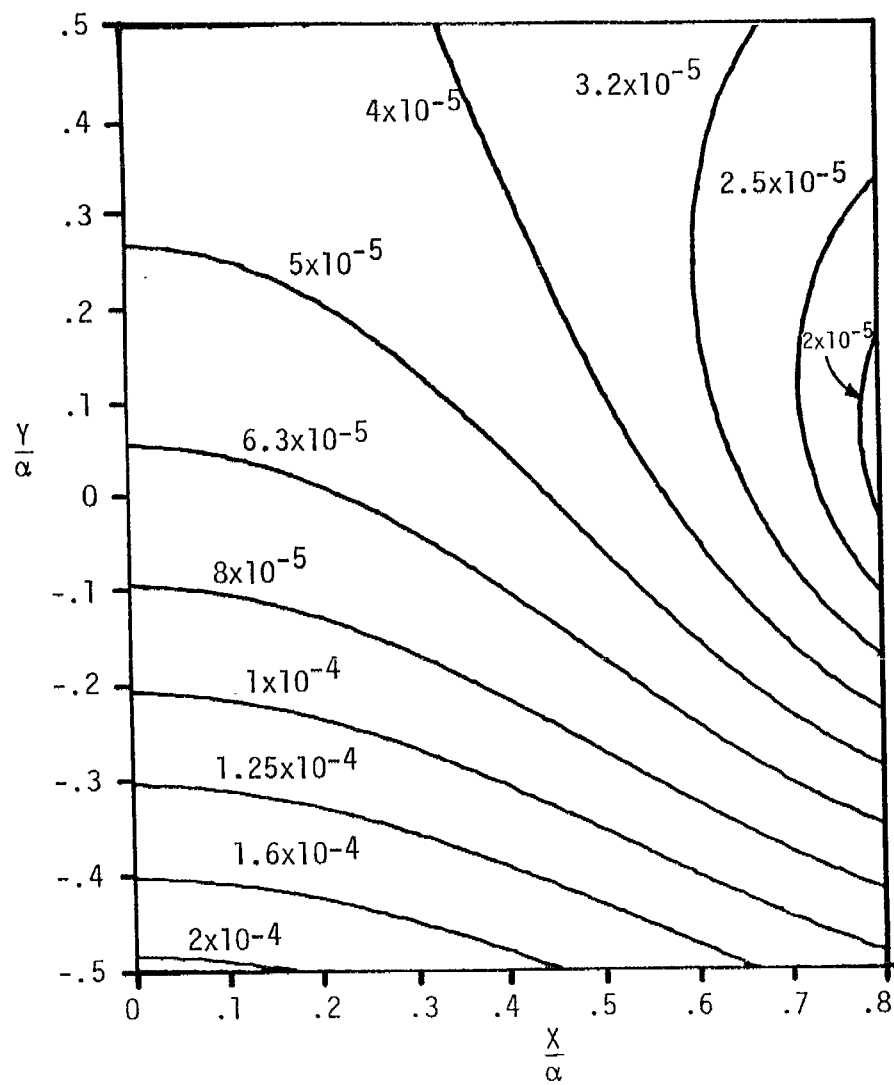
A. $b = \beta$
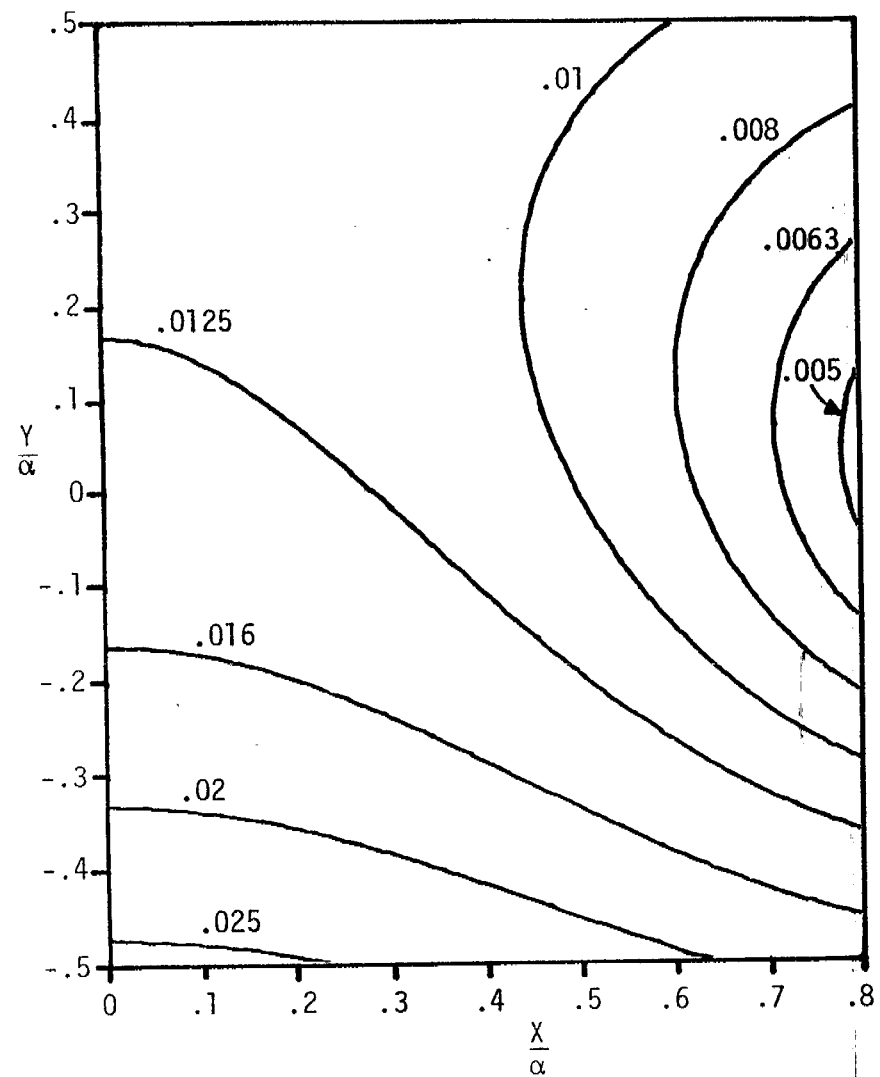
B. $b = \beta - \gamma$

FIGURE 44. ERROR CONTOUR OF FIELD DEVIATION FOR $\Delta e^{(B)}$ $\frac{\beta}{\alpha} = 2$ $\frac{\gamma}{\beta} = .1$

A. $b = \beta$

B. $b = \beta - \gamma$

A. b = β
B. b = β-γ
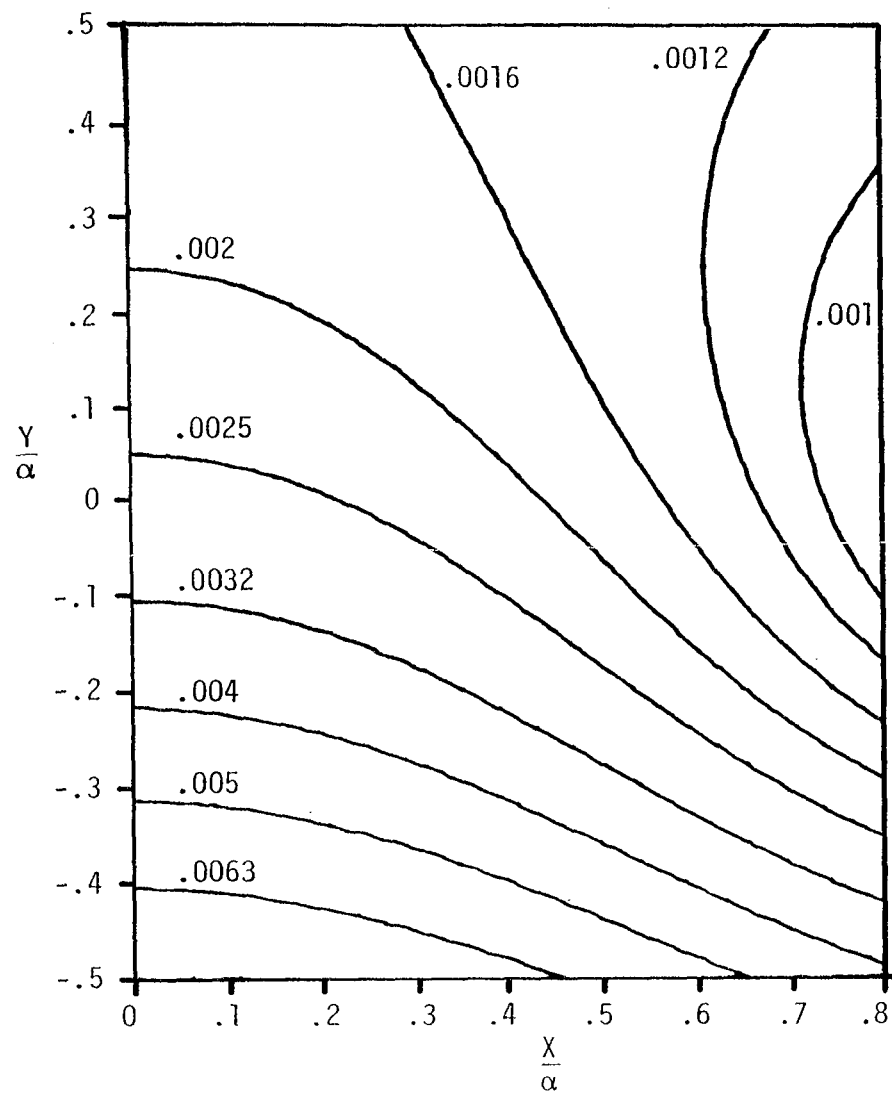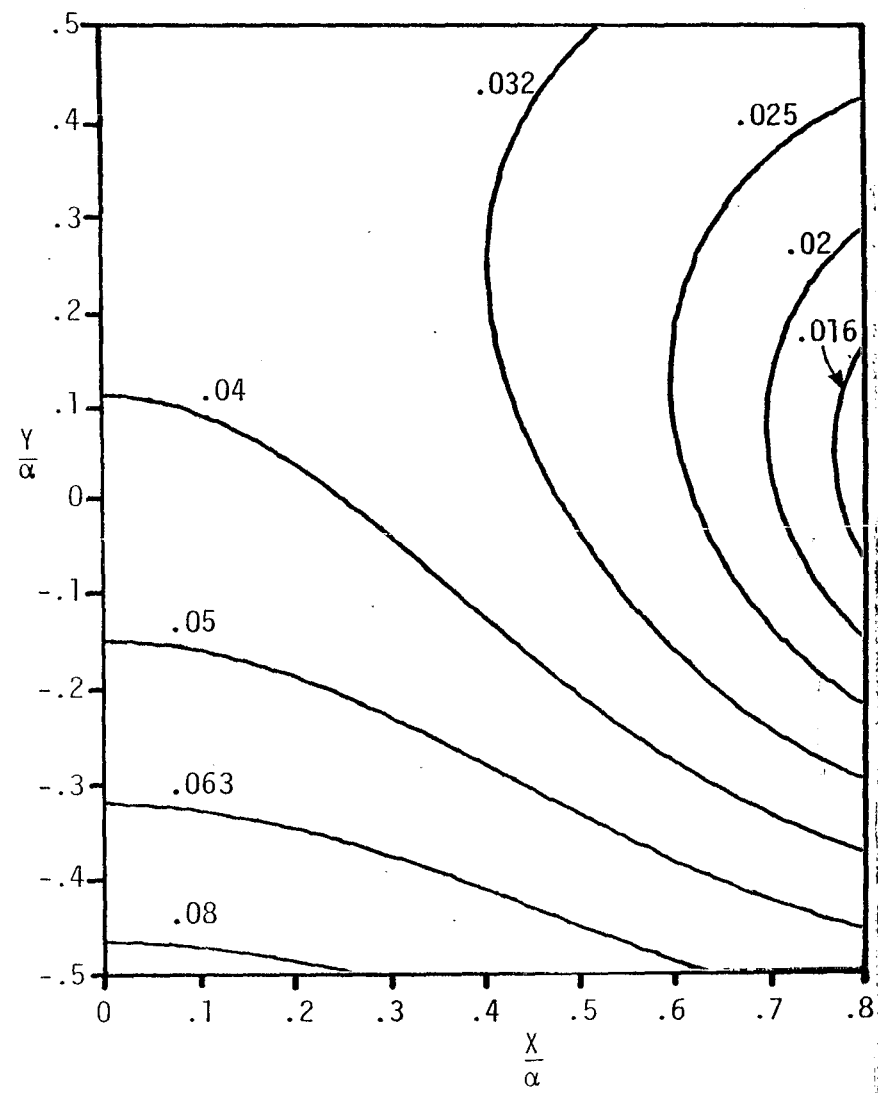
FIGURE 45. ERROR CONTOUR OF FIELD DEVIATION FOR $\Delta e^{(B)}$ $\frac{\beta}{\alpha} = 2$ $\frac{\gamma}{\beta} = .25$
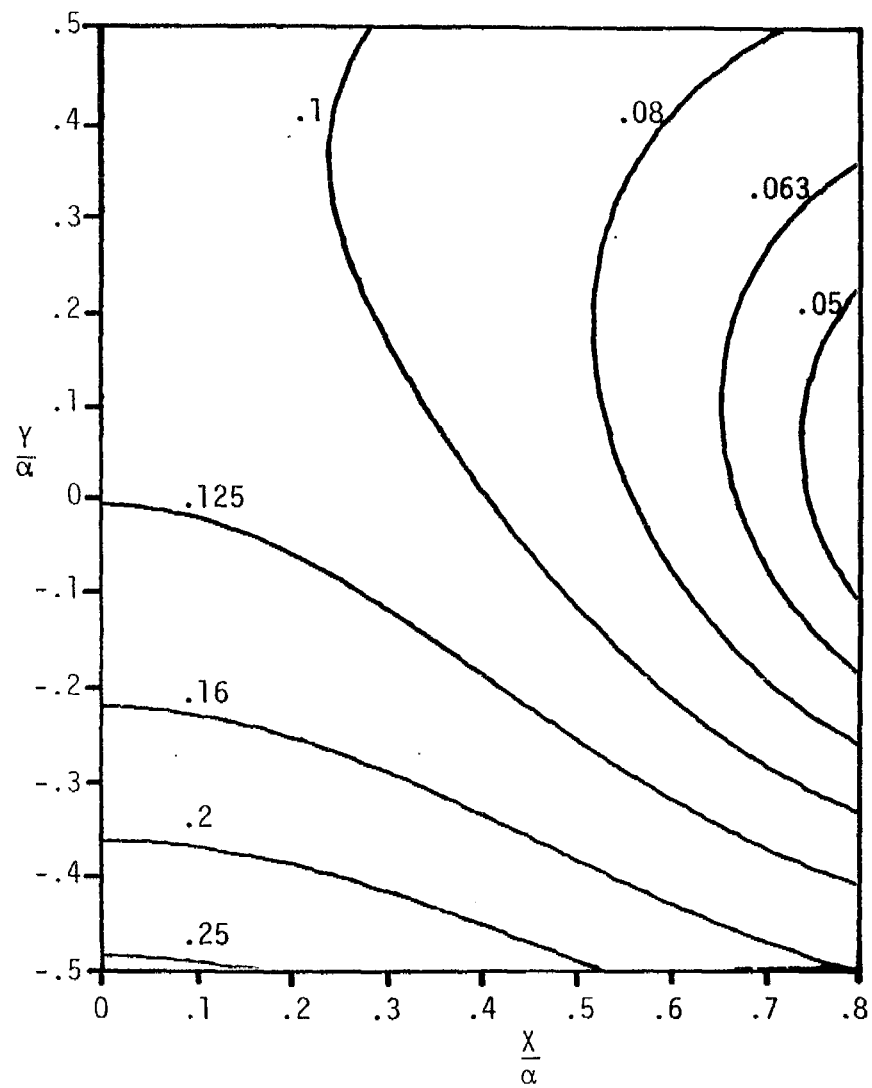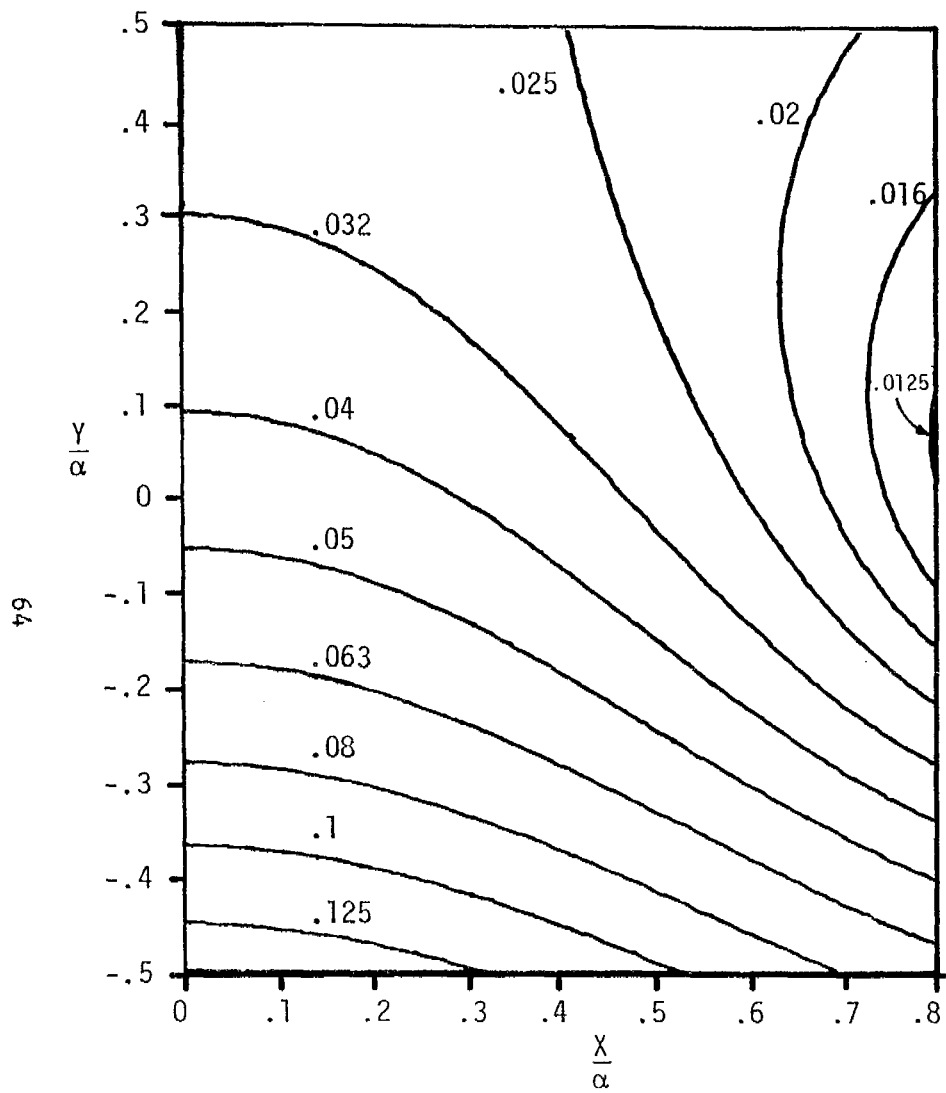
FIGURE 46. ERROR CONTOUR OF FIELD DEVIATION FOR $\Delta e^{(B)}$ $\quad \frac{\beta}{\alpha} = 2 \quad \frac{\gamma}{\beta} = .5$

A. $b = \beta$

B. $b = \beta - \gamma$

64

A. b = β-α

B. b = β-γ
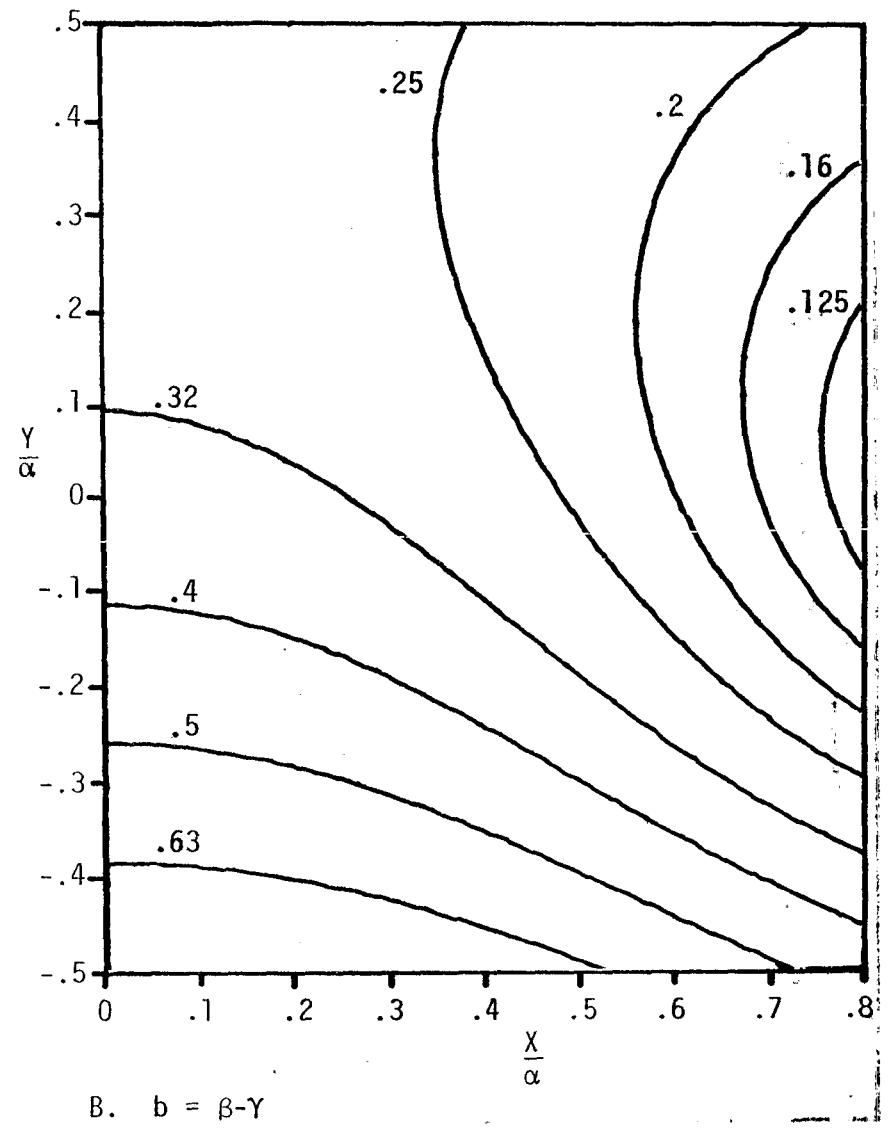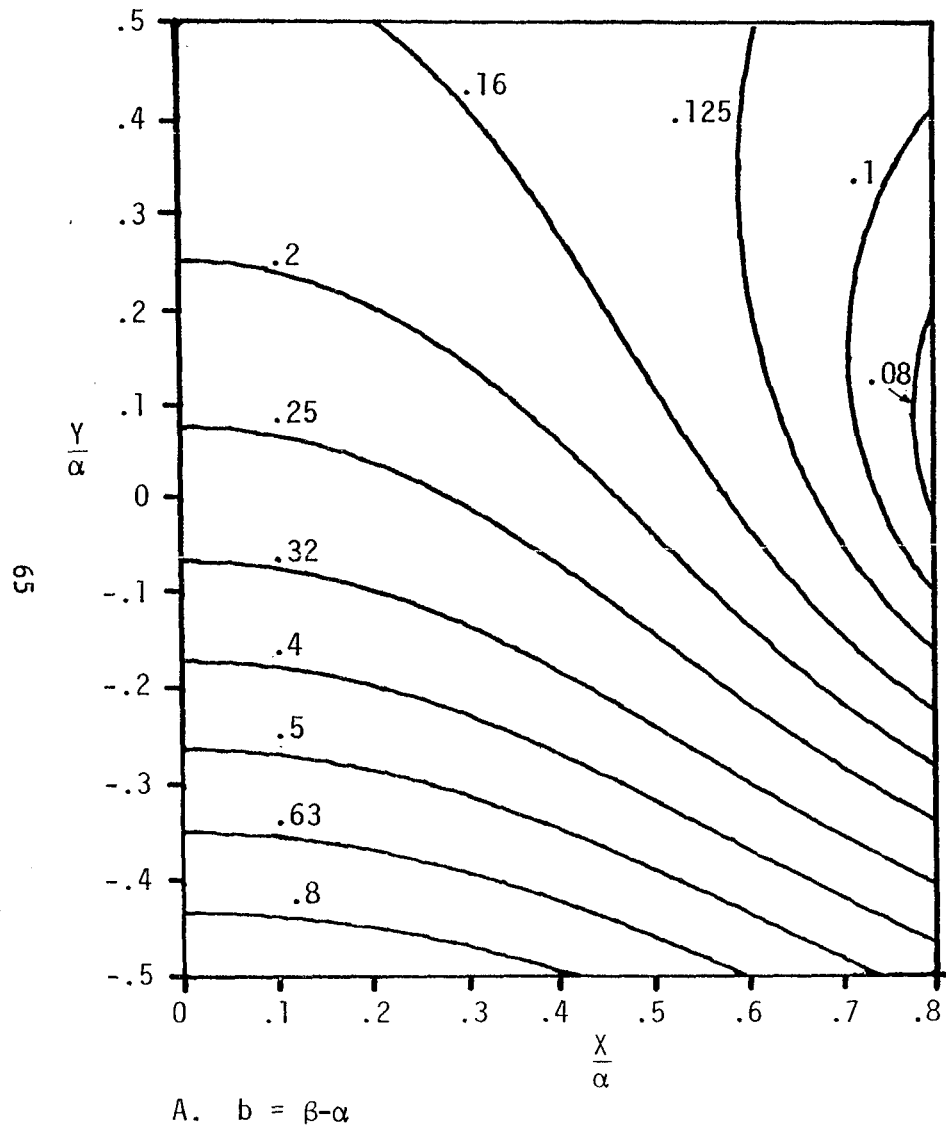
FIGURE 47.   ERROR CONTOUR OF FIELD DEVIATION FOR $\Delta e^{(B)}$ $\frac{\beta}{\alpha} = 2$ $\frac{\gamma}{\beta} = .75$
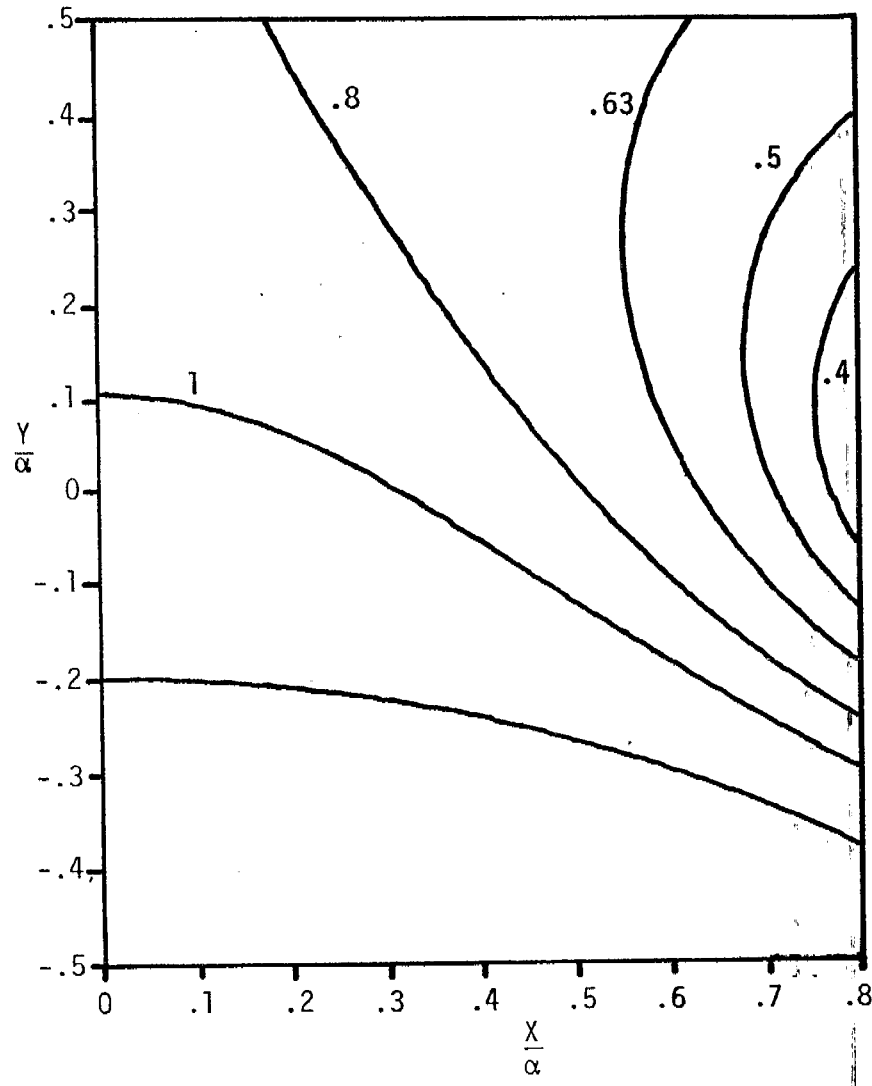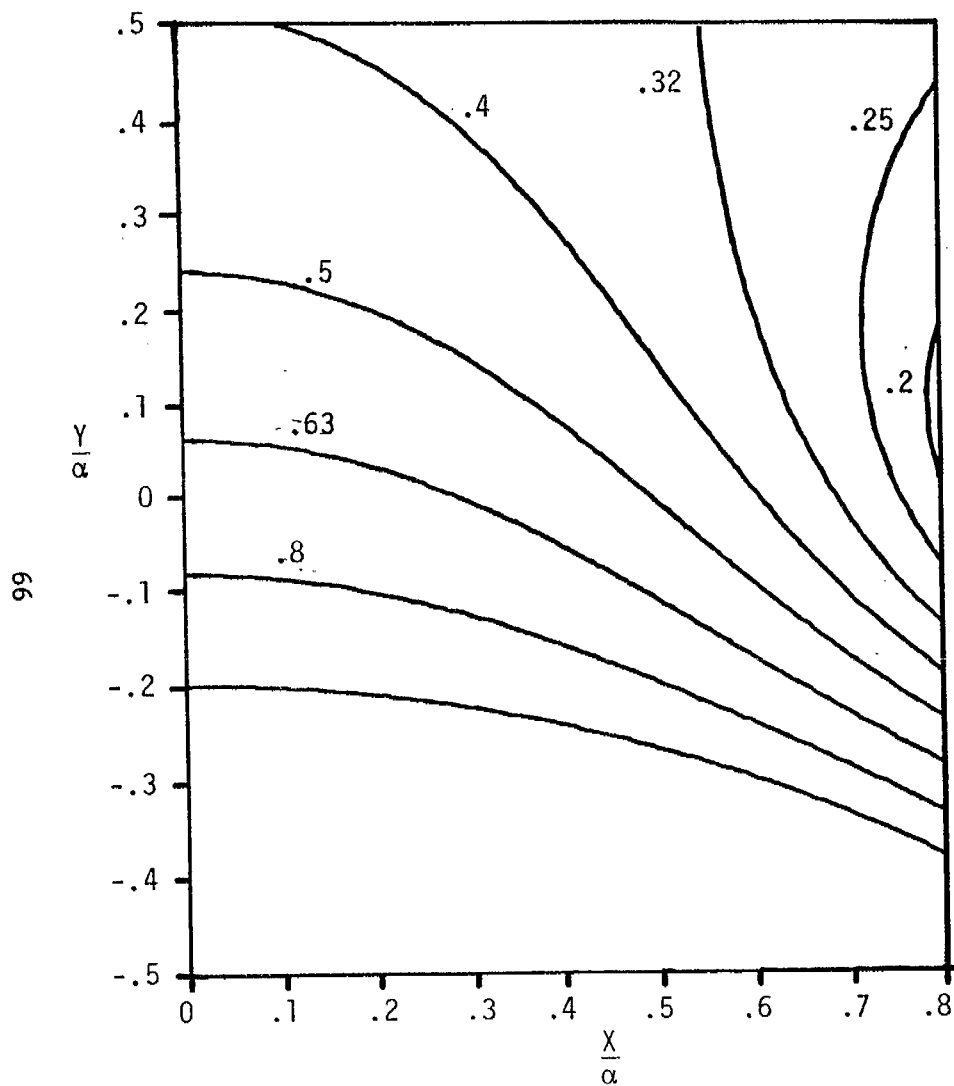
FIGURE 48. ERROR CONTOUR OF FIELD DEVIATION FOR $\Delta e^{(B)}$ $\frac{\beta}{\alpha} = 2$ $\frac{\gamma}{\beta} = .9$

A. $b = \beta$

B. $b = \beta - \gamma$

A. $\frac{Y}{\alpha} = 0$

B. $\frac{Y}{\alpha} = .05$
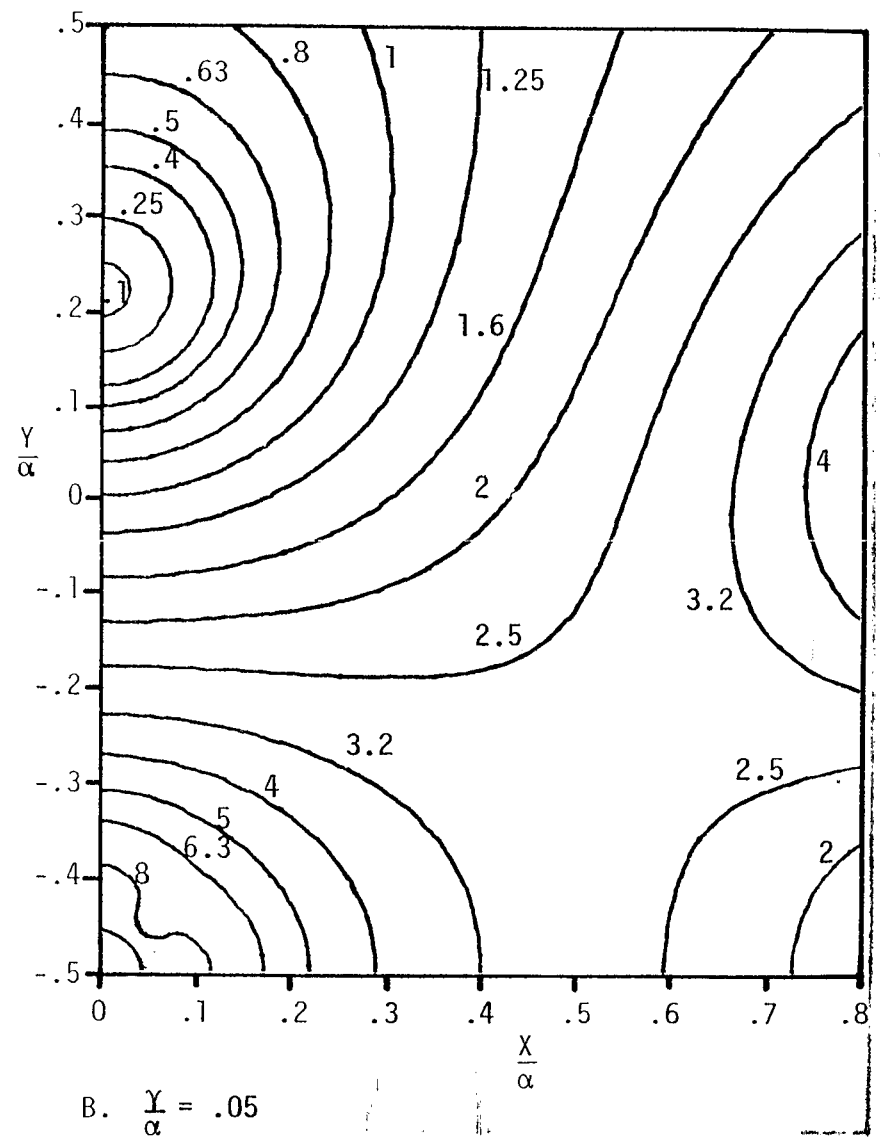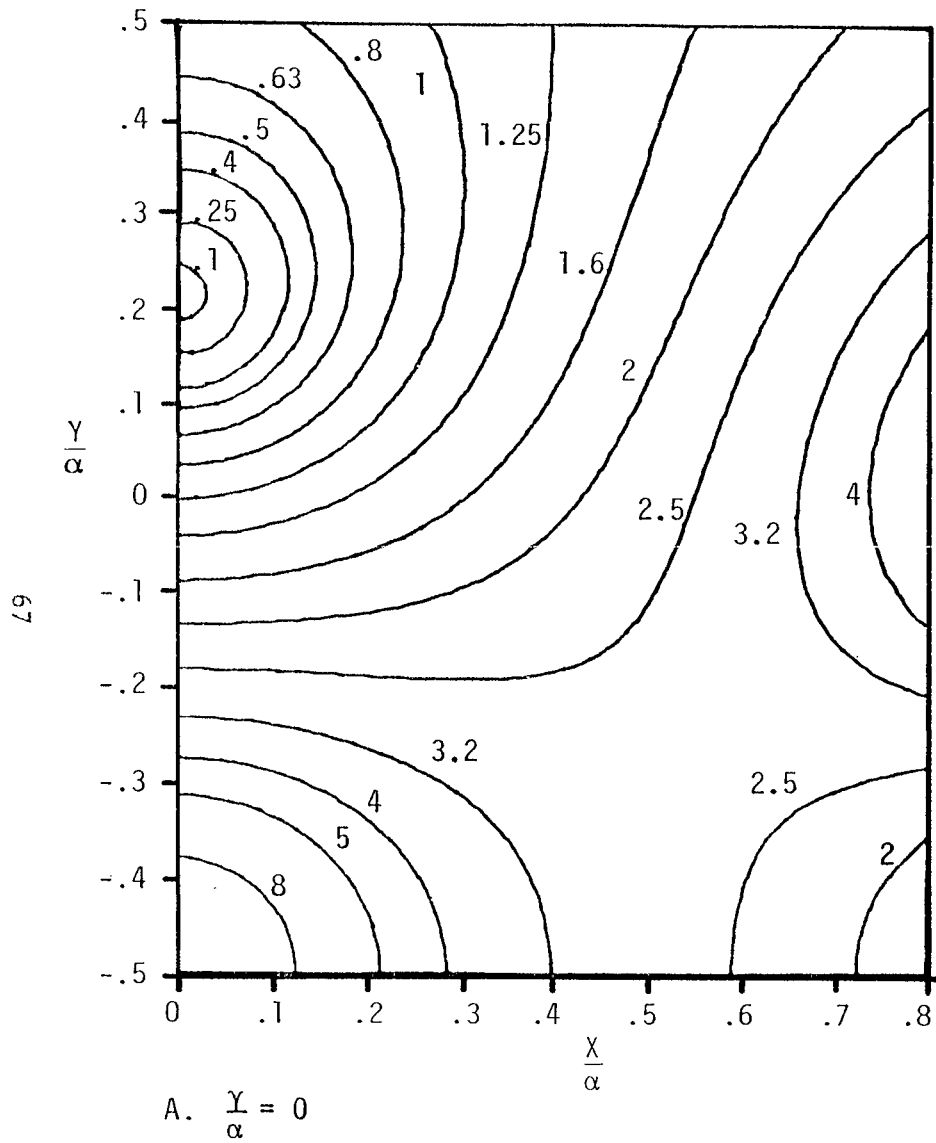
FIGURE 49. UNIFORMITY CONTOURS OF $U^{(B)}$ FOR $\frac{\beta}{\alpha} = .5$
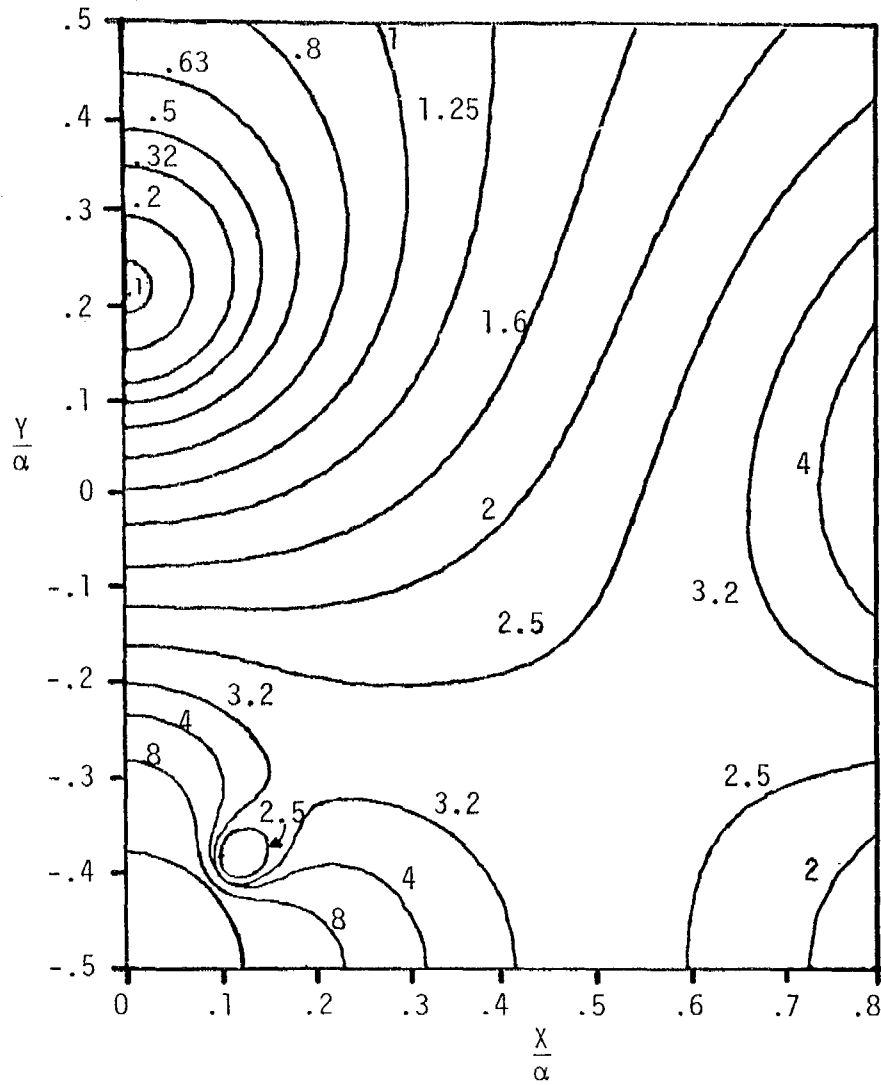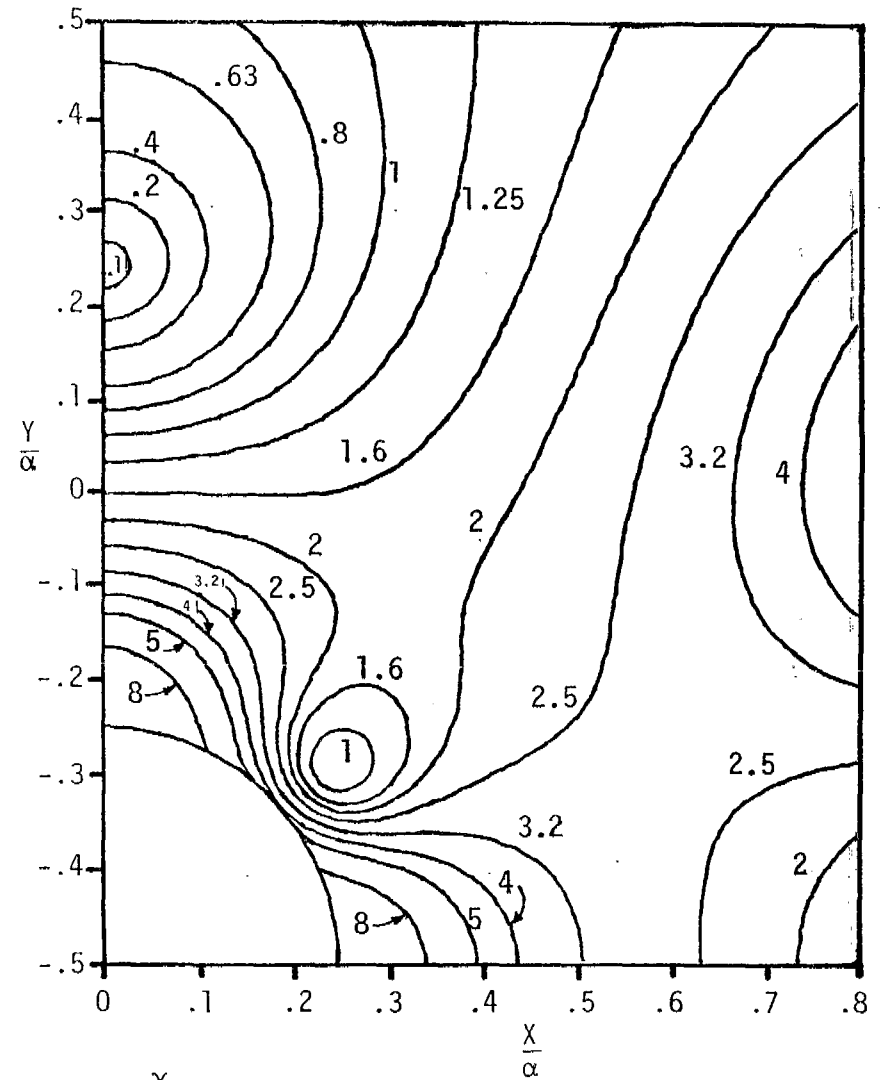
FIGURE 50. UNIFORMITY CONTOURS OF $U^{(B)}$ FOR $\frac{\beta}{\alpha} = .5$

A. $\frac{Y}{\alpha} = .125$

B. $\frac{Y}{\alpha} = .25$
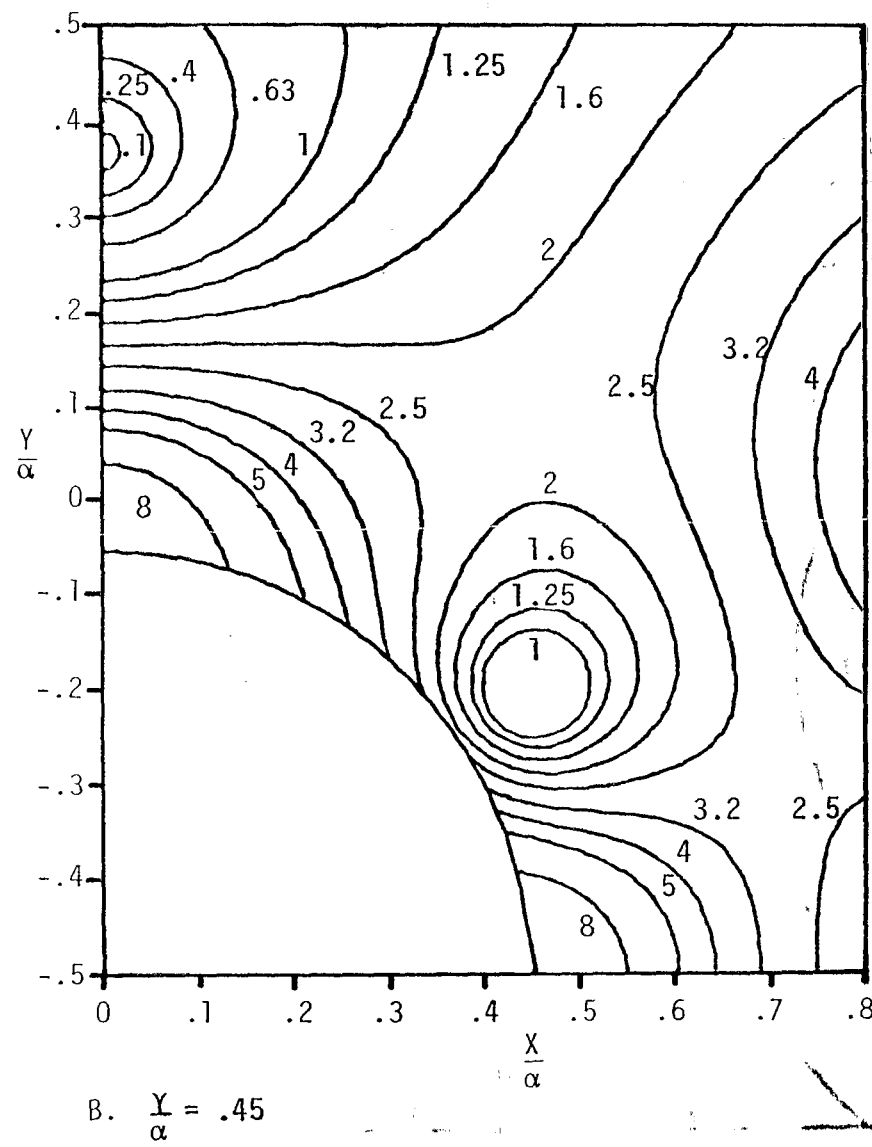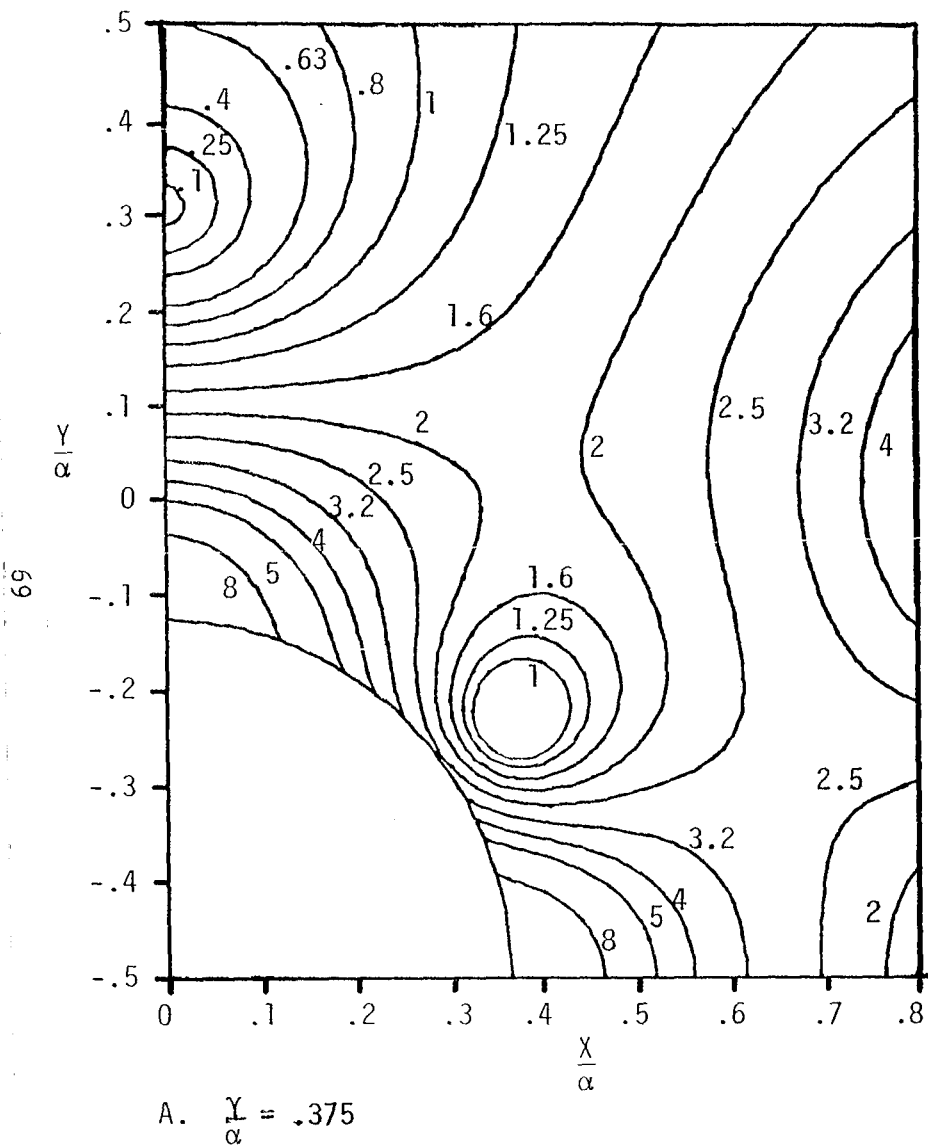
FIGURE 51. UNIFORMITY CONTOURS OF $U^{(B)}$ FOR $\frac{\beta}{\alpha} = .5$
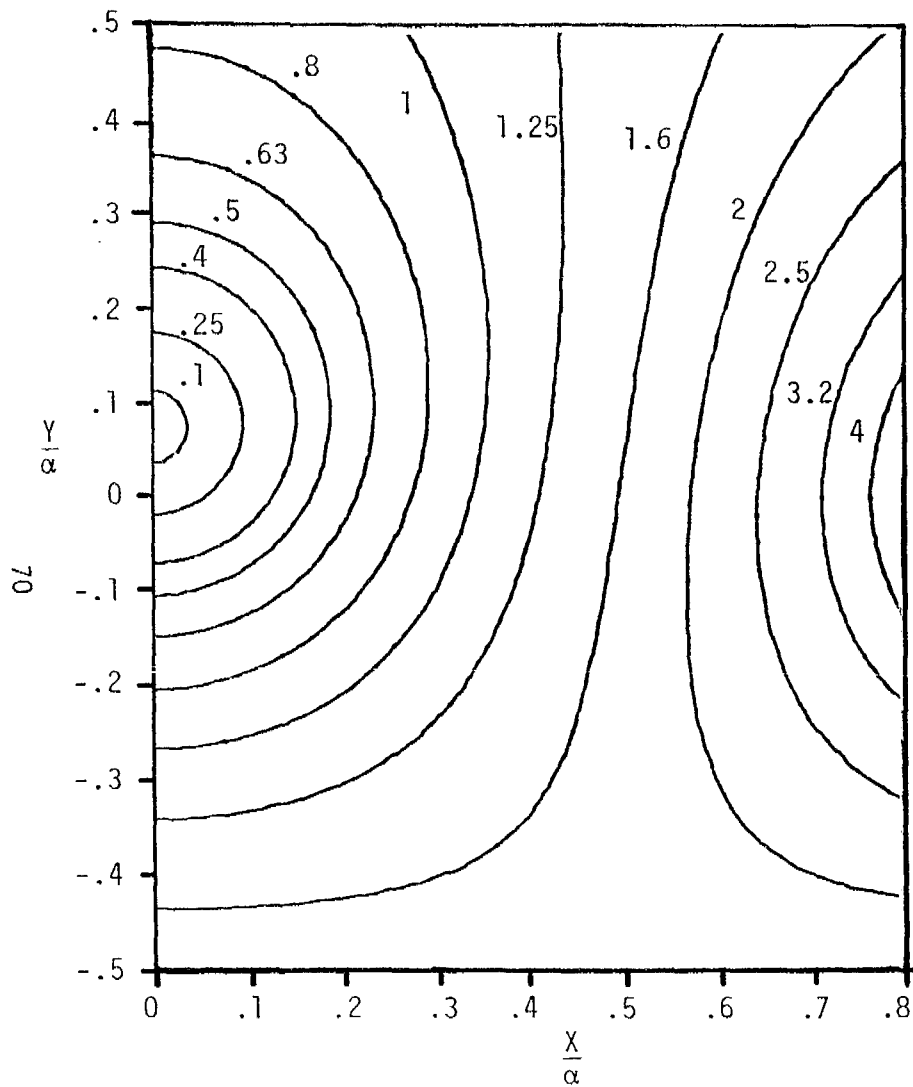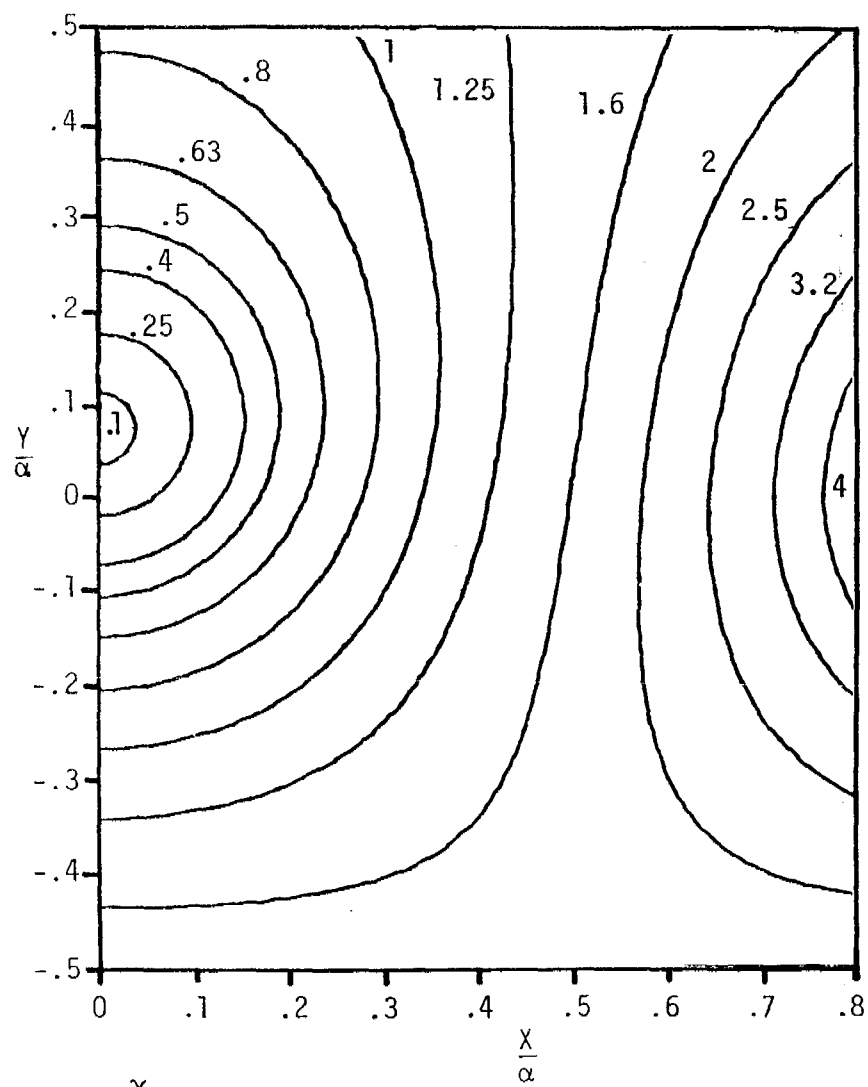
FIGURE 52. UNIFORMITY CONTOURS OF $U^{(B)}$ FOR $\frac{\beta}{\alpha} = 1$

A. $\frac{Y}{\alpha} = 0$

B. $\frac{Y}{\alpha} = .1$
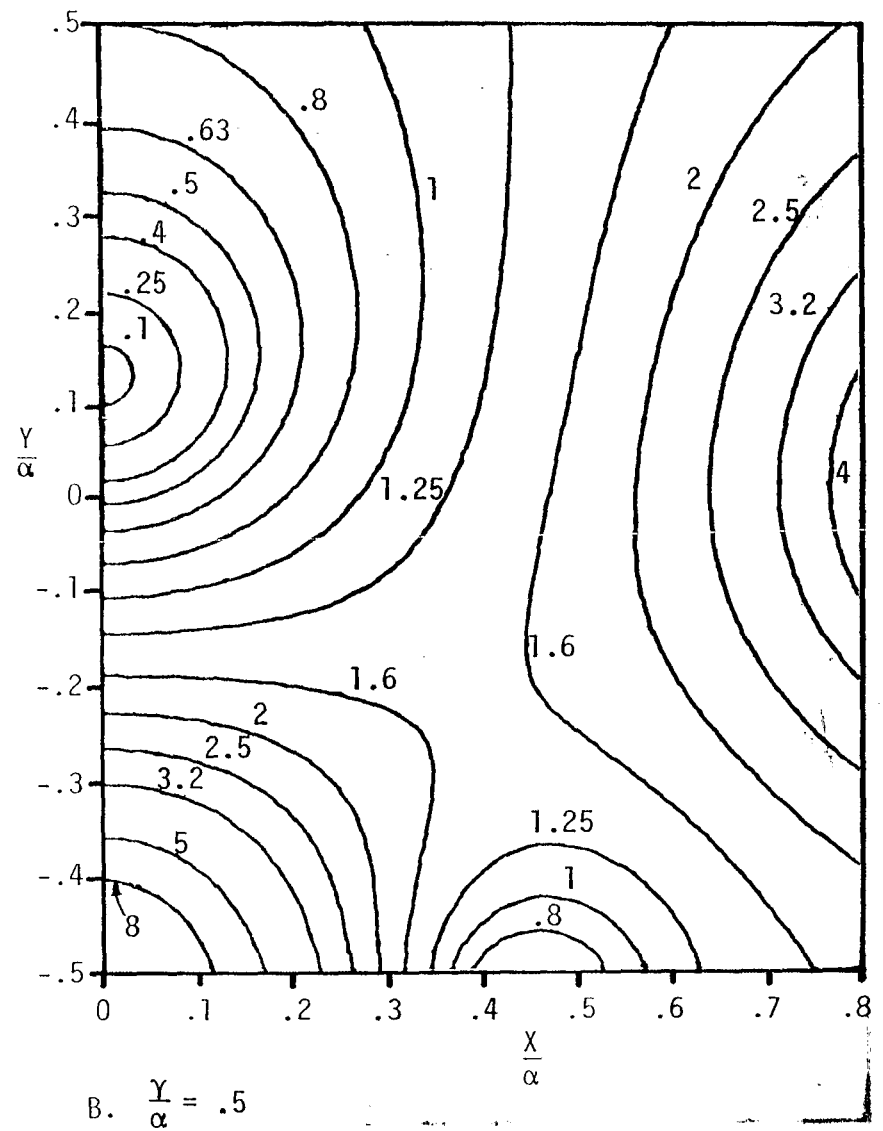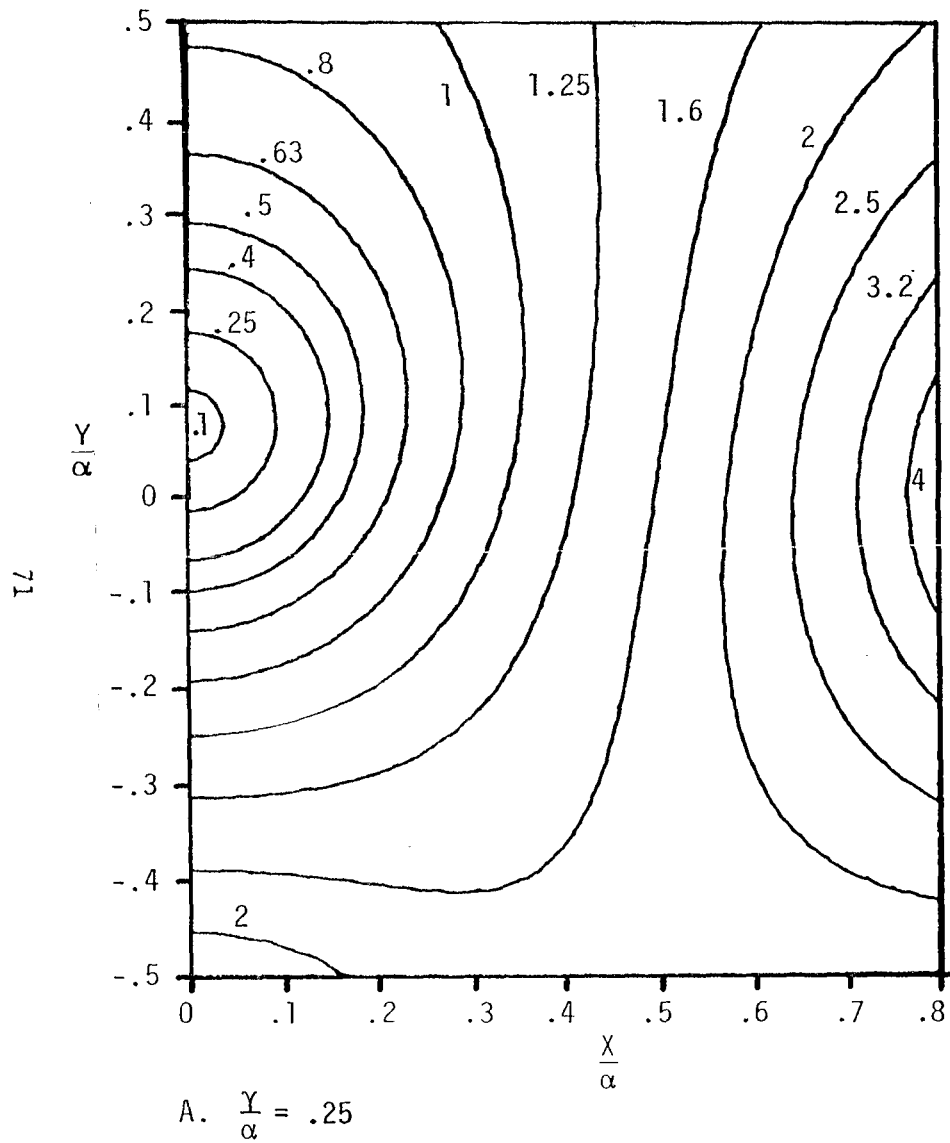
FIGURE 53. UNIFORMITY CONTOURS OF $U^{(B)}$ FOR $\frac{\hat{B}}{\alpha} = 1$

A. $\frac{Y}{\alpha} = .25$

B. $\frac{Y}{\alpha} = .5$

71

A. $\frac{Y}{\alpha} = .75$

B. $\frac{Y}{\alpha} = .9$
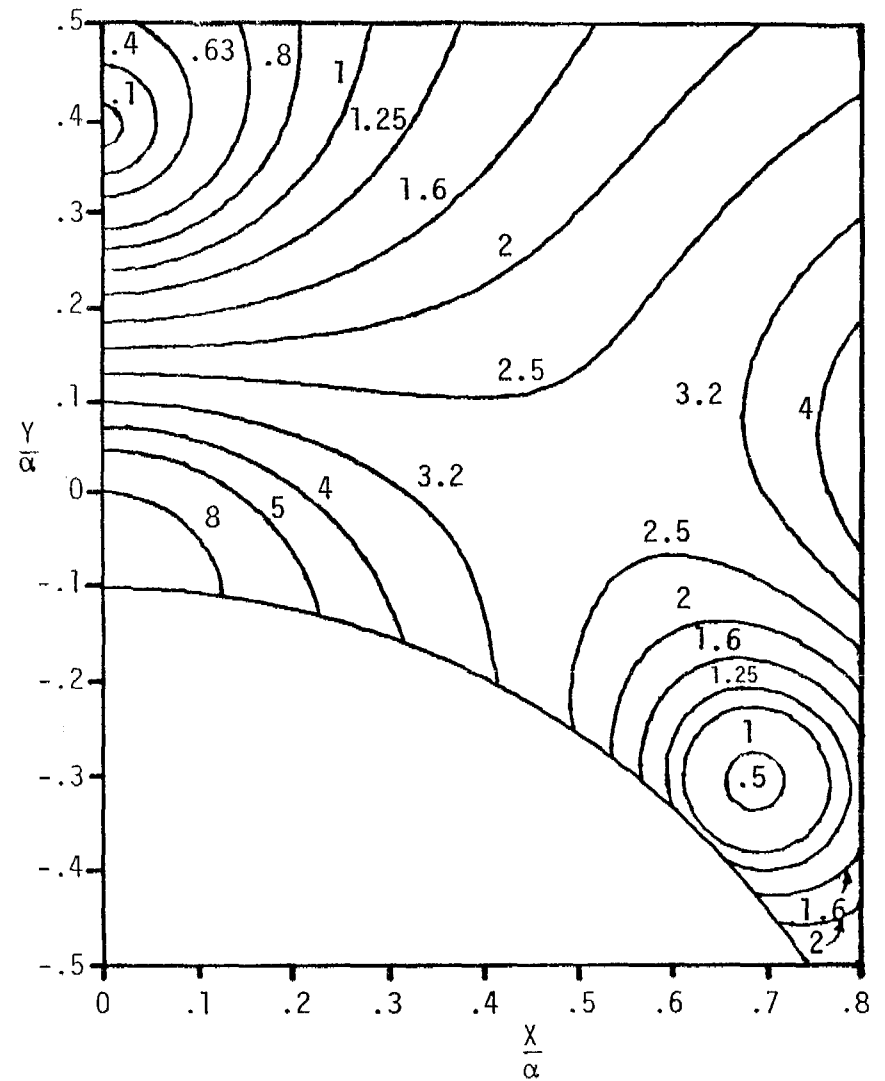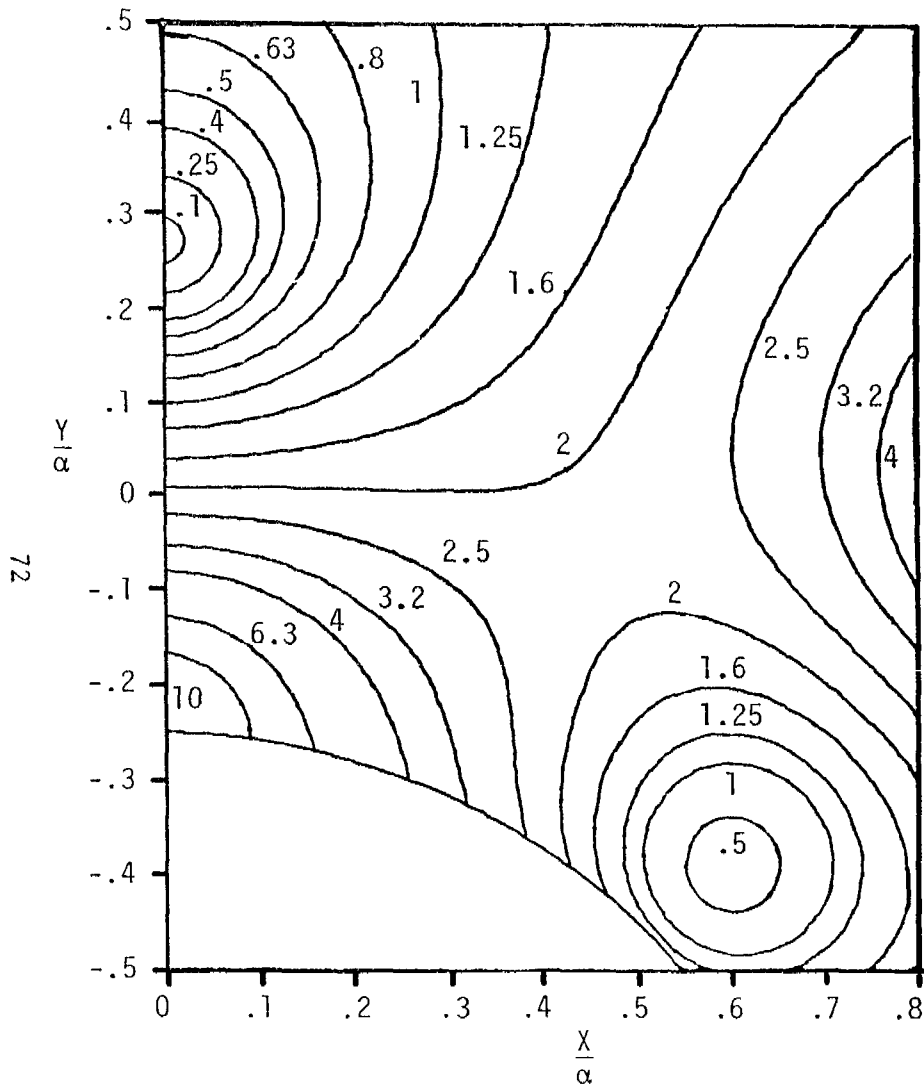
FIGURE 54. UNIFORMITY CONTOURS OF $U^{(B)}$ FOR $\frac{\beta}{\alpha} = 1$
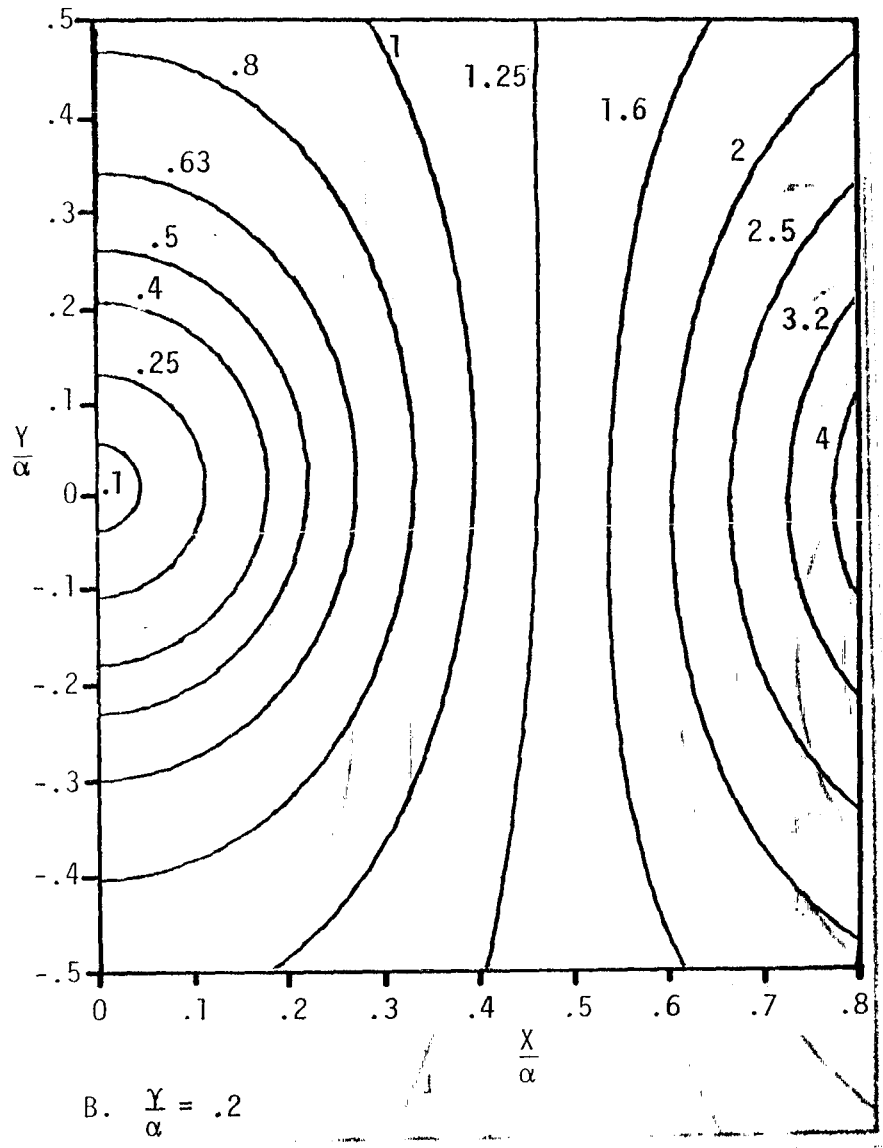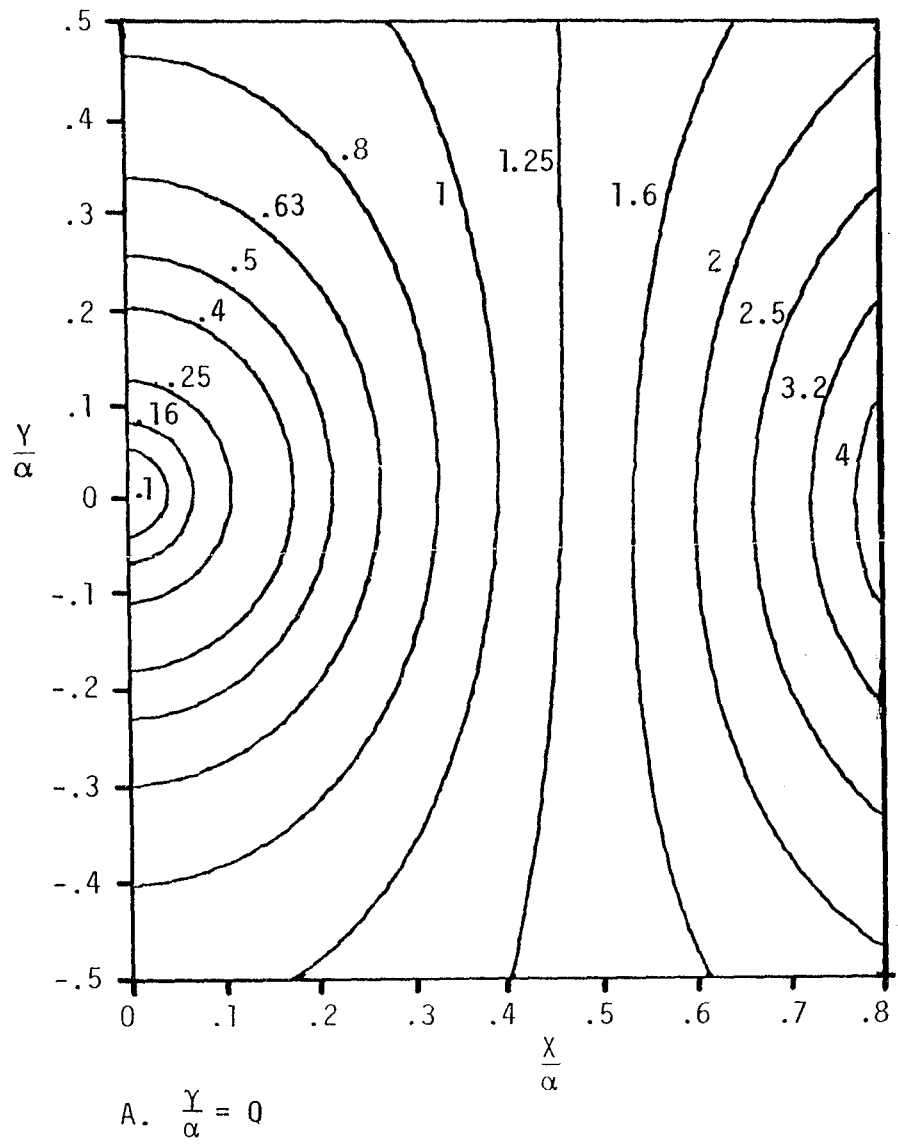
FIGURE 55. UNIFORMITY CONTOURS OF $U^{(B)}$ FOR $\frac{\beta}{\alpha} = 2$
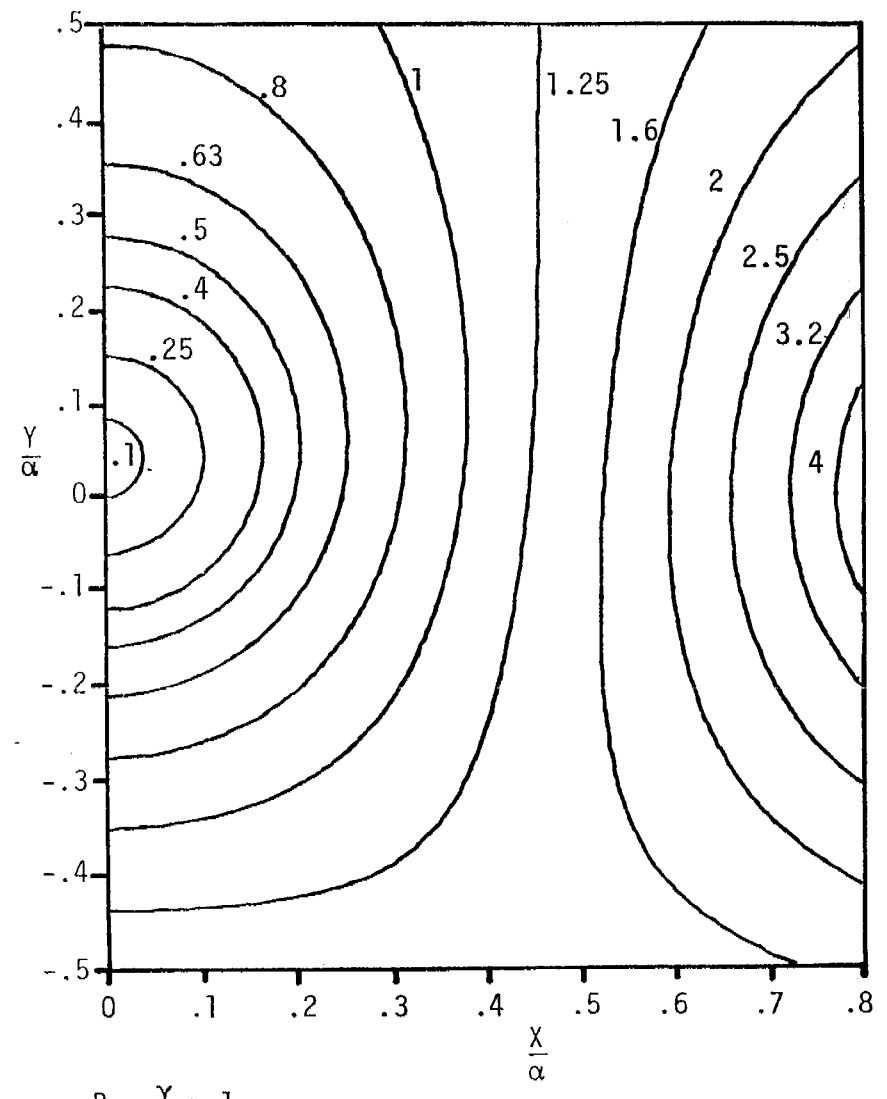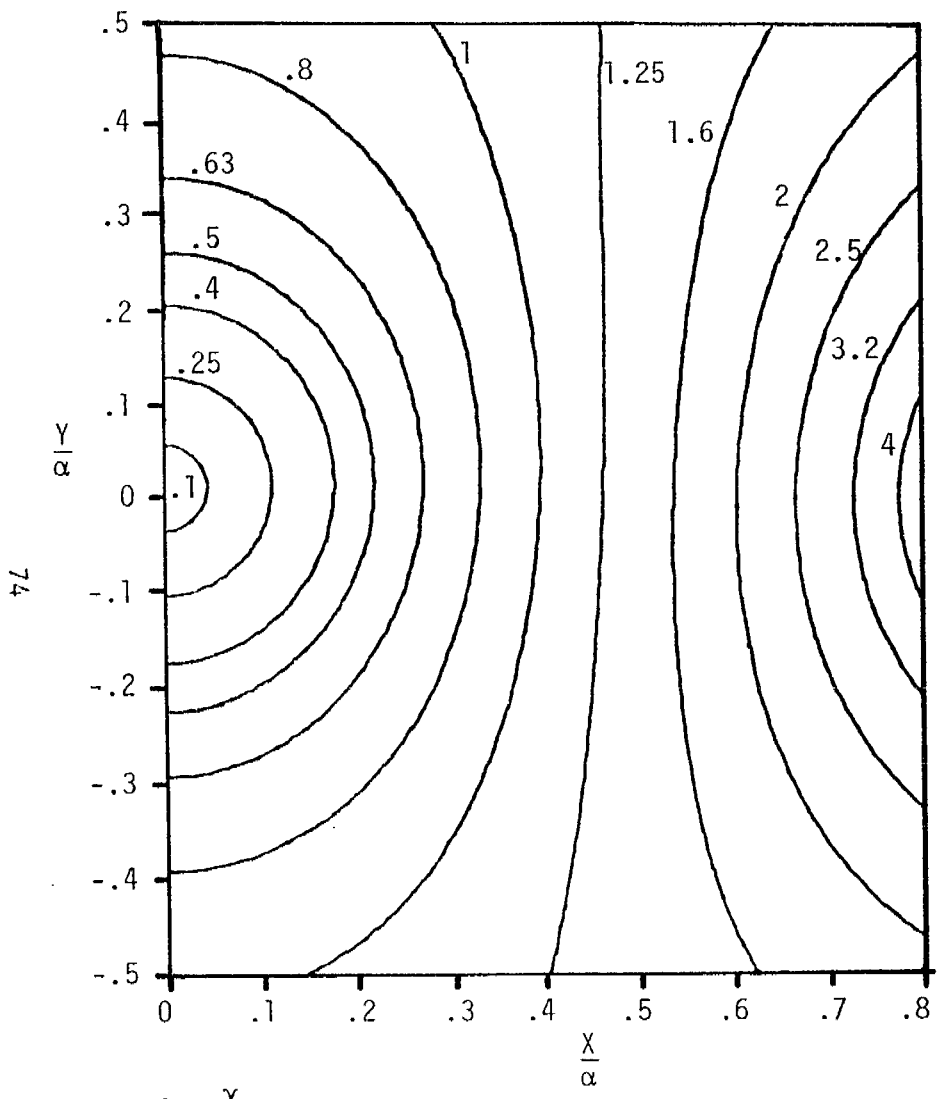
FIGURE 56. UNIFORMITY CONTOURS OF $U^{(B)}$ FOR $\frac{\beta}{\alpha} = 2$

A. $\frac{Y}{\alpha} = .5$

B. $\frac{Y}{\alpha} = 1$

74
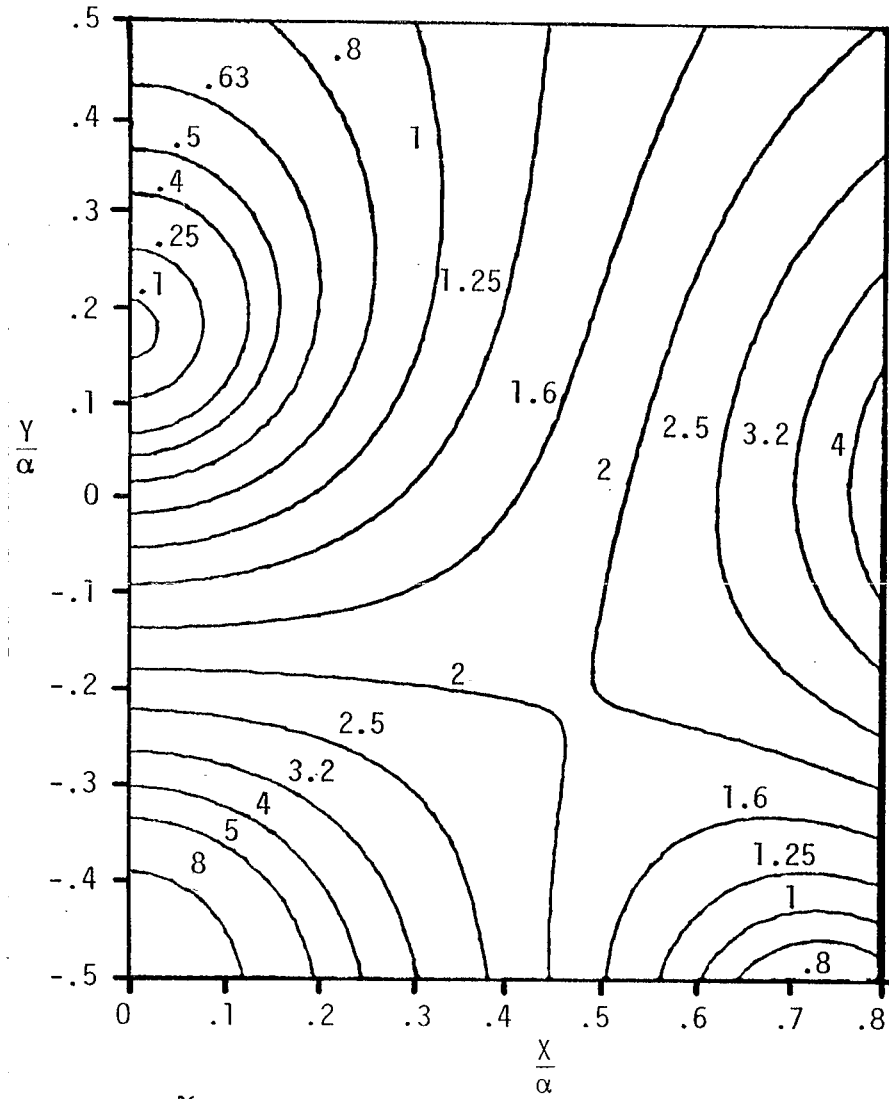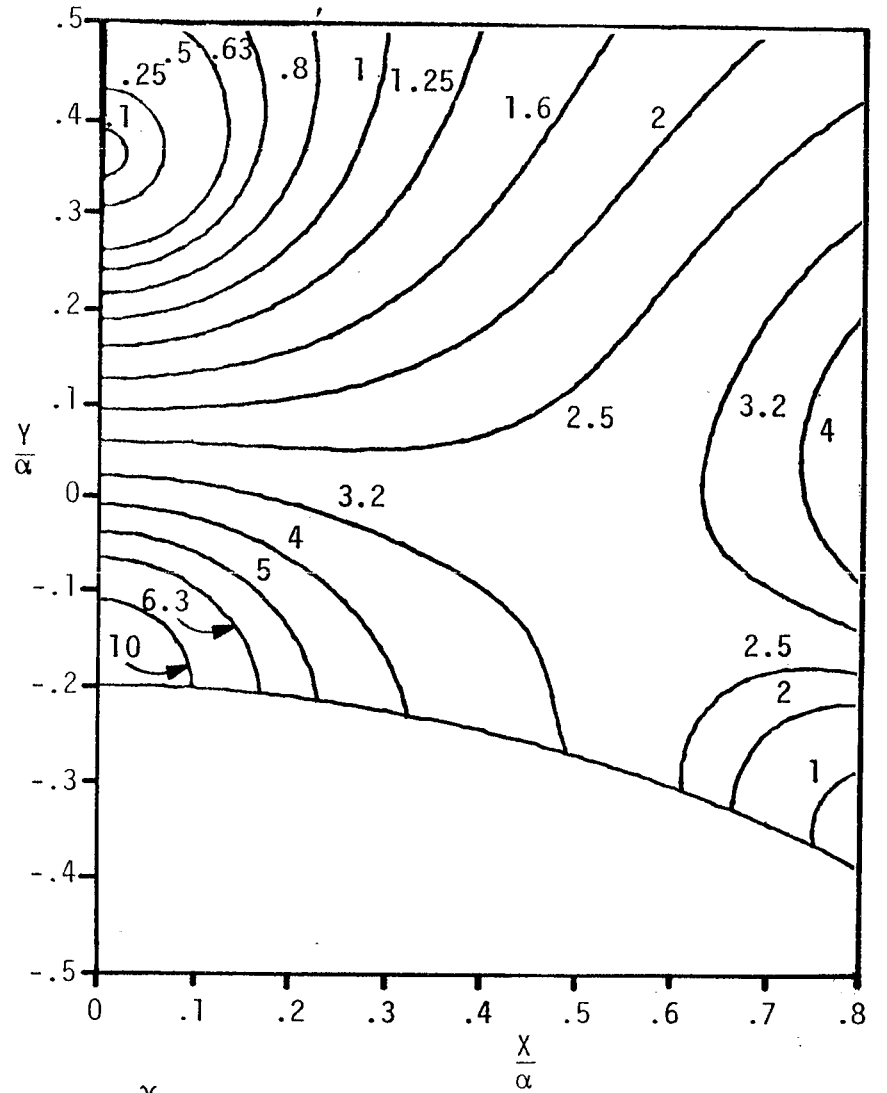
FIGURE 57. UNIFORMITY CONTOURS OF $U^{(B)}$ FOR $\frac{\beta}{\alpha} = 2$

A. $\frac{\Upsilon}{\alpha} = 1.5$

B. $\frac{\Upsilon}{\alpha} = 1.8$